A Reproduced Copy

OF

NASA CR-166,570

Reproduced for NASA

by the

NASA Scientific and Technical Information Facility

NASA CONTRACTOR REPORT 166570

Comparison of Frequency-Domain and Time-Domain Rotorcraft Vibration Control Methods

N.K. Gupta

Integrated Systems, Inc.
Palo Alto, California

CONTRACT NAS2-11271
April 1984

NASA

NASA CONTRACTOR REPORT 166570

Comparison of Frequency-Domain and Time-Domain Rotorcraft Vibration Control Methods

N.K. Gupta
Integrated Systems, Inc.
Palo Alto, California

April 1984

Prepared for
Ames Research Center
under Contract NAS2-11271

National Aeronautics and
Space Administration

Ames Research Center
Moffett Field, California 94035

PREFACE

This report analyzes characteristics of active control design methods for rotorcraft vibration reduction. The frequency-domain formulation is compared against the recently proposed time-domain approach.

The research was conducted under the sponsorship of the National Aeronautics and Space Administration, Ames Research Center, through Contract NAS2-11271.

TABLE OF CONTENTS

TABLE OF SYMBOLS

A, B	- weighting matrices in the time domain control design approach
A_i's	- coefficients in an autoregressive moving average representation of rotorcraft vibration
B	- innovation covariance
C	- control gain in the frequency-domain approach
C_1, C_2, C_3	- control gain in the time-domain approach
E(.)	- expected value of a quantity
F,G,H,D	- matrices which describe rotorcraft system dynamics in the time domain
$\Gamma(j\omega)$	- filter spectrum
G	- gain
Im(.)	- imaginary part of a matrix
j	- $\sqrt{-1}$
J	- penalty function for time domain or frequency-domain control design approach
K	- Kalman estimator gain
ln(.)	- natural logarithm

L	- likelihood function
m	- number of measurement channels
M	- sample points per vibration cycle
n	- measurement noise or modeling error also index for control update in the frequency-domain approach
N	- spectrum of n
N	- number of blades
P	- parameter vector
q	- number of inputs
Re(.)	- real part of a matrix
s	- number of state variables in the time-domain description
$s(j\omega)$	- frequency dependent weighting matrix for maximum-likelihood estimation
t	- parameters in T represented as a vector
T	- transfer matrix
T_m	- modeled transfer function
T_T	- true transfer function
v_i	- measurement noise at the ith time sample point
v_n	- measurement noise in vibration harmonics

V, V_n - covariance of measurement noise

w - vibration source

W - spectrum of random noise w

W_z, W_θ, $W_{\Delta\theta}$ - weighting functions in performance index

x - state vector

y - time history of vibration output

z - harmonic of the vibration level

z_n - rotorcraft vibration harmonic over the nth measurement cycle

z_o - open loop vibration

Greek

Γ - noise distribution matrix

Δ - sampling interval

$\Delta(.)$ - change in any quantity from one update point to the next

δ_n - defined as v_{n-1} (delayed version of measurement noise in the frequency domain

η_n - noise added to transfer matrix to ensure that the Kalman filter does not start ignoring future measurements

θ_n - harmonic of the input over the nth cycle

λ - eigenvalue of matrix

ν - innovations (difference between a measurement and its expected value based on past data)

ξ - vector representing outputs of an undamped filter at the vibration frequency if the input to the filter is rotorcraft vibration

ξ_n - defined as ν_n

π - 3.14159

$\sum$ - covariance of estimation error in T

τ - control input update interval for the frequency-domain approach

Φ - state transition matrix for parameter estimating Kalman filter, transition matrix for discrete state-space transition

ϕ - azimuth reference angle for applied control input

ψ - rotor azimuth angle

Ω - rotor speed

ω - frequency

ω_v - vibration frequency

Superscripts

$\hat{\cdot}$ - estimate

$\tilde{\cdot}$ - error in estimate

$*$ - complex conjugate

Subscripts

c - cosine term, or controller

d - disturbance related transfer function

i - ith sample point in the time domain

m - measured value

max - maximum value

n - nth sample point in the frequency domain

r - sample point for estimation

s - sine term

t - true value

v - vibration

SECTION 1
INTRODUCTION

1.1 BACKGROUND

One of the major difficulties in the acceptance of rotorcraft for both commercial and military applications is the mechanical vibration level. There are several significant vibration sources in rotorcraft, including rotors, transmission systems, and engines. Rotor and fuselage flexibilities amplify the effects of the vibration sources. The level and spectrum of vibration varies along the fuselage. The transmission of rotor blade cyclic loads into the fuselage represents a major source of vibration. It is easily shown that the major components of transmitted forces are at N/rev, 2N/rev, 3N/rev ... etc., where N is the number of rotor blades [1,2].

Without control, the vibration levels in rotorcraft may exceed 0.25 g--significantly higher than those for fixed-wing aircraft. For a four-bladed rotor turning at 240 rpm, the vibration would occur at 16Hz, 32Hz, 48Hz, ... etc. At these frequencies and levels, the vibration degrades both the pilot/passenger ride quality and increases maintenance requirements. Reduction of rotor-induced vibration is of major importance in future rotorcraft developments.

For many years, mass-spring-damper systems have been used for rotorcraft vibration reduction. These systems are heavy and have a limited effectiveness range. Considerable research has recently been done on 'active' techniques, which reduce vibration by directly changing the blade pitch which produces aerodynamic forces to counterbalance the vibration loads. This report studies two approaches that have been proposed for the active control of helicopter vibration.

1.2 ACTIVE CONTROL OF ROTORCRAFT VIBRATION

Two approaches have been proposed to reduce rotor-induced vibration in helicopters through active control of rotor blade pitch angle--one based on frequency-domain analysis and the other based on a time-domain model. The frequency-domain approach using multicyclic feedback control is the more established approach. It has been studied theoretically and validated in certain wind tunnel experiments [3]. The frequency-domain approach uses a model which relates amplitudes and phases of vibration and multicyclic inputs. The time-domain approach uses a model which relates the time history response of vibration with input time history. It has been possible to use this model because of recent work in frequency-shaped modern control design methodology [4]. It has been tested on a detailed rotor systems research aircraft (RSRA) simulation, which includes fuselage flexibilities but does not include rotor aeroelastic effects [5]. Both approaches have been studied in this report to evaluate potential advantages and disadvantages.

1.3 SUMMARY OF KEY WORK

The key results from this research are as follows:

(i) There are many similarities but important differences between the frequency-domain and time-domain formulations of the active rotorcraft vibration suppression problem (see Sections 2 and 3). Both approaches are similar to the extent that they are formulated to control vibration at discrete frequencies. The major differences in their behaviors arise because the time-domain approach updates the control at each sample point while the frequency domain approach updates the control after several vibration cycles.

(ii) System identification techniques are available for both the time-domain and the frequency-domain approaches. These techniques can be used off-line or in real-time. The system identification approach used to identify the local frequency-domain model can be extended for improved accuracy.

(iii) Both the time-domain and the frequency-domain approaches have been analyzed for transient behavior, robustness, susceptibility to various noise sources, and implementation complexity.

(iv) Both random measurement noise and low-frequency modulation of the uncontrolled vibration (caused by pilot inputs, gusts or other process noise sources) has been studied. The low-frequency modulation of the vibration can cause significant errors in the identified models.

(v) The theoretical developments have been partially validated using simplified linear simulations.

(vi) Further work is necessary to develop a fully-adaptive time-domain controller and to study its robustness and performance characteristics.

1.4 SUMMARY OF REPORT

The report is organized as follows.

Section 2 of the report summarizes the frequency-domain and the time-domain methods and their variations.

Section 3 compares, evaluates and extends the two approaches for helicopter vibration control.

Section 4 shows simulation results based on a simplified model.

Section 5 gives the summary, conclusions and proposed work for future research.

SECTION 2

DESCRIPTION OF TIME-DOMAIN AND FREQUENCY-DOMAIN METHODS

There are two basic characteristics of the helicopter vibration problem that directly impact the active control design and implementation.

(i) The high-frequency nature of rotorcraft vibration necessitates high-bandwidth actuators, sensors and control processors. The vibration frequency in most rotorcraft is high enough such that aeroelastic and structural modes will be within the control bandwidth when active control is used. Aeroelasticity can cause rotorcraft dynamics in the neighborhood of the vibration frequency to change substantially from one flight condition to another.

(ii) The control action is desired in the neighborhood of widely separated discrete frequencies.

All previous approaches are able to simplify the basic feedback control design approach by developing suppression techniques to explicitly control disturbances at discrete frequencies. The time-domain approach and the frequency-domain approach differ in the manner in which this characteristic is utilized, i.e.,

(1) The frequency-domain approach attempts to minimize the N/rev (2N/rev, etc.) Fourier transform component of the vibration output, through the use of a performance index which depends on Fourier components of inputs and outputs.

(2) The time-domain approach optimizes a performance index with large penalty on helicopter response which is narrow-band filtered at the vibration frequency. This makes it feasible to use a time-domain dynamic model and update the control law at each sample point.

In this section, the essential characteristics of these approaches are described. This description forms the basis of the developments of the next section.

2.1 FREQUENCY-DOMAIN ROTORCRAFT VIBRATION CONTROLLER

The frequency-domain approach is based on rotorcraft behavior at the discrete vibration frequencies. Various formulations can be used. They all require a combination of identification and feedback control computation steps.

2.1.1 Model Form

The control design model for the frequency-domain approach describes the relationship between the N/rev harmonics of the control inputs and the vibration at desired locations on the rotorcraft. Other dependent variables like blade loads may be substituted for vibration. A different model is needed for each vibration frequency. A dependent variable may be a performance parameter or any other quantity of interest, e.g., blade loads. Using notation of Ref. [3], let z_n and θ_n be the N/rev harmonics of the dependent-variable vector and the control vector, respectively. In steady-state, assuming linearity, z_n and θ_n are related by a transfer matrix, T,

$$z_n = T\theta_n + z_0 \ . \tag{2.1}$$

where z_0 is the N/rev harmonic of the open-loop vibration level. If the linearity does not hold over the entire range of controls, θ_n, a locally linear model may be used

$$z_n - z_{n-1} = T_n(\theta_n - \theta_{n-1}) \ . \tag{2.2}$$

In the frequency domain vibration control design approach, vibration levels are measured at desired points on the rotorcraft and z_n is computed through harmonic analysis. A three-step procedure is then used (i) to identify certain model parameters, (ii) to compute desired feedback gain values, and (iii) to compute harmonic components of the desired feedback inputs. A schematic diagram of the frequency-domain vibration control law is shown in Figure 2-1.

2.1.2 Identification Step

The identification is a key step in the overall procedure because T varies substantially with flight condition, loading and other operating variables. z_0 depends on the flight condition as well as the gust environment and pilot inputs. The model of Equation (2.2) does not explicitly take this variation into consideration (it assumes z_0 is constant). z_0 will typically vary more than T.

The identification problem consists of estimating both T and z_0 if the model of Equation (2.1) is used. When the model described by Equation (2.2) is used, only T needs to be estimated. If T is assumed known or does not vary too much, z_0 needs to be identified in the global model and no parameter needs to be estimated for the local model.

Various forms of least-squares and Kalman filter may be used to solve the identification problem [3]. All recursive approaches, including the Kalman filter, are of the form (where t_n is the unknown parameter vector, which includes all elements of T and z_0, if necessary)

$$\hat{t}_n = \hat{t}_{n-1} + K_n(z_n - \hat{z}_n) , \tag{2.3}$$

$\hat{t}_n$ is the best estimate of the parameters based on first n harmonic cycles. $\hat{z}_n$ is the best estimate of z_n and can, in general, be written as

$$\hat{z}_n = \hat{T}_n\theta_n + \hat{z}_o \tag{2.4}$$

or

$$\hat{z}_n = \hat{z}_{n-1} + \hat{T}_n (\theta_n - \theta_{n-1}) \tag{2.5}$$

The gain K_n can be obtained by solving estimation error covariance equations or be based on least-squares or stochastic gradient equations. A Kalman filter formulation has often been used [3]. It is necessary to consider T and z_0 models driven by white nose such that the gain K_n stays finite. Exponential windows may, alternatively, be used to ensure that K_n is not reduced below an acceptable limit.

2.1.3 Gain Computation and Control Input Determination

The so-called 'deterministic controller' computes the feedback gains by minimizing a quadratic function of the form

$$J = z_n^T W_z z_n + \theta_n^T W_\theta \theta_n + \Delta\theta_n^T W_{\Delta\theta} \Delta\theta \tag{2.6}$$

The control law is of the form

$$\Delta\theta_n = C \begin{bmatrix} z_{n-1} \\ \theta_{n-1} \end{bmatrix} \tag{2.7}$$

where

$$C = -(T^T W_z T + W_\theta + W_{\Delta\theta})^{-1} \; (T^T W_z \vdots W_\theta) \tag{2.8}$$

assuming that the first matrix on the right-hand side is invertible. Note that if $T^T W_z T$ were invertible, W_θ and $W_{\Delta\theta}$ could be set to zero without the control activity becoming infinite at any time point.

Extensions of the deterministic controller, described above, include stochastic methods, where gains are computed based on errors in parameter estimates. This can lead to either a cautious control law or a dual controller. The main effect of these extensions is to add a positive semidefinite term to $(T^T W_z T + W_{\Delta\theta})$ in Eq. 2.8, thus reducing the gain. In many cases, a similar effect could be achieved by modifying W_θ or $W_{\Delta\theta}$ [3].

2.1.4 Implementation of the Frequency-Domain Controller

The frequency-domain vibration controller involves several steps, which are repeated at regular intervals. Figure 2-2 shows the details of the implementation for a four-bladed rotor. The input is updated once per several vibration cycles (typically once per rev or four vibration cycles

for a four-bladed rotor). The control update sampling rate is therefore once per multiple vibration cycles.

2.1.5 Summary

The frequency-domain approach uses a steady-state model, one of various identification procedures (see Section 2.1.2) and one of several gain determination procedures (see Section 2.1.3) for the computation of the feedback control law. Harmonic analysis methods are needed to determine harmonic contents of the vibration at the N/rev frequencies. Sine and cosine wave reconstruction generates the time domain inputs. Typically a control input is applied and the rotor is allowed to reach a pseudo-steady state in several vibration cycles. Measurements are then taken for one or more cycles of vibration. With a small computation delay, the control input can then be updated. The control inputs are thus updated every four to ten cycles of vibration. Table 2-1 from Ref. [3] summarizes various options in the frequency-domain vibration controller implementation.

Since the control harmonics θ_n are changed continually, the rotorcraft may not be in steady state when the measurements are taken. Waiting for the rotorcraft to stabilize may cause unacceptable delays in computing feedback inputs. Thus, an autoregressive moving-average (ARMA) form of the model may be more appropriate where z_n depends on past values of z and current and past values of θ. Such models are difficult to use and have not been studied, though they have been mentioned by Johnson [3]. Such models could offer potential advantages in the frequency-domain vibration control designs, though they require higher computation time.

2.2 TIME-DOMAIN APPROACH

The time-domain approach uses a model defined in the state-space form together with a quadratic performance index to design a feedback control law. The standard time-domain approach uses a performance index, which places equal penalties on states, outputs, and controls at all frequencies. A direct application of this approach to the rotorcraft vibration

suppression control design is not successful because unnecessarily high control activity occurs over a wide frequency region. The wide band nature of the controller also requires an accurate rotorcraft model over a broad frequency region, a model which is difficult to obtain because it might span many blade and fuselage structural modes.

A recent extension of the linear-quadratic-Gaussian time domain methodology makes it feasible to place large penalties on outputs at selected frequency. This extension is called the frequency-shaping methodology [6]. Application of this methodology to rotorcraft vibration control leads to acceptable designs.

2.2.1 Model for the Time-Domain Controller

The model for the time-domain control design problem starts with equations in the state variable form. If u, y and x are control, outputs (or dependent variable) and state time histories respectively, the dynamic model takes the form (assuming linearity)

$$\dot{x} = Fx + Gu \,,$$
$$y = Hx + Du + w \qquad (2.9)$$

The state variables represent translation, rotational or modal displacements and velocities or possibly nonphysical quantities relating inputs and outputs. w is the vibration source. The dynamics must include the effects of rigid-body and rotor states as well as aeroelasticity and structural dynamics states. For a rotorcraft in forward flight, F, G, H, and D are periodic functions of time.

The vibration frequency in rotorcraft is high enough such that the blade aeroelastic modes and fuselage structural modes are important. The model used for vibration control must include the gain and phase changes produced by all the modes up to and beyond the vibration frequency. Normally this model could be very complex; however, the narrow-band nature of rotorcraft vibration simplifies the model needed for vibration control design since the model needs to be accurate near the helicopter vibration

frequency. Thus, a detailed model for each mode is not necessary. A narrow-band model could be approximated by a time-invariant reduced-order model. The time-invariant model describes the output in the neighborhood of N/rev resulting from inputs in the neighborhood of N/rev. It would not, for example, show harmonics in the output when inputs are applied at N/rev.

2.2.2 Control Design Approach

The time-domain approach uses a state-space model and optimizes a cost functional that places a large penalty on fuselage accelerations at vibration frequencies. The solution to the optimal control problem leads to a feedback law where the fuselage accelerations are first filtered by undamped, second-order systems. This vibration control solution has been possible due to a recent extension of the well-known optimal control formulation. The extension allows frequency-dependent penalty functions on states and controls [6].

Considering the model defined by (2.9), we select a cost functional which places large penalties on the vibration output at the vibration frequency. The following quadratic cost functional can be used because the penalty at the vibration frequency, ω_v, is infinite.

$$\int_{-\infty}^{\infty} \left(y^* A y \frac{\omega_v^4}{(\omega^2-\omega_v^2)^2} + u^* B u\right) d\omega , \qquad (2.10)$$

where y represents those variables in which the vibration must be reduced. Note that there is infinite penalty on the component of y at the vibration frequency. y could be components of translational or rotational velocity or acceleration at various points on the fuselage.

The time-domain solution is obtained by defining an additional variable vector ξ as follows

$$\frac{y\omega_v^2}{\omega_v^2-\omega^2} = \xi \qquad (2.11)$$

$$\ddot{\xi} + \omega_v^2 \xi = \omega_v^2 y \ , \tag{2.12}$$

$$y = Hx + w \ ,$$

and

$$J = \int (\xi^T A \xi + u^T B u) dt \ . \tag{2.13}$$

The resulting control law is

$$u = C_1 x + C_2 \xi + C_3 \dot{\xi} \ , \tag{2.14}$$

and the gains are obtained via an optimal control design program. Because of the multiplicity of open-loop eigenvalues, a Schur form (Appendix A and Ref. [7]) algorithm must be used. If necessary, the states x may be derived from a state estimator based on measurements, y. The method is very robust because it can be shown that stability will ensure that the vibration is completely controlled.

The basic procedure can be extended to incorporate implementation difficulties and other requirements as follows:

(1) The feedback of rotor states is eliminated by solving for rotor states in terms of fuselage accelerations [8].

(2) Actuator/sensor dynamics are included by adding more states.

(3) The gains can be scheduled with flight conditions, if necessary. Extensive scheduling is not likely to be needed because of the high margin and zero-to-infinity gain margin [8].

Thus, once the model is defined, the entire control design procedure is straightforward. The model can be obtained in an online procedure or it can be derived off-line. In the off-line procedure, the control gains are computed and stored. Only the control input is determined in real time. To date, the time-domain approach has only used simulation derived models.

2.3 Relationship of the Frequency-Domain and Time-Domain Models

The frequency-domain model of Equations (2.1) or (2.2) and the time-domain model of (2.9) are closely related. To demonstrate the relationship, we shall show procedures to convert one model form into the other.

Conversion from the time-domain to the frequency-domain representation is obtained simply by computing the transfer function between y and u at the vibration frequency ω_v. In the following, z_n and θ_n represent complex variables, with real and imaginary parts representing cosine and sine components. Note that the time-domain representation results in the same transfer matrix for both the cosine and the sine parts.

$$z_n = y(j\omega_v) = \underbrace{H(j\omega_v I - F)^{-1}G}_{T_n} \underbrace{u(j\omega_v)}_{\theta_n} + \underbrace{w(j\omega_v)}_{z_o}$$
$$= T_n\theta_n + z_o \quad . \tag{2.15}$$

Conversion from the frequency-domain representation to the time-domain representation is non unique. Without giving any proof, we shall state that the simplest time-domain representation for a general frequency-domain transfer matrix is as follows (assuming the order of y is the same or more than the order of u)

$$\begin{aligned} \dot{x} &= u \ , \\ y &= Hx + Du + w \ . \end{aligned} \tag{2.16}$$

The order of the state vector equals the number of independent variables

$$\begin{aligned} x(j\omega_v) &= \frac{1}{j\omega_v} u(j\omega_v) \\ y(j\omega_v) &= \left(\frac{1}{j\omega_v} H + D\right) u(j\omega_v) + w)j\omega_v) \ . \end{aligned} \tag{2.17}$$

Thus, if we choose

$$H = -\omega_v \, \mathrm{Im}(T_n) \ ,$$

$$D = \mathrm{Re}(T_n) \qquad (2.18)$$

and $$w(j\omega_v) = z_0 \ .$$

The time-domain representation of (2.11) can be made equivalent to a general frequency-domain model. Note that the open-loop representation is neutrally stable. The closed-loop design will, of course, be stable as long as H is full rank and all elements of y are to be controlled.

2.4 SUMMARY

This chapter summarized the time-domain and the frequency-domain methods for active control of rotorcraft vibration. The next chapter analyzes each of the techniques to enable an understanding of the relative tradeoffs in using the two methods.

SECTION 3

ANALYSIS OF TECHNIQUES

There are several significant considerations in the use of an active feedback control design technique in real systems. These include performance under nominal and off-design conditions, ease of design, reliability, maintainability, implementation complexity, and robustness. Some of the more important analytical considerations are as follows:

Identification of Mathematical Models for Helicopter Vibration Control Design - All feedback control design methods require a mathematical model to describe the relationships between applied control inputs and measured outputs. These models may, in general, be developed from theoretical analysis or experimental data. For helicopter vibration control design, system identification methods with experimental data are desirable because the model is required over a narrow frequency band and the theoretical analysis is likely to be very complex. Both real-time and off-line parameter estimation methods must be considered.

Robustness - The active vibration control system must continue to operate satisfactorily and stably with errors in parameters and models used for control law design. In addition, the steady-state vibration level must be relatively insensitive with respect to weighting functions used in control design.

Transient Behavior - The time delay between changes in the vibration and the rotorcraft approaching steady-state vibration should be small. This provides adequate performance in transient flight conditions and in the presence of gusts, which have correlation times of 1 sec. or even less. Stability of the control law during the transient must be established. As has been shown recently, many adaptive control methods may have very poor transient response.

Susceptibility to Noise - The measurements taken on-board a helicopter are likely to be very noisy because of significant vibration and air turbulence. The techniques must be reasonably insensitive to measurement and process noise.

Implementation Considerations - The effect of the active control design approach on actuator, sensors, control processor requirements is important because these will impact the overall cost of the helicopter with active vibration control system.

During the course of this research, each of these issues was studied. In the following sections of this chapter, the most significant results are shown.

3.1 SYSTEM IDENTIFICATION

This section discusses a selection of algorithms to identify helicopter models suitable for use in vibration controller design and implementation. Emphasis has been placed on deriving mathematical models from measured control inputs and vibration response data. Previous techniques are extended to develop low order models that hold primarily in the immediate neighborhood of the vibration frequency. Both batch and recursive forms of identification methods are discussed. Batch methods are suitable for off-line identification, while recursive methods might be applicable to real-time identification as well as adaptive implementations. A major portion of the discussion is restricted to time-domain model identification since identification of frequency-domain models has been covered previously.

Either an off-line or a real-time (on-line) approach may be used for the development of models from test data. If the off-line system identification approach is used, three steps are required to derive the control law (Figure 3-1).

In the first step, a test is planned and conducted, where preselected multicyclic inputs are applied to the helicopter and the resulting response is measured and recorded. Then, the data is used in a batch mode to derive a highly accurate model of the helicopter in the operating regions of interest. The identified model or its simplified form is used to derive the control law. Prior to implementation, the control law is evaluated for robustness and proper performance over the entire range of operating conditions. Failure modes are also tested and redundancy is built to avoid catastrophic results in case of failure. Implementation follows.

In the on-line approach, all of the above steps are combined. The identification is done on-board in the helicopter and the control law is computed using the resulting model. Significant off-line planning and analysis are, nevertheless, needed to ensure robustness of algorithms to noise, failures, and sudden changes in model forms. The control law may be

updated continuously or at certain intervals. Such methods are referred to as 'self-tuning' or 'adaptive.'

Not surprisingly, the basic methods are similar in off-line and on-line implementations. In either case, the model needs to be good only in the neighborhood of the vibration frequency. The model complexity must be kept low both to simplify on-board implementation complexity and because unnecessarily complex models can lead to sensitive and nonrobust control laws. The key to designing good control laws for helicopter vibration reduction is to identify a low-order mathematical model in the neighborhood of the vibration frequency and to develop a robust control scheme that can use this model.

The next subsection summarizes system identification methods for the derivation of the model for frequency-domain control design. Methods to derive applicable time-domain models are discussed in a subsequent subsection.

3.1.1 Identification of Frequency-Domain Models

Johnson [3] provides a summary of the system identification methods that may be used for the frequency-domain models. We shall show the basic results for the local model (extensions of the results to other models are straightforward).

$$\Delta z_n = z_n - z_{n-1} = T\Delta\theta_n \tag{3.1}$$

Let v_n be the measurement noise in z_n, i.e.,

$$z_{nm} = z_n + v_n \tag{3.2}$$

The most common off-line procedure is the least-squares. Substituting (3.2) in (3.1), we get

$$\Delta z_{nm} = z_{nm} - z_{n-1,m}$$

$$= (z_n + v_n) - (z_{n-1} - v_{n-1})$$

$$= (z_n - z_{n-1}) + (v_n - v_{n-1})$$

$$= T\Delta\theta_n + e_n \qquad (3.3)$$

where $e_n = v_n - v_{n-1}$. The estimation model is defined by Eq. (3.3) with noise e_n. Note that e_n is correlated with $e_{n-1}(= v_{n-1} - v_{n-2})$ and $e_{n+1}(= v_{n+1} - v_n)$. If V is the covariance of the measurement noise v_n, and the noise has a Gaussian distribution, the least-squares estimate based on $z_1, z_2 \ldots, z_{n+1}$ minimizes

$$(e_1^T, e_2^T, \ldots, e_n^T) \begin{bmatrix} 4V & -V & 0 & \cdot & \cdot & \cdot & 0 \\ -V & 4V & \cdot & \cdot & \cdot & \cdot & \cdot \\ 0 & \cdot & \cdot & \cdot & \cdot & \cdot & \cdot \\ \cdot & \cdot & \cdot & \cdot & \cdot & \cdot & 0 \\ \cdot & \cdot & \cdot & \cdot & \cdot & 4V & -V \\ 0 & \cdot & \cdot & \cdot & & -V & 4V \end{bmatrix}^{-1} \begin{bmatrix} e_1 \\ e_2 \\ \cdot \\ \cdot \\ \cdot \\ e_n \end{bmatrix} \qquad (3.4)$$

The estimation problem is often simplified by neglecting the off-diagonal terms in the covariance matrix. The resulting solution is

$$T_N = \left[\sum_{n=1}^{N} (z_{n+1,m} - z_{nm}) V^{-1} \Delta\, \theta_{n+1}^T\right] \left[\sum_{n=1}^{N} \Delta\theta_{n+1} V^{-1}\, \Delta\theta_{n+1}^T\right]^{-1} \qquad (3.5)$$

The most efficient solution is much more complex (see the following).

The least-squares solution can be converted into a recursive form in which the estimate for N+1 measurements can be obtained from the estimate with N measurements and estimation error covariance equations. A window is usually needed in recursive estimation to ensure that the estimation error covariance does not become too small because a small estimation covariance makes the parameter estimates less sensitive to new measurements. A Kalman filter can also be used in recursive estimation. For the application at hand, the Kalman filter formulation simply formalizes the approach to the development of windows in recursive estimation.

We shall again start with the local model and develop an optimal Kalman filter noting the correlation between successive measurements. One formulation is as follows.

$$T_n = T_{n-1} + \eta_n$$

$$\zeta_n = \xi_{n-1} = v_{n-1}$$

$$\xi_n = v_n$$

$$\Delta z_{nm} = T_n \Delta\theta_n - \zeta_n + \xi_n \qquad (3.6)$$

The noise η_n is added to ensure that the Kalman filter does not start ignoring future measurements. The formulation of Equation (3.6) is interesting for two reasons. First, two additional state vectors are needed to model the correlation; secondly, in the extended formulation, there is no measurement noise.

The Kalman filter estimator for the model of Equation (3.6) takes the form

$$\hat{T}_n = \hat{T}_{n-1} + (\Delta z_{nm} - \hat{T}_n \Delta\theta_n - \hat{\zeta}_n) K_{1n}$$

$$\hat{\zeta}_n = \hat{\xi}_{n-1} + K_{2n}(\Delta z_{nm} - \hat{T}_n \Delta\theta_n - \hat{\zeta}_n)$$

$$\hat{\xi}_n = \Delta Z_{nm} - \hat{T}_n \Delta\theta_n - \hat{\zeta}_n \qquad (3.7)$$

K_{1n} is a gain vector (row) and K_{2n} is a scalar. These gains are obtained by solving the covariance equations. These covariance equations must be solved in real-time, in general, because the measurement equations involve the input distribution matrix $\Delta\theta_n$. The window size is controlled by selecting covariances of noise sources η_n and v_{n+1}. The estimator is usually simplified by using the assumption of uncorrelated measurement noise in Δz_{nm}.

$$\hat{T}_n = \hat{T}_{n-1} + (\Delta z_{nm} - \hat{T}_n \Delta\theta_n) K_{1n} \qquad (3.8)$$

Estimation Error Analysis

The error in the estimate of T_n depends on the measurement noise covariance v_n, assumed covariance of w_n, and the estimation procedure. The error covariance for the exact procedure of Equation (3.7) can be determined by solving the covariance equations corresponding to the Kalman filter. Usually, the error covariance will be computed for the T matrix one row at a time.

The estimator model of Equation (3.8) will give larger estimation errors than those obtained from the optimal estimation of Eq. (3.7) (computed for a single measurement and one row at a time). In the following, it is useful to consider T_n as a row vector:

$$\tilde{T}_n^T = \tilde{T}_{n-1}^T - K_{1n}^T \Delta\theta_n^T \tilde{T}_{n-1}^T - K_{1n}^T \xi_n + K_{1n}^T \zeta_n \qquad (3.9)$$

$$= (I - K_{1n}^T \Delta\theta_n^T)\, \tilde{T}_{n-1}^T - K_{1n}^T \xi_n + K_{1n}^T \zeta_n$$

Let

$$\sum_n = \text{Covariance} \begin{bmatrix} \tilde{T}_n^T \\ \zeta_n \\ \xi_n \end{bmatrix} \qquad (3.10)$$

Then

$$\sum_n = \Phi_{n-1} \sum_{n-1} \Phi_{n-1}^T + V_{n-1} \qquad (3.11)$$

where

$$\Phi_n = \begin{bmatrix} (I - K_{1n}^T \Delta\theta_n^T) & K_{1n}^T - K_{1n}^T & \\ 0 & 0 & I \\ 0 & 0 & 0 \end{bmatrix} \qquad (3.12)$$

$$V_n = \begin{bmatrix} 0 & 0 & 0 \\ 0 & 0 & 0 \\ 0 & 0 & E(v_n v_n^T) \end{bmatrix} \qquad (3.13)$$

Equation (3.11) is solved to determine the error in the estimation of the transfer matrix, T, using the simplified Kalman filter of Equation (3.8). This estimation error covariance depends on K_{1n} $\Delta\theta_n$ and measurement noise. These error covariances must be compared with the optimal Kalman filter (3.7) to determine if the simplified filter is adequate for vibration control.

3.1.2 Time-Domain Model Identification

3.1.2.1 Rotorcraft Model Development

A general linear model of a helicopter about a trim condition may be written as

$$\dot{x} = F(\psi)x + G(\psi)u \qquad (3.14)$$

where x is the state vector, which may include position, velocity, angles, angular rates, rotor states and flexible modes. u is the control input vector, and ψ is the azimuth location of a reference point on the rotor with respect to a reference point in the fixed frame. Also

$$\dot{\psi} = \Omega \qquad (3.15)$$

where Ω is the rotor speed. For a constant speed rotor, $\psi = \Omega t$. Hence, Equation (3.14) is periodic with respect to time with periodicity Ω. Outputs y may be written similarly as follows.

$$y = H(\psi)x + D(\psi)u + w \tag{3.16}$$

where w is the open-loop uncontrolled vibration.

A linear helicopter model valid in the neighborhood of the $N\Omega$ vibration frequency can be developed in many different ways (N is the number of blades on the rotor). One approach simply computes the $N\Omega$ sine and cosine components of the output, y, without any input and then with sine and cosine inputs at $N\Omega$. The data collected in this form may be used together with the model transformation of Section 2.3 to get an approximate time domain representation. N/rev inputs produce higher harmonic responses at $2N\Omega$, $3N\Omega$, ..., etc., which are essentially ignored. This approach gives the transfer matrix formulation utilized for much work on higher harmonic control [2]. The formulation ignores the transients caused by changes in control levels at higher harmonic frequencies. Thus, controls based on these models must have update intervals much longer that the transient time constant. Johnson [3] proposes a more sophisticated model which partially accounts for control transients.

$$z_n = \sum_{i=1}^{N} a_i z_{n-i} + \sum_{i=0}^{N} T_i \theta_{n-i} \tag{3.17}$$

where z_n represents the sine and cosine components at $N\Omega$ in the output.

The time-domain representation is simplified in two stages. First, modes which are very far from the vibration frequency are eliminated through model reduction. Several methods are available to achieve this model reduction. Secondly, if the inputs is of the form $u = u_o \cos(N\Omega t + \phi)$ and we are interested in the responses at and around $N\Omega$, above equations can be simplified to a time invariant model, which well be written as

$$\dot{x} = Fx + Gu + \Gamma w(N\Omega t) \tag{3.18}$$

$$y = Hx + Du \tag{3.19}$$

Note that all matrices in Eq. (3.18) and (3.19) will, in general, be functions of ψ. In the above derivation, we assume that u_o and ϕ are constant or slowly time-varying.

The model of Equations (3.18) and (3.19) can be identified using the maximum likelihood approach. The maximum likelihood approach selects model parameters F, G, H and D by minimizing the likelihood function, which is a function of the innovations sequence and the estimated innovations covariance. The likelihood function is defined as follows:

$$L = \sum_{k=1}^{n} \nu_k^T B^{-1} \nu_k \tag{3.20}$$

where ν_k, $k = 1, 2, \ldots, n$ is the innovation sequence and B is the estimated innovations covariance. The matrix B can be considered as a weighting matrix. The innovations are obtained from a state estimating Kalman filter (chapter 13, Ref. [9]).

If the maximum likelihood described above is used for estimation, the resulting model will have all the rotorcraft modes, which are excited by the inputs and measured by the instruments. Since the model is desired around the N/rev vibration frequency, the maximum likelihood method should be extended such that innovations in the region of the vibration frequency are given a higher weighting (innovations correspond to differences between the estimated model and the measurements). This can be achieved by reformulating the likelihood function in the frequency domain by using Parseval's theorem.

$$L(j\omega) = \sum_{i=-\omega_{max}}^{\omega_{max}} \nu_i^*(j\omega)\, B^{-1}\, \nu_i(j\omega) \tag{3.21}$$

where ν_i is the Fourier transform of the innovations and ν_i^* is its complex conjugate. To emphasize errors in the neighborhood of the N/rev frequency the likelihood function should be extended to include a frequency varying term $s(j\omega)$, where $s(j\omega)$ is large at N/rev and small elsewhere.

$$L(j\omega) = \sum_{i=-\omega_{max}}^{\omega_{max}} [\nu_i^*(j\omega)\, B^{-1}\, \nu_i(j\omega)]\, s(j\omega) \tag{3.22}$$

$s(j\omega)$ is, thus, a weighting function. Selection of $s(j\omega)$ will determine model fidelity (e.g., frequency range over which the model is valid, complexity (e.g., model order), and estimation error. An example of $s(j\omega)$ is

$$s(j\omega) = \frac{\omega^2}{(\omega_v^2 - \omega^2 + .1\ \omega\omega_v)^2}$$

The extended maximum likelihood method can be implemented using the following algorithm.

Step 1: Define a new innovation $\bar{\nu}$ as

$$\bar{\nu}_i(j\omega) = \nu_i(j\omega)\ s^{1/2}(j\omega) \qquad (3.23)$$

Step 2: Develop a Kalman filter whose outputs are $\bar{\nu}_i(j\omega)$. Since the model is linear, any frequency shaping applied to $u(j\omega)$ and $y(j\omega)$ will lead to the same shaping in the innovations.

Step 3: Pass u and y through a filter represented by $s^{1/2}(j\omega)$.

Step 4: Use these modified u and y for parameter estimation. This procedure is shown in Figure 3-2.

3.1.2.2 Model Form and Model Order Selection

The model form used in identification can be quite general. In particular, the specific forms for F, G, Γ, H and D can be selected for any canonical structure, which can be described as a general set of linear input-output relationships. Three of the forms are shown here. Each of these structures represents a state model with minimum number of parameters for a given model order.

Controllable Canonical Form

$$F = \begin{bmatrix} 0 & 1 & 0 & \cdots & 0 \\ 0 & & \ddots & & \vdots \\ \vdots & & & \ddots & \vdots \\ \vdots & & & & 0 \\ 0 & \cdots & \cdots & 0 & 1 \\ x & x & x & \cdots & x \end{bmatrix}, \quad G = \begin{bmatrix} 0 & x & \cdots & x \\ 0 & x & \cdots & x \\ \vdots & \vdots & & \vdots \\ \vdots & \vdots & & \vdots \\ \vdots & \vdots & & \vdots \\ 1 & x & \cdots & x \end{bmatrix} \quad (3.24)$$

H is general

Real Diagonal Form

$$F = \begin{bmatrix} \begin{bmatrix} x & x \\ x & x \end{bmatrix} & \begin{matrix} 0 \\ 0 \end{matrix} & \cdots & \begin{matrix} 0 \\ 0 \end{matrix} \\ \begin{matrix} 0 & 0 \end{matrix} & \begin{bmatrix} \ddots \end{bmatrix} & & \begin{matrix} 0 \\ \vdots \end{matrix} \\ \vdots & & \begin{bmatrix} \ddots \end{bmatrix} & \begin{matrix} \vdots \\ 0 \end{matrix} \\ \begin{matrix} 0 & 0 \end{matrix} & \cdots & \begin{matrix} 0 \end{matrix} & \begin{bmatrix} x & x \\ x & x \end{bmatrix} \end{bmatrix} \quad G = \begin{bmatrix} 0 & x & \cdots & x \\ 1 & x & & x \\ 0 & x & & x \\ 1 & x & & x \\ \vdots & \vdots & & \vdots \\ \vdots & \vdots & & \vdots \\ \vdots & \vdots & & \vdots \\ 0 & x & & x \\ 1 & x & & x \end{bmatrix} \quad (3.25)$$

H is general

Autoregressive Moving-Average (ARMA) Form

If y is the output and u is the input, a discrete ARMA form is similar to Equation (3.17) except the outputs are used directly rather than the harmonic components at $N\Omega$.

Suitable model order depends on the required model fidelity and the nature of helicopter dynamics in the neighborhood of $N\Omega$. Many tests have been proposed for selection of model order [10]. If the ARMA-type representation is used, an adaptive ladder filter might be suitable to select model order [11]. The baseline approach is to overspecify the model

order. The extra poles generally cancel the extra zeros in the identified model.

Selection of Model From for Time-Domain Vibration Control Design

The autoregressive moving average form and controller canonical form have larger universal errors than the real diagonal form. Thus, they are suitable when the time-domain rotorcraft model needed for vibration control is of low order. The maximum desired order for these forms depends on the accuracy of the computer used for system identification and to implement vibration control, but will usually be less than ten. The numerical conditioning in the real diagonal form does not degrade with increasing model order. Thus, this form is preferred when a higher order rotorcraft model is desired.

Simple identification algorithms may be used with controller canonical and autoregressive moving-average (ARMA) forms. If significant structural modes move around the vibration frequency as the flight condition is varied, the model order may have to be estimated in real-time. Simple algorithms exist to estimate model order for ARMA forms [11].

Recent work in ladder-form realizations of ARMA models provides an approach to alleviate numerical conditioning problems in ARMA models.

3.1.2.3 Estimation Error Control

The estimation error will be controlled by selecting a time record over which the model for the helicopter does not change appreciably and by choosing the filter in Equation (3.23), such that its bandwidth is neither too narrow nor too broad. If the filter is too narrow (in the limit a single discrete frequency), the level of the signal is decreased and the estimation error increases. If the filter is too wide, the signal includes dynamics of no interest to the vibration control problem. Even though a theoretical analysis can be performed to analyze the effects of filter bandwidth on estimation error (see Section 3.1.2.4), the selection of the bandwidth will vary from one rotorcraft to another. The selection will be

guided by the frequencies of structural modes, sensor errors, variations in rotor speed and rotorcraft transient behavior in gusts and turbulence.

3.1.2.4 Error Analysis

The error in estimate of the model order and system parameters is determined by postulating a true model, the noise sources and the range of frequencies over which the model is desired.

Let the true model be described in terms of the response of the helicopter to sinusoidal inputs at various frequencies. For any flight condition, the rotorcraft response amplitude and phase at each frequency depends on input amplitude as well as phase because the rotorcraft has a nonlinear behavior. Mathematically, the true model is of the form

$$y(j\omega) = T_t(j\omega, u(j\omega)) + \text{noise} \tag{3.26}$$

The noise is a combination of sensor errors and gusts. We shall assume that a linear model of the following form is desired.

$$y_m(j\omega) = T_m(j\omega,p)\ u(j\omega) \tag{3.27}$$

where a parameter vector p will be selected to best fit the measured response. We can define a new error term to combine the process and measurement noise and the differences in model form

$$y(j\omega) = T_m(j\omega,p)\ u(j\omega) + n(j\omega) \tag{3.28}$$

Let $N(j\omega)$ be the spectrum of process and measurement noise and modeling error. Since we are primarily interested in behavior around the vibration frequency, significantly more weighting will be given to the model accuracy about that frequency. Let the weighting matrix be $W(j\omega)$.

The signals y and u are passed through a filter with response $F(j\omega)$ prior to minimization; therefore, the parameter estimation problem involves minimization of the following with respect to p.

$$\frac{1}{2}\int_{\omega} F(j\omega)y(j\omega)-T_m(j\omega,\hat{p})F(j\omega)u(j\omega)\ {}^{*}R\ F(j\omega)y(j\omega)-T_m(j\omega,p)F(j\omega)u(j\omega)\ d\omega \tag{3.29}$$

where $(.)^*$ represents the complex conjugate of $(.)$ and R is a frequency independent weighting matrix. For optimization, the derivative of the above with respect to p is zero (remember that $F(j\omega)$ is a scalar). By substituting for y from Equation (3.28) into Equation (3.29) we get:

$$\int_{\omega}\left[\frac{\partial(T(j\omega,\hat{p})u}{\partial p}\right]^{*}(F^{*}(j\omega)RF(j\omega))\left[(T_m(j\omega,p)-T_m(j\omega,\hat{p}))\ u(j\omega)+n(j\omega)\right]d\omega = 0 \tag{3.30}$$

Expanding $T_m(j\omega,p)$ in a Taylor series

$$T_m(j\omega,p) = T_m(j\omega,\hat{p}) + \frac{\partial T_m(j\omega,\hat{p})}{\partial\hat{p}}\ \Delta p \tag{3.31}$$

We get (dependence on $j\omega$ is implied)

$$\underbrace{\int\left[\frac{\partial T_m u}{\partial\theta}\right]^{*}(F^{*}RF)\ \frac{\partial T_m u}{\partial p}\ d\omega}_{A}\ \Delta p + \underbrace{\int\left(\frac{\partial(T_m u)}{\partial p}\right)^{*}(F^{*}RF)\ n(j\omega)d\omega}_{B} = 0 \tag{3.32}$$

i.e., $A\ \Delta\ p + \int B(j\omega)\ n(j\omega)d\omega = 0$

The covariance of $\Delta\ p$ is

$$E\ (\Delta p\ \Delta p^{T}) = A^{-1}\int B(j\omega)\ N(j\omega)\ B^{*}(j\omega)d\omega\ A^{-1} \tag{3.33}$$

It is possible to show that the estimation error is minimized if $F(j\omega)$ is selected such that (see Appendix B).

i.e., $R^{1/2}\ F(j\omega) \approx [N(j\omega)]^{1/2}$ (3.34)

The symmetric square root is taken for $N(j\omega)$. Note that $F(j\omega)$ is a scalar, while the $N(j\omega)$ is a matrix. This equality cannot be realized in practice unless we consider one measurement at a time.

3.2 ROBUSTNESS

The robustness of both the frequency-domain and the time-domain vibration control laws are analyzed. The stability and the performance results are studied first for a fixed gain controller. Stability conditions for a controller where parameters are identified in real-time are very difficult to analyze and are the subjects of intense research in control theory [13].

3.2.1 Frequency-Domain Controller

In this analysis, we assume that the correct model for helicopter multicyclic vibration output for time interval n is written as

$$z_n = T\theta_n + z_0 \tag{3.35}$$

where z, θ and z_0 are the vectors of sin and cosine components of closed loop vibration, applied input and open-loop vibration. T is the transfer matrix. We consider two controllers

$$\text{Controller 1:} \quad \theta_n = -G_n \hat{z}_{0,n-1} \tag{3.36}$$

$$\text{Controller 2:} \quad \Delta\theta_n = -G_n z_{n-1}$$

$$\theta_n = \theta_{n-1} + \Delta\theta_{n-1} \tag{3.37}$$

$z_{0,n-1}$ represents the estimated open-loop vibration at time $n-1$. z_{n-1} is the measured closed-loop vibration. The first controller may be referred to as the open-loop control law while the second has the closed-loop form. In

the following section, stability and noise sensitivity of each of these controllers is analyzed.

Stability Conditions for Fixed Gain

In a fixed-gain controller G_n is constant. To analyze the stability of the open-loop control law, it is necessary to study variations in z_0 caused by pilot inputs, gusts, and changes in flight conditions. Let z_{0_n}, $\hat{z}_{o_n}$ and $\tilde{z}_{o_n}$ be the true, the estimated and the estimation error in open-loop vibration at cycle n.

$$\hat{z}_{0_n} = z_{0_n} + \tilde{z}_{0_n} \tag{3.38}$$

then,

$$z_n = T(-G_n(z_{0_{n-1}} + \tilde{z}_{0_{n-1}})) + z_{0_n} = z_{0_n} - TG_n z_{0_{n-1}} - TG_n \tilde{z}_{0_{n-1}} \tag{3.39}$$

For constant open-loop vibration, z_{0_n}

$$E(z_n) = (I-TG)z_0 - TG\ E(\tilde{z}_{0_{n-1}}) \tag{3.40}$$

If the bias error in the estimation of z_{0_n} is zero, then the average value and variance of the residual vibration are given by the following equations:

$$E(z_n) = (I-TG)z_n \tag{3.41}$$

$$\text{Var}\ (z_n) = Z_n = TG\ E(\tilde{z}_{0_{n-1}} \tilde{z}_{0_{n-1}}^T)G^T T^T = TG\ N_{n-1}\ G^T T^T \tag{3.42}$$

where N_{n-1} is the variance of the estimation error in open-loop vibration. The mean value of the vibration is small if $(I-TG)$ is small. If T were square and invertible, G could be selected to be T^{-1} to reduce the mean value of vibration to zero. The same would also hold if T had more

columns than rows and it were full rank. In addition, the closed-loop vibration level is proportional to the estimation error in open-loop vibration.

With a constant G, the open-loop controller will not become unstable as long as $\tilde{z}_{0_{n-1}}$ is uncorrelated with z_{n-1}. A poor selection of G will lead to insufficient vibration reduction or even an increase of vibration.

Correlation between $\tilde{z}_{0_{n-1}}$ and z_{n-1} can be analyzed as follows. If A represents the projection of $\tilde{z}_{0_{n-1}}$ on z_{n-1}, then $\tilde{z}_{0_{n-1}}$ can be written in the form

$$\tilde{z}_{0_{n+1}} = Az_{n+1} + \text{noise} \tag{3.43}$$

where the additive noise does not correlate with z_{n-1}. Equation (3.42) then modifies to

$$Z_n = TGAZ_{n-1}A^T G^T T^T + \text{additional term} \tag{3.44}$$

This equation is stable if the eigenvalues of TGA have absolute value less than one. Since TG is of unit order and A must be much smaller than one to ensure system stability.

The basic dynamics of the closed-loop helicopter vibration control law is obtained by substituting the control law of Equation (3.37) in the dynamic model of Equation (3 35).

$$z_n - z_{n-1} = T\Delta\theta_n = -TG\, z_{n-1} \tag{3.45}$$

If z_{n-1} is estimated without error, the stability of the closed-loop dynamics depends upon the following

$$\text{Abs (eig(I-TG))} = \text{Abs (1-eig(TG))} \leq 1$$

The eigenvalues of TG must lie within the unit circle shown in Figure 3-3. If the number of outputs to be controlled exceeds the number of available inputs, TG is rank deficient and some of its eigenvalues are at the

origin. The difference between the number of inputs and outputs is the number of zero eigenvalues (Figure 3-3).

To understand the stability conditions, it is necessary in particular to analyze the behavior of the eigenvalues of TG, that are not at the origin. The eigenvalues at origin will stay there because the rank of TG can never exceed the rank of t for any value of G. Suppose first that T is known exactly and that the G is selected to minimize the vibration to the extent feasible

$$G = (T^TQT)^{-1}\ T^TQ \tag{3.46}$$

where Q is a weighting matrix.

$$TG = T(T^TQT)^{-1}T^TQ$$

$$(TG).(TG) = (T(T^TQT)^{-1}T^TQ)(T(T^TQT)^{-1}T^TQ) = T(T^TQT)^{-1}T^TQ = TG \tag{3.47}$$

For any matrix where $(.)^2 = (.)$, every eigenvalue is zero or one [12]. The right eigenvectors of the eigenvalues at unity lie in the subspace of T, e.g., they represent the parts of the vibration which are directly controlled from the input.

$$(TG)T = [T(T^TQT)^{-1}T^TG]\ T = I.T \tag{3.48}$$

and the left eigenvectors lie in the subspace of T^TQ. The right and left eigenvectors for unit eigenvalues describe errors in T that cause the largest perturbation in closed-loop eigenvalues. This will be discussed next. Using the small matrix perturbation theory, the perturbation in the eigenvalues of T at unity based on perturbation in G is given by [12].

$$\Delta\lambda = (T^TQT)^{-1}[T^TQ(T\Delta G)T] = \Delta GT \tag{3.49}$$

If $\hat{T}$ the estimate of T is written as

$$\hat{T} = T-\Delta T \tag{3.50}$$

then

$$\Delta G = (T^TQT - \Delta T^TQT - T^TQ\Delta T + \Delta T^TQ\Delta T)^{-1} (T^T+\Delta T^T)Q - (T^TQT)^{-1}T^TQ$$

$$= (T^TQT)^{-1} \Delta T^TQ - (T^TQT)^{-1} (\Delta T^TQT+T^TQ\Delta T)(T^TQT)T^TQ \qquad (3.51)$$

Ignoring second and higher order terms in ΔT . Therefore

$$\Delta\lambda = -(T^TQT)^{-1} T^TQ\Delta T \qquad (3.52)$$

The perturbation in eigenvalue therefore depends on error in estimating the transfer matrix as well as the condition of T^TQT. If T^TQT is nearly singular a small relative change in ΔT can cause a very large perturbation in the eigenvalues.

One approach to reduce the sensitivity is to add a positive definite matrix to (T^TQT) in the expression for G. This gives the more common control gain

$$G = (T^TQT+A)^{-1} (T^TQ+B) \qquad (3.53)$$

Now TG has the same number of eigenvalues at the origin since the ranks of T and G have not changed. The remaining eigenvalues are not necessarily at unity. To ensure that the remaining eigenvalues are at unity A and B are related as follows (with this condition TG . TG = TG).

$$BT = A \qquad (3.54)$$

This appears to be a good choice since it places the eigenvalues farthest away from the unit circle. The effect of a small perturbation with the above condition on the eigenvalues of TG is as follows

$$\Delta\lambda = (T^TQT+A)^{-1} (T^TQ+B)\Delta T \qquad (3.55)$$

If A is selected properly the condition number of the matrix to be inverted can be improved leading to more robustness.

Other Modeling Errors

In the previous analysis, only errors in T were studied and the model $\Delta Z = T\Delta\theta_k$ was assumed to be the true model. In rotorcraft there is one more error source introduced by pilot and gust inputs. These inputs change the uncontrolled vibration level. Let us then assume that the true model is of the form

$$\Delta z_k = T\Delta\theta_k + \Delta z_{ok} \tag{3.56}$$

Note that Δz_{ok} represents the difference between the uncontrolled vibration level over two consecutive control updates and can be thought of as the rate of change of the uncontrolled vibration. This error can be very large if the pilot input or gust spectrum has frequency content in the neighborhood of the control update rate, even if the actual variation in uncontrolled open-loop vibration is small. The closed loop dynamics are

$$\Delta z_k = -TG\, z_{k-1} + \Delta z_{ok} \tag{3.57}$$

$$z_k = (I-TG)z_{k-1} + \Delta z_{ok} \tag{3.58}$$

If Δz_{ok} has frequency components near the poles of $(I-TG)$, then the open-loop variation Δz_{ok} can be further amplified in the closed loop vibration z_k in the steady state. This could seriously degrade the performance of the closed-loop control law, if the natural frequencies of the external vibration matches the closed loop frequency.

3.2.2 Time-Domain Controller

The robustness of the time domain controller is analyzed most effectively by using robustness theory which is most effectively applied in the frequency domain. Let $G(j\omega)$ and $C(j\omega)$ represent the transfer function equivalents of the rotorcraft and the vibration controller in the frequency domain (see Figure 3-4). The closed-loop system of Figure 3-4 is stable if the encirclement count of the map $\det[I + G(j\omega)\, C(j\omega)]$ around

the origin, evaluated on the Nyquist contour equals the number of unstable poles of GC [14].

Assume now that the controller is stable for the nominal plant. Let $G_p(j\omega)$ represent the set of perturbed plant transfer function, which may be written as

$$G_p(j\omega) = (I + \varepsilon\, \Delta G(j\omega))\, G(j\omega) \tag{3.59}$$

where $0 \leq \varepsilon \leq 1$. It is easy to show [13] that the closed-loop system is stable if

$$\bar{\sigma}\, [G(j\omega)\, (I + G(j\omega)\, C(j\omega))^{-1}] < 1/\, \bar{\sigma}\, (\Delta G(j\omega)) \tag{3.60}$$

for all $0 \leq \omega \leq \infty$ where $\bar{\sigma}(.)$ represents the maximum singular value of a matrix. The above equation represents a sufficient condition but not one that is necessary. Therefore, it may represent a conservative bound. Nevertheless, structure of the inequality is a major aid in understanding the robustness of the time domain controller.

The time domain vibration controller is designed such that $C(j\omega)$ has a complex pole pair at $\pm j\omega_v$. Therefore, $C(j\omega)$ is theoretically infinite in the neighborhood of the vibration frequency. It has been observed that the optimal control formulation selects controller transfer function such that $G(j\omega_v)\, C(j\omega_v)$ is nearly real and positive. If we assume that $G(j\omega)$ is a stable transfer function, then because of the frequency-shaping selected in the vibration controller design, $C(j\omega)$ will be small away from the vibration frequency. The Bode and Nyquist charts for the vibration controller will then be as shown in Figure 3-5. Because of the phase behavior at the vibration frequency and a small closed-loop gain elsewhere, the Nyquist chart will be mostly to the right of +1. This shows that the phase angle of the rotorcraft transfer function must change by about 90° in the neighborhood of the vibration frequency before the controller becomes unstable.

3.3 TRANSIENT RESPONSE

The transient response of the vibration control system determines the rate at which the initial vibration and the effect of gusts and other disturbances are eliminated. A fast transient response is desirable consistent with good steady-state performance, stability and robustness. This section shows achievable transient response settling times with both the frequency-domain and the time-domain controllers.

The transient settling time will be combination of the time required for system identification and for feedback control assuming both are performed on-line. The delay in each of the two steps should be isolated to understand the weak elements in obtaining fast response.

Transient requirements can be very stringent. In a gusty environment the transient settling times should be much shorter than the correlation times of the gust field. Otherwise vibration caused by gust inputs will never be reduced or eliminated.

3.3.1 Frequency-Domain Approach

The control input in the frequency domain approach is updated after several vibration cycles (typically once per rev or four vibration cycles for a four-bladed rotor). The control update sampling rate is therefore once per several vibration cycles. Thus, any disturbance which changes vibration may take at least one rotor cycle before compensation starts.

The transient response of a discrete update system is defined by the eigenvalues of the closed-loop dynamics matrix. The slowest component of the closed loop response corresponds to the largest eigenvalue of the closed loop dynamic matrix (except the eigenvalues on the unit circle).

$$\lambda max = |\lambda max\ (I-TG)| \tag{3.61}$$

If τ is the update time, the vibration will be reduced to within 5% of the steady state value in

$$\ln(.05)*\tau/\ln(\lambda max) + \text{average delay in update} = -3\tau/\ln(\lambda max) + \tau/2$$

$\tau/2$ represents average delay between the update intervals.

The key, therefore, is to keep the eigenvalues of $(I-TG)$ as close to zero as possible. That requires an accurate knowledge of the transfer matrix T because the value of the gain G is computed using the estimated value of T. Thus, if T were in error the eigenvalues of $(I-TG)$ will be nonzero.

3.3.2 Time-Domain Approach

Let the open-loop input-to-output and disturbance-to-output models for the helicopter be $G(j\omega)$ and $G_d(j\omega)$. The vibration controller is designed with transfer function $C(j\omega)$.

The closed-loop disturbance response is

$$G_d(I+GC)^{-1} \tag{3.62}$$

In the time domain approach the measurements are passed through an undamped filter with frequency at $\pm j\omega_v$. If the measurements are y, the output of the filter is (see Equation 2.11)

$$\xi = \frac{1}{s^2 + \omega_v^2}\, y$$

and the control law may be written as (see Equation 2.14)

$$u = C_1 x + C_2 \xi + C_3 \dot{\xi}$$

Let the transfer function between the estimated state and the output, y, be $T_f(s)$. Then

$$u = \left[C_1 T_f(s) + \frac{(C_2 + C_3 s)}{\omega^2 + \omega_v^2} \right] y$$

$$= \left[\frac{C_1 T_f(s)(s^2 + \omega_v^2) + (C_2 + C_3 s)}{s^2 + \omega_v^2} \right] y$$

Since C has a pole pair at $\pm j\omega_v$, $(I+GC)^{-1}$ has a zero pair there. The closed-loop design places a pole pair approximately at $-\sigma \pm j\omega_v$. Assuming that there are no rotorcraft poles in the neighborhood of the vibration frequency, the closed-loop behavior for vibration disturbances can be approximated to

$$G_d(I+GC)^{-1} \underset{\omega \to \omega_v}{\approx} \frac{K(s^2+\omega_v^2)}{(s^2+2\xi\omega_v s+\omega_v^2)} \tag{3.63}$$

where K is some gain. The response of the closed-loop system to input $\cos(\omega_v t)$ is

$$K \exp(-\xi_v \omega_v t)\,[\cos(\omega_v t) + \xi_v \sin(\omega_v t)] \tag{3.64}$$

Thus, the time constant for the vibration to reduce to within 5% of the steady state value is

$$\frac{3}{(\xi_v \omega_v)} \tag{3.65}$$

Thus, if $\omega_v = 100$ rad sec^{-1} and $\xi_v = 0.1$, the vibration will be reduced to within 5% of the steady state value within .3 sec.

This may seem to imply that the convergence time can be reduced arbitrarily by increasing ξ_v. Increasing ξ_v, however, expands the range around ω_v where the closed-loop gain is large. This will make the system less robust with respect to modeling errors far away from the vibration frequency.

3.4 SUSCEPTIBILITY TO NOISE

The rotorcraft is subject to a variety of disturbances. For the purpose of studying the behavior of vibration reducing control laws, all external or internal inputs applied to the rotorcraft away from the N/rev frequency will be considered as unwanted disturbances.

This section describes typical rotorcraft disturbances and then analyzes the effects of these disturbances on the behavior of closed-loop vibration control systems.

2.4.1 Rotorcraft Disturbances

Three classes of rotorcraft disturbance inputs are of interest:

(a) external gust and turbulence inputs;

(b) pilot and stability augmentation system (SAS) inputs, and;

(c) measurement noise sources.

We shall describe each of these disturbance sources to study their effects on rotorcraft vibration controller.

External gust and turbulence are stochastic inputs in the low frequency region of the spectrum. Assuming a Dryden or VonKarman spectra, the flow field variations apply a random force and moment input to the rotorcraft. Most of the power in the spectra is typically below 1/2 Hz. Gusts and turbulence affect the flow field around the rotor leading to an increase in the open-loop vibration level. The affected flow field may also impact the transfer matrix between the N/rev inputs and the associated rotorcraft responses. The major effect is likely to be the change in the open-loop vibration level.

The pilot inputs are deterministic time functions whose spectrum is mostly limited to one Hz or less. These inputs can also change the open-loop vibration significantly and affect the transfer matrix temporarily. Pilot inputs may also produce significant changes in flight condition which have more permanent effects on open-loop vibration and transfer matrices. The pilot inputs can cause a low-frequency modulation of the open-loop vibration level. Such modulation places demanding requirements on the vibration control algorithms.

Measurement noise is a combination of random and systematic error sources like bias and scale factor errors.

In the following, we will analyze the effects of each of these errors on closed-loop rotorcraft performance.

3.4.2 Frequency-Domain Approach

Let the average open-loop vibration in the absence of gusts and pilot inputs be $w_0\cos(\omega_v t+\phi)$ where w_0 is the vibration amplitude and ϕ is an arbitrary phase angle. The effects of pilot, SAS and gust inputs is represented as a time-dependent $w_0(t)$. The measurement noise is modeled as a random additive term, v. The $w_0(t)$ has spectrum mostly in the low frequency region.

Consider a discrete implementation, where the vibration frequency is ω_v rad $\sec^{-1}$ and the data is sampled at n points per vibration cycle. Thus, the sampling rate is $n\omega_v/2\pi$ per second and the sampling interval is written as

$$\Delta = \frac{2\pi}{n\omega_v} \tag{3.66}$$

The ith time domain sample in the measurement is given by

$$y_i = w_o\left(\frac{2\pi i}{n\omega_v}\right)\cos\left(\frac{2\pi i}{n} + \phi\right) + v_i \tag{3.67}$$

The sin and cosine components at the vibration frequency are determined as follows (assuming the averaging is done over kth vibration cycle)

$$\begin{aligned} z_{c_k} &= \frac{2}{n}\sum_{i=1}^{n}\left[y_i\cos(2\pi i/n)\right] \\ &= \frac{2}{n}\left[\sum_{i=1}^{n} w_o\left(\frac{2\pi i}{\omega_v n}\right)\cos\left(\frac{2\pi i}{n}+\phi\right)\cos\left(\frac{2\pi i}{n}\right)\right. \\ &\quad \left. + \sum_{i=1}^{n} n_i\cos\left(\frac{2\pi i}{n}\right)\right] \\ &= \frac{1}{n}\left[\sum_{i=1}^{n} w_o\left(\frac{2\pi i}{\omega_v n}\right)\cos\phi + \cos\left(\frac{4\pi i}{n}+\phi\right)\right. \\ &\quad \left. + 2\sum_{i=1}^{n} n_i\cos\frac{2\pi i}{n}\right] \end{aligned}$$

$$= \frac{1}{n}\left[\cos\phi \sum_{i=1}^{n} w_o\left(\frac{2\pi i}{\omega_v n}\right) + \sum_{i=1}^{n} w_o\left(\frac{2\pi i}{n}\right)\cos\left(\frac{4\pi i}{n} + \phi\right)\right.$$

$$\left. + 2\sum_{i=1}^{n} n_i \cos\left(\frac{2\pi i}{n}\right)\right] \qquad (3.68)$$

All the summations in the above equations are taken with i varying from $(k-1)n$ to kn. If there were no error sources, the result would be $\cos\phi$. The first two terms produce deterministic errors while the last term gives random errors.

To understand the effects of pilot inputs, consider w_o to be a single low-frequency sine wave. The effect of a general w_o can be determined by superposition

$$w_o(t) = \cos(\omega_d t + \psi) \qquad (3.69)$$

where ψ is phase at the initial time. The three terms in equation (3.68) are simplified as follows:

First Term:

$$\sum_{i=(k-1)n+1}^{kn} w_o \frac{2\pi i}{\omega_v n} = \sum_{i=(k-1)n+1}^{kn} \cos\left(\frac{2\pi i \omega_d}{n\omega_v} + \psi\right)$$

$$\approx \frac{n\omega_v}{\pi\omega_d} \sin\left(\frac{\pi\omega_d}{\omega_v}\right) \sin\left(\frac{\pi\omega_d}{\omega_v} + \frac{2\pi(k-1)\omega_d}{\omega_v}\right)$$

$$\approx n \sin\left(\frac{\pi\omega_d}{\omega_v} + \frac{2\pi(k-1)\omega_d}{\omega_v}\right) \quad \text{for} \quad \omega_d << \omega_v \qquad (3.70)$$

Second Term:

$$\sum_{i=(k-1)n+1}^{kn} w_o \left(\frac{2\pi i}{n}\right) \cos\left(\frac{4\pi i}{n} + \phi\right) = \sum_{i=(k-1)n+1}^{kn} \cos\left(\frac{2\pi\omega_d i}{\omega_v n} + \psi\right) \cos\left(\frac{4\pi i}{n} + \phi\right)$$

$$\approx 0 \quad \text{for} \quad \omega_d << \omega_v \tag{3.71}$$

Third Term:

This is a random noise term. Its mean value is assumed zero and the covariance is computed as follows (where r is the covariance of the random noise)

$$\text{cov}\left[\sum_{i=1}^{n} n_i \cos\frac{2\pi i}{n}\right]$$

$$= E \sum_{i=1}^{n} n_i^2 \cos^2 \frac{2\pi i}{n}$$

$$= r \sum_{i=1}^{n} \cos^2 \frac{2\pi i}{n}$$

$$= \frac{rn}{2} \tag{3.72}$$

because the expected value of a cosine wave over its entire cycle is one-half.

The noise in the harmonic cosine component (and similarly in the sine component) consists of two parts--a slowly varying function consisting of a sum of sine wave and random noise. The random noise increases the root-mean-square (RMS) residual vibration in the closed-loop and will impact the identification procedures to some extent. The first error term could cause major deterioration in identification accuracy because Δz_k could occur with zero $\Delta\theta_k$.

In addition to the additive noise in the measurement of the average open-loop vibration, pilot, SAS and disturbance inputs may also cause variations in the input to measured response transfer matrix. No analytical

models are available to determine the level of the changes in transfer matrix caused by a certain size gust input. These effects are difficult to analyze in the frequency domain formulation but could be significant in the performance of the overall controller.

3.4.3 Time-Domain Formulation

In the time domain formulation the model is

$$\dot{x} = Fx + Gu$$

$$y = Hx + Du + w \tag{3.73}$$

where w represents the time history of the open-loop vibration. Sampled measurements at n samples per vibration cycle are

$$y_{m_i} = Hx(i\Delta) + Du(i\Delta) + w(i\Delta) + v_i \tag{3.74}$$

where v_i is measurement noise. The controller is of the form

$$x_{c_{i+1}} = \phi_c x_{c_i} + G_c y_{m_i} \tag{3.75}$$

$$u(i\Delta) = H_c x_{c_i} + D_c y_{m_i} \tag{3.76}$$

The state equations for the system may also be sampled

$$x_i \triangleq x(i\Delta), \quad \text{etc.} \tag{3.77}$$

$$x_{i+1} = \phi x_i + G_d u_i \tag{3.78}$$

$$y_i = Hx_i + Du_i + w_i \tag{3.79}$$

In the time-domain formulation, the entire control law and system are defined by a set of linear differential or difference equations. Therefore

an appropriate Lyapunov equation needs to be solved to compute steady-state root-mean-square vibration levels [7]. The steady-state response could be determined more accurately by modeling w_i with an appropriate spectrum. An approximate analysis can also be performed in the continuous time-domain representation. Appropriate Lyapunov equations are easy to derive.

An adaptive controller or a real-time system identification implementation could have difficulties here because of the low frequency modulation of the open-loop vibration. This problem could be handled by updating the model only after several sample points, or by placing a lower confidence on previous open-loop vibration estimate.

3.5 IMPLEMENTATION CONSIDERATIONS

Three issues are important in implementation: (a) actuator requirements, (b) sensor requirements, and (c) computational capability. Any approach for active vibration reduction requires actuators which can produce sufficient deflection of the swashplate at the N/rev vibration frequency. Thus, similar actuators are needed for either approach. The only difference is that the commanded input at N/rev is changed in steps in the frequency-domain approach and smoothly in the time-domain approach. The sensor requirements are also similar in the two approaches. Thus, the major difference may arise because of the computation requirements required in the two approaches.

This section discusses specifically the number of computations which must be performed in real-time to implement frequency domain and time domain control laws. To develop a uniform approach to compare the two approaches, the following notation will be used

N = number of blades

n = number of samples per vibration cycle

m = number of measurement channels

q = number of independent inputs

3.5.1 Frequency-Domain Control Law

Table 3-1 shows the various steps in the frequency-domain control law. The number of computations required in an all-digital implementation are also shown. The computations are based on a Kalman filter parameter estimator and a continuous control formulation. The number of calculations required for other frequency-domain formulations is similar.

3.5.2 Time-Domain Control Law

Table 3-2 shows the number of calculations required for a time domain controller implemented in discrete form if all identification is performed off-line.

The additional number of calculations for on-line parameter estimation is given in Table 3-3 for various approaches which are applicable for helicopter vibration reduction (s is the number of state variables). These calculations include the control computation as well.

The fixed-gain time domain controller requires very few computations for implementation. The number of computations required for scheduled gain control law is also similar. The computation time will go up by a factor of s^2 where s is the number of states. Depending upon the complexity of the helicopter model and the possible presence of structural modes in the neighborhood of the vibration frequency, the increase could be an order of magnitude.

3.5.3 Comparisons

The time-domain approach requires fewer computations than the frequency-domain approach if a fixed gain (or scheduled gain) controller can be used in the time-domain formulation. The real-time computations are about the same for the time-domain and the frequency-domain controller if the model needed for the time domain control must be identified on-line.

SECTION 4
SIMULATION RESULTS

This section discusses simulation results. The results have been organized to address specific issues in the implementation and use of the time-domain and frequency-domain methods.

Section 4.1 describes the model used in the analysis of this chapter. The data is based on a wind-tunnel test performed at NASA 40 x 80 Foot Wind Tunnel. Every attempt has been made to obtain results with wide applicability. The procedure for comparison and evaluation is summarized

Section 4.2 covers system identification methods and results achievable under noisy conditions. The following section describes the effect of closing the control loop assuming model parameters are known. The simultaneous identification and control problem is discussed in Section 4.4. Section 4.5 gives a short summary.

4.1 HELICOPTER MODEL AND EVALUATION APPROACH

The model used in the analysis is based on helicopter vibration data collected in the NASA 40 x 80 Foot Wind Tunnel (McCloud and Chopra [15]). Table 4-1 shows transfer matrices calculated from experimental wind-tunnel data for the Kaman 7.02-m diameter rotor. It is a four-bladed rotor turning at 300 rpm giving the vibration frequency of 20 Hz. Higher harmonic control was applied through the controllable twist rotor. The data was collected with 2/rev, 3rev and 4/rev inputs in the rotating frame. For the purpose of our modeling we assume transfer matrices are available at 3/rev, 4/rev and 5/rev inputs. Note that the transfer matrix coefficients corresponding to the 2/rev input and the longitudinal response are very small and unreliable.

A state variable model was developed using the cosine and sine components of the response. ϕ, G, H and D matrices for one possible choice of the state variable model, which reproduces the transfer matrix,

are shown in Table 4-2. The model was used to simulate responses of the helicopter to multicyclic inputs. Discrete models are used throughout. Models based on the cosine components were used in design while models based on both sine and cosine components were used in validation.

In the analysis presented here, it is assumed that 4/rev vertical, lateral and longitudinal harmonics are measured every 6° of the rotor azimuth angle. Thus, 60 data points are collected for every rotor revolution or 15 points for every vibration cycle. The effect of measurement noise level on estimation accuracy is studied parametrically.

The frequency-domain and the time-domain approaches are compared on a one-to-one basis. The comparison consists of three parts:

(a) Identification step with no closed-loop control

(b) Control design step (assuming the model is estimated a priori), and

(c) Closed-loop controller with real-time identification and control.

The time domain formulation is based on the frequency-domain model obtained from the wind tunnel tests. The evaluation procedure, therefore, has been extended as shown in Figure 4-1 to accommodate this model form.

4.2 SYSTEM IDENTIFICATION

System identification techniques are used in the time domain and the frequency domain. The corresponding results are compared.

The 4/rev inputs are applied simultaneously in all channels in the nonrotating systems. The phase and amplitudes are changed randomly in all three channels at the end of each rotor cycle. The maximum amplitude is about .005 in the nondimensional units represented by the data (Figure 4-2). Data is collected for 25 rotor cycles giving a total of 1501 points over 5 seconds. Noise free rotorcraft response to this input is shown in Figure 4-3.

Noise free measurements are studied first. Then three cases with measurement noise and noise due to pilot inputs are evaluated. Thus, four cases are studied in all.

(i) Noise-free measurements (Figure 4-3)

(ii) Measurements with white random noise (noise RMS is 5% of the open-loop vibration level). The response is shown in Figure 4-4.

(iii) Measurements with white random noise (RMS is 25% of the open-loop vibration level). The corresponding measurements are given in Figure 4-5.

(iv) A 0.85 Hz pilot input or gust disturbance, which causes the open-loop uncontrolled vibration to vary ± 25% about its nominal open-loop value (0.85 Hz is selected to be less than 1 Hz and to not coincide with any of the vibration frequency subharmonics). The variation in open-loop vibration is shown in Figure 4-6a. The response of the rotorcraft is shown in Figure 4-6b.

4.2.1 Frequency-Domain Formulation

Cosine and sine components are extracted from the measured responses. Δz_k are computed from the sine and cosine responses. Note that one out of four vibration cycles is used for identification, because the rest of the vibration cycles are used to ensure that the output has reached steady state prior to measuring the response.

The correct transfer matrix as well as the estimated values after 25 cycles are shown in Table 4-3.

The rate at which parameters converge for 5% noise are shown in Figure 4-7 (two sample runs). A corresponding plot for 25% noise level is given in Figure 4-8. The convergence time can be more than one second.

4.2.2 Time-Domain Formulation

A batch maximum likelihood technique is used in the time domain. Identified parameters for the four cases are given in Table 4-4. Figures 4-7 and 4-8 shows convergence of parameters in the time-domain model. Convergence time is substantial and will depend upon the shape of the filter used.

4.2.3 Comparison

The models estimated without noise are the same as the simulated models. 5% noise degrades the models to some extent and 25% noise causes a significant error, which may degrade the accuracy of the controller and may make it unstable.

Pilot inputs which cause modulation of the open-loop vibration are the most troublesome.

4.3 EVALUATION OF THE CONTROL LAW

Several control laws are designed both in the time-domain and the frequency domain. The effect of measurement noise and pilot inputs is studied. Trade-offs between residual vibration and speed of response are established.

4.3.1 Frequency-Domain Formulation

The closed-loop system is simulated by collecting data over one vibration cycle, setting aside one vibration cycle for computation and then applying the computed feedback input. Nothing is done for the following two vibration cycles. Thus the feedback control signal is computed and updated once every rotor cycle.

In the following, two sets of plots are shown for each case. The first plot shows the sensor measurements, which include both the measurement noise and the rotorcraft vibration. The second plot shows the actual vibration of the rotorcraft. While the second plot shows the vibration the crew and the airframe experiences, the first plot indicates the quality of signal used for control.

Sine and cosine components z_k of the vibration along the three axes are extracted. Based on the previous measured values of z_{k-1}, Δz_k is computed. This is multiplied by the gain matrices to compute inputs for feedback.

The following gain matrices are used.

(1) $G = T^{-1}$, since there are three inputs and three controls (each with a sine and a cosine component) in our example, it is possible to make this choice. This is the fastest possible controller, leading to vibration reduction in about four vibration cycles, under ideal conditions.

(2) $G = \alpha T^{-1}$ where $\alpha < 1$. The time constant increases as α is decreased from one.

(3) $G = (T^T Q T + A)^{-1}(T^T Q + B)$, Q is set to identity, and A and B are varied.

The results for measurements with and without noise are shown in Figures 4-9 to 4-19 and are summarized in Table 4-5. As a general conclusions as the gains are reduced the steady-state vibration response due to measurement noise goes down but the convergence time goes up. The presence of pilot-induced open-loop vibration can significantly degrade the closed-loop results and high gains are needed to minimize the impact of this effect on closed-loop performance.

4.3.2 Time-Domain Formulation

In the time domain formulation, the basic dynamic model of the rotorcraft is extended to include frequency-shaping of helicopter vibration. This gives a 9-state formulation for the three-axis problem. The control-law is designed by optimizing a quadratic cost functional in the states of the intended system and the input. The model in the discrete formulation has the form:

$$x_{i+1} = \phi x_i + G_d u_i \tag{4.1}$$

$$x'_i = 2*\cos(\omega_v \Delta t) x'_{i-1} + x'_{i-2} + y_i \tag{4.2}$$

Note that the second equation has open loop poles at $\cos(\omega_v \Delta t) \pm j \sin(\omega_v \Delta t)$. These poles have a continuous frequency of ω_v and are on the unit circle. The baseline control law minimizes

$$J = E[x_i'^T x_i' + b\, u_i^T u_i]$$

The nominal value of b is 3×10^8. The control law is of the form

$$u_i = C_1 x_i + C_2 x'_i + C_3 x'_{i-1}$$

Table 4-6 shows the closed-loop eigenvalues of the time domain controller with $b = 3 \times 10^8$. The absolute value of the closed-loop eigenvalues is also shown. As is well known for digital systems, the distance of the closed-loop eigenvalues away from unit circle is a measure of system convergence time (the farther the eigenvalue the better the convergence time). The convergence time for the open-loop vibration to reduce to 5% for the three complex eigenvalue pairs is as follows:

$-3/\ln(.989)$, $-3/\ln(.9766)$ and $-3/\ln(.9737)$ sample points

or 271, 123 and 113 sample points. Thus, the worst case convergence time is 271 sample points.

With sampling time of 300 per second, the convergence time for various modes varies between .375 and .98. To this must be added the state estimation delay to determine the overall convergence time.

Figure 4-19 shows the response of the closed-loop system when there is no measurement noise. The convergence time varies from 0.3s to 0.6s. Figures 4-20 and 4-21 show the helicopter vibration response and measured outputs in the presence of 5% white Gaussian noise. Note that the measurement is very noisy even in steady state (representing mostly measurement noise). The vibration is reduced to a low value within about the same convergence time as before.

Corresponding rotorcraft vibration and measured time histories for 25% measurement noise are shown in Figures 4-22 and 4-23. Note that there is a significant increase in the closed-loop vibration level due to the noise.

The response of the closed-loop system is computed with a pilot, SAS or gust input which causes a modulation of the open-loop rotorcraft vibration. The modulation has a magnitude equal to 25% of the open-loop vibration with a frequency of 0.85 Hz (see Figure 4-6a). Figure 4-24 shows the closed-loop response of the system. The response is modulated at 1.70 Hz and has a magnitude of about 10% of the open-loop value.

The closed-loop responses for the baseline controller are summarized in Table 4-7. The RMS value of residual vibration for noisy measurements is also determined statistically. actual simulated values are close to the statistically determined quantities. For this controller 25% white Gaussian measurement noise does not appear to cause major problems. Pilot-induced responses could be important.

To study the behavior of the closed-loop system with variations in transient response time, two additional control laws are designed. In the first one, the control penalty is reduced by a factor of ten to 3×10^7 and in the second one by a factor of one hundred to 3×10^6. These penalty reductions will cause the closed-loop eigenvalues to migrate away from the unit circle causing the transient response to be faster. Figure 4-26 shows the closed-loop response with 5% noise level and $b = 3 \times 10^7$ (medium speed controller). The response of the medium speed controller with pilot-induced variations in open-loop vibration is shown in Figure 4-26. A comparison of Figures 4-20 and 4-25 shows that increasing the speed (or gain) of the controller increases the residual closed-loop vibration due to measurement noise. A similar comparison of Figure 4-23 and 4-26 indicates that the reverse is true of pilot induced variations in open-loop vibration. Thus, in the design of closed-loop control system for rotorcraft vibration control a trade-off must be established to ensure that reasonable residual vibration is obtained both in the presence of measurement noise and open-loop variations in rotorcraft vibrations.

The magnitude of the eigenvalues and the corresponding convergence times in terms of the number of sample points is given in Table 4-8. Transient response can be significantly accelerated by simply decreasing the control weighting.

Table 4-9 shows the RMS steady-state vibration level for the three controllers with 25% measurement noise and with pilot-induced variation in open-loop vibration. The faster response causes an amplification of the measurement noise. It is very beneficial for pilot induced input.

The controllers with faster response are also less robust. Modeling errors farther away from the vibration frequency can drive the controller unstable or degrade performance.

4.4 REAL-TIME ESTIMATION AND CONTROL

This section discusses the implementation of vibration control laws where the system identification and feedback control functions are performed in real-time rather than off-line. The issues of significance are

(i) Stability problems in the presence of noise,

(ii) The intervals over which the model must be updated,

(iii) Steady-state response, and

(iv) Need for caution or dual control.

These areas are studied through simulation in the following subsections.

4.4.1 Frequency-Domain Formulation

The frequency-domain control law is simulated using the Kalman filter estimates and gains from Section 4.3.1. Results in the presence of three different kinds of noise sources (discussed in Section 4.2) are shown in Figures 4-27 to 4-29. Note significant performance degradation when pilot-induced inputs modulate open-loop helicopter vibration levels.

4.4.2 Time-Domain Formulation

The time-domain approach is implemented as follows:

- Control law updated every rotor revolution and is based on the solution to a Riccati equation
- Identification performed recursively, updating parameter values at every sample point
- Estimation accuracy computed using information matrix
- The entire procedure is implemented in square-root form
- Sampled-data control design and covariance analysis

Results in the absence of measurement noise are shown in Figure 4-30. Figure 4-31 expands the first 500 data points and shows the building of control and filtered state.

A white-Gaussian noise with an RMS value of .6 is added to the measurements. The measured time histories are shown in Figure 4-32. The actual accelerations with closed-loop control are given in Figure 4-33. Closed-loop system appears well controlled.

The corresponding time histories for noise within $\pm$ 1/rev around the vibration frequency (a two pole filter is used with white noise input) are shown in Figure 4-34 and 4-35. Note that there is significant helicopter vibration in the steady-state. Part of the steady-state vibration is due to parameter estimation error and partly because of feeding measurement noise directly into the plant.

SECTION 5
SUMMARY, CONCLUSIONS AND FUTURE WORK

The analysis presented in this report compares the frequency-domain and the time-domain approaches for effectiveness, robustness and implementation complexity. The study has attempted to point out the advantages and disadvantages of both approaches.

5.1 CONCLUSIONS

The following conclusions may be drawn based on the theoretical analysis presented here and the simulation results based on one specific model form.

System Identification Methods

System identification methods are available for both the frequency-domain and the time-domain approaches. These techniques may be implemented on-line in a recursive mode or off-line in a batch mode. The off-line approach can give more accurate models for specific flight conditions. To track parameter variations, the on-line approach will have to use a past-fading approach.

It is necessary to base models on data in the immediate neighborhood of the vibration frequency. Appropriate approaches which make this possible have been specified for the time-domain approach.

When local models are used in the frequency-domain approach the pseudo measurement noise is non-white. Use of appropriate noise models can give improved results.

Robustness

The time-domain approach appears to be more robust (has higher gain and phase margins). Most of this robustness is available mainly because the inputs can be updated more frequently. However, it appears that gain scheduling can be used in the frequency-domain approach as in the time-domain approach. More points may be needed in the frequency-domain approach than in the time-domain.

Transient Response

When the rotorcraft is operating at one-flight condition and the open-loop vibration is constant, transient response in the frequency-domain is superior to that in the time-domain if the transfer matrix is known exactly. The settling time in the frequency-domain is about one rotor cycle. If any of the above conditions do not hold, the transient settling time can increase substantially. The faster settling time also places certain closed-loop eigenvalues nearer the unit circle with possible impact on robustness. The transient response for the time-domain controller may be made arbitrarily fast. However, faster response reduces robustness because it increases gain away from the vibration frequency. In practice, the transient settling time will be determined by a priori confidence in the model and the distance of structural modes from the vibration frequency.

Susceptibility to Noise

Both techniques are highly susceptible to noise, particularly variations in open-loop vibration due to pilot inputs and noise. The residual vibration increases as the transient settling time is reduced.

Implementation Complexity

Both approaches require similar actuators and sensors. The time-domain controller is easier to implement even with on-line identification.

5.2 FUTURE RESEARCH

Future research should be performed along the following directions:

(i) Establish definitive relationships between robustness, transient response and susceptibility to noise for each of the two techniques.

(ii) Study the effects of other kinds of noise sources.

(iii) Further simulations for both approaches.

(iv) Perform wind-tunnel and flight tests for each of the two approaches to provide an understanding of the impact of unmodeled parts of the system on closed-loop behavior.

REFERENCES

1. Shaw, J., and N. Albion, 'Active Control of the Helicopter Rotor for Vibration Reduction,' Paper No. 80-68, 36th Annual Forum of the American Helicopter Society, Washington, DC, 1980.

2. Molusis, J.A., C.E. Hammond, and J.H. Cline, 'A Unified Approach to the Optimal Design of Adaptive and Gain-Scheduled Controllers to Achieve Minimum Helicopter Rotor Vibration,' 37th Annual Forum of the American Helicopter Society, New Orleans, LA, May 1981.

3. Johnson, W., 'Self-Tuning Regulators for Multi-Cyclic Control of Helicopter Vibration,' NASA Technical Paper 1996, March 1982.

4. Gupta, N.K., and R.W. DuVal, 'A New Approach to Active Control of Rotorcraft Vibrations,' AIAA Journal of Guidance and Control, Nov.-Dec. 1981.

5. Gregory, C.Z., Jr., and N.K. Gupta, Rotorcraft Vibration Controller Design and Evaluation, ISI Report No. 14, Prepared by Integrated Systems, Inc. for NASA-Ames Research Center under Contract NAS2-10951, April 1982.

6. Gupta, N.K., 'Frequency-Shaping of Cost Functionals: Extensions of LQG Design Methods,' AIAA Journal of Guidance and Control, Vol. 3, No. 6, Nov.-Dec. 1980, pp. 529-535.

7. MATRIX$_x$™: A Program for Model Building, Simulation, Control Design and System Identification, User's Guide, 1983 (available from Integrated Systems, Inc.).

8. DuVal, R., and N.K. Gupta, 'Continuous Rotorcraft Vibration Suppression Without Rotor Feedback,' Presented at the American Helicopter Society Workshop on the Technology for Jet Smooth Ride, Paper No. 10, Hartford, CT.

9. Bryson, A.E., and Y.C. Ho, Applied Optimal Control, Ginn Blaisdell, 1969.

10. Shah, S.C., and G.F. Franklin, 'Internal Model Adaptive Control,' IEEE Conference on Decision and Control, San Diego, CA, Dec. 1981.

11. Lev-Ari, H., 'Nonstationary Lattice-Filter Models,' Ph.D. Dissertation, Stanford University, Stanford, CA, Dec. 1983.

12. Gantmacher, F.R., Theory of Matrices, Chelsea, New York, 1959.

13. Kosut, R.L., C.R. Johnson and B.D.O. Anderson, 'Conditions for Local Stability and Robustness of Adaptive Control Systems,' to be presented at the 22nd IEEE Decision and Control Conference, San Antonio, Texas, Dec. 14-16, 1983.

14. Doyle, J.C., and G. Stein, 'Multivariable Feedback Design: Concepts for a Modern/Classical Synthesis,' IEEE Trans. Automatic Control, Vol. AC-26, No. 1, pp. 4-17, 1981.

15. Chopra, I., and J.L. McCloud, III, 'A Numerical Simulation Study of Open-Loop and Adaptive Multicyclic Control Systems,' Journal of the American Helicopter Society, Vol. 28, No. 1, pp. 63-77, January 1983.

TABLE 2-1. SUMMARY OF PAST WORK ON REGULATORS FOR HELICOPTER VIBRATION ALLEVIATION
(Taken from Ref. [3]. All references may be found in that report.)

Regulator type	Reference	Investigation	Identification	Controller	Notes
Invariable open loop	Kretz et al. (1973a,b)	Experiment	Least squares	$J = z^T z$	
	McCloud and Kretz (1974)	Experiment	Least squares	$J = z^T z$	
	McCloud (1975)	Theory	Least squares	$J = z^T W_z z$	
	McCloud and Weisbrich (1978)	Experiment	Least squares	$J = z^T W_z z$	
	Brown and McCloud (1980)	Experiment	Least squares	$J = z^T W_z z + \dot{z}^T W_{\dot{z}} \dot{z}$	
	Sissingh and Donham (1974)	Experiment	Direct inverse	Direct inverse	
	Powers (1978)	Experiment	Various methods	Direct inverse	
	Wood et al. (1980)	Experiment	Various methods	Direct inverse	
Invariable closed loop	Shaw and Albion (1980)	Experiment	Direct inverse	Direct inverse	Δt = 1 rev
	Shaw (1980)	Theory	Direct inverse	Direct inverse	
Adaptive open loop	Hammond (1980)	Experiment	Kalman filter, T and z_0	$J = z^T W_z z$, caution	Δt = 1 rev, Δ
	Molusis et al. (1981)	Experiment	Kalman filter, T and z_0; or only z_0	$J = z^T W_z z$, caution	Rate limit, Δ
Adaptive closed loop	Shaw (1980)	Theory	Kalman filter, local T	Direct inverse	
	Taylor, Farrar, and Miao (1980)		Kalman filter, local T	$J = z^T W_z z$	Δt = 1-2 rev, rate limit, Δ
	Taylor et al. (1980)	Theory			

[a] Included in the theoretical development, but not used in applications.

TABLE 3-1. COMPUTATIONS REQUIRED TO IMPLEMENT FREQUENCY DOMAIN CONTROLLER (LOCAL MODEL APPROACH)

Step No.	Description	Relevant Equations	No. of Computations* Per Rotor Cycle
1	Harmonic Analysis	$z_{ic} = \sum_{t=1}^{nN} y_i \cos \frac{2\pi t}{n}$ and $z_{is} = \sum_{t=1}^{nN} y_i \sin \frac{2\pi t}{n}$ $i = 1, 2, 3 \ldots m$ } Equivalent to FFT for a few spectral lines	$2nmN$ (Note: FFT will require more computations, but is not necessary)
2	Feedback Controller	$\theta_k = C_1 z_{k-1} + C_2 \theta_{k-1}$	$4qm$
3	Control Time History Generation	$u_t = \begin{matrix} \cos 2\pi t/n \\ \sin 2\pi t/n \end{matrix}$	$2nqN$
4	Identification (Simplified Kalman Filter Formulation)	$\hat{T}_k = \hat{T}_{k-1} + (\Delta z_k - \hat{T}_k \Delta\theta_k) K_k^T$ $K_k = M_k \theta_k / (\gamma_k + \Delta\theta_k^T M_k \theta_k)$ $M_k = (I - K_{k-1} \Delta\theta_{k-1}^T) M_{k-1} (I - K_{k-1} \Delta\theta_{k-1}^T)^T + K_{k-1} K_{k-1}^T r_{k-1} + Q_{k-1}$	
5	Gain Computation (Cautious Controller)	$C_1 = -D\hat{T}^T W_z$ $C_2 = DW\Delta\theta$ $D = (\hat{T}^T W_z \hat{T} + W_\theta + W_{\Delta\theta})^{-1}$	

* One computation is approximately one multiplication plus one addition.

TABLE 3-2. NUMBER OF COMPUTATIONS FOR FIXED-GAIN TIME-DOMAIN VIBRATION REDUCTION CONTROL LAW

Step	Description	Related Equations	No. of Computations Per Sample Point
1	Filter	$\ddot{z} + \omega_v^2 z = a$	2m
2	Control Law	$u = C_0 x + C_1 z + C_2 \dot{z}$	3mq

TABLE 3-3. NUMBER OF COMPUTATIONS FOR FULLY-ADAPTIVE TIME-DOMAIN CONTROL LAW

Id update	Computational Complexity	Numerical Behavior	Suitability for adaptive control implementation
Unmodified Kalman update	$(6s^2+8s+1)m$	poor, results in 'burst instability'	Numerically unacceptable
U-D factored covariance update with regularization	$(6s^2+8s)m$ information	good, inappropriate for fixed-point arithmetic	Easy implementation of minimum variance type control laws, difficult to exploit a-priori Can use a-priori structure and information directly. Can be used with variety of control design algorithms.
Potter square root	$(12s^2+7s+3)m$	reasonable needs square roots	Good

TABLE 4-1. TRANSFER FUNCTION $Tx10^2$ FOR 80 KNOTS AND 100 KNOTS (FROM REF. [6])

Response harmonics	Fixed flight conditions			Control harmonics					
	CST	CLR	CNR	2 cos	2 sin	3 cos	3 sin	4 cos	4 sin
Vertical acceleration									
4 cos	16.34	1.01	1.33	15.17	-2.02	18.73	56.22	102.96	20.05
4 sin	68.45	0.71	4.76	4.85	22.50	54.65	17.76	21.91	67.35
Lateral acceleration									
4 cos	-40.94	0.65	0.32	0.73	8.98	-20.52	-2.79	9.34	-8.19
4 sin	21.45	0.59	0.14	5.52	6.91	2.80	-21.07	20.52	1.93
Longitudinal acceleration									
4 cos	2.69	0.02	0.10	0.98	-0.26	0.05	-2.28	3.89	0.62
4 sin	3.62	0.04	0.12	-0.42	1.11	2.04	-0.09	-0.22	1.71

Response harmonics	Fixed flight conditions			Control harmonics					
	CST	CLR	CNR	2 cos	2 sin	3 cos	3 sin	4 cos	4 sin
Vertical acceleration									
4 cos	111.68	0.46	6.53	12.03	-15.82	82.38	-126.26	114.58	45.61
4 sin	66.93	2.88	6.18	0.19	-25.69	39.40	83.33	-10.84	104.82
Lateral acceleration									
4 cos	23.40	0.81	-4.49	5.63	4.48	1.60	-30.59	16.35	-11.22
4 sin	-44.47	0.43	0.23	-3.79	-4.59	19.25	-32.39	5.19	7.68
Longitudinal acceleration									
4 cos	5.27	0	0.19	0.09	0.01	2.14	-5.72	2.61	-1.28
4 sin	6.18	0.11	0.16	0.64	-1.55	2.08	0.73	-1.29	3.02

TABLE 4-2. STATE-SPACE DESCRIPTION MATRICES FOR ROTORCRAFT VIBRATION AT 80 KNOTS

$$\Phi = \begin{bmatrix} 0.4000 & 0.0000 & 0.0000 \\ 0.0000 & 0.4000 & 0.0000 \\ 0.0000 & 0.0000 & 0.4000 \end{bmatrix} \quad G_d = \begin{bmatrix} 0.6000 & 0.0000 & 0.0000 \\ 0.0000 & 0.6000 & 0.0000 \\ 0.0000 & 0.0000 & 0.6000 \end{bmatrix}$$

Based on

$$H1 = \begin{bmatrix} 104.1444 & -134.8268 & 40.4742 \\ -97.5373 & -52.4049 & 26.9036 \\ 1.0457 & -98.4880 & -198.2593 \end{bmatrix} \quad D1 = \begin{bmatrix} 173.7178 & -81.1690 & 52.7490 \\ -56.9288 & -45.0650 & 4.3788 \\ 4.6005 & -25.6997 & -196.6914 \end{bmatrix}$$

$$H2 = \begin{bmatrix} 95.3033 & -147.2091 & 39.4285 \\ -38.9294 & -79.3323 & -52.5713 \\ 2.9470 & -305.4933 & -195.6688 \end{bmatrix} \quad D2 = \begin{bmatrix} 132.1210 & -90.7718 & 53.0735 \\ -24.5194 & -80.6299 & -43.9430 \\ 3.7123 & -165.9383 & -151.6213 \end{bmatrix}$$

cos	sin	
0.1634	0.6845	Vertical
-0.4094	0.2145	Lateral
0.0269	0.0362	Longitudinal

where

$$x_{i+1} = \Phi x_i + G_d u_i$$

$$y_i = H_1 x_i + D_1 u_i : \text{cosine components}$$

$$y_i = H_2 x_i + D_2 u_i : \text{sine components}$$

TABLE 4-3. IDENTIFIED VALUES OF TRANSFER MATRICES FOR VARIOUS CONDITIONS

4-3a. No Measurement Noise (Simulation Values)

248.4905	-126.9578	5.3513	59.2212	-55.4642	0.5946
-177.9708	-82.6902	-96.4113	-76.6687	-29.7998	-56.0047
81.8083	23.6948	-339.0359	23.0155	15.2986	-112.7393
-59.2212	55.4642	-0.5946	248.4905	-126.9578	5.3513
76.6687	29.7998	56.0047	-177.9708	-82.6902	-96.4113
-23.0155	-15.2986	112.7393	81.8083	23.6948	-339.0359

4-3b. 5% Measurement Noise

228.7618	-115.5355	4.1620	61.1591	-79.8408	-0.0975
-201.2055	-79.3397	-96.4760	-62.2130	-16.3239	-55.7717
86.2400	19.3265	-337.7200	20.5434	18.8274	-114.1909
-34.8128	64.6834	-1.0120	239.5251	-123.9286	4.2645
49.0249	18.5928	56.6752	-176.1633	-84.5502	-97.9689
-38.7759	-23.0295	113.7915	67.2966	35.6074	-339.7685

4-3c. 25% Measurement Noise

318.8766	-102.2032	3.6299	94.2875	-77.8795	3.0921
-226.8184	-51.7225	-101.0769	-91.5136	-12.6879	-56.5297
48.7592	29.2625	-334.6284	76.3503	-12.6542	-109.4967
-139.5581	20.8387	-1.0341	153.3878	-138.1573	8.5748
21.1616	82.6690	57.3932	-150.7690	-60.6836	-96.8024
-27.7391	-36.9317	117.2422	73.8549	51.1235	-339.7697

4-3d. Pilot-Induced Variation in Open-Loop Vibration and No Noise

243.2912	-146.3046	5.7786	88.4342	-54.3660	2.4589
-159.9086	-10.3621	-98.0988	-186.9508	-33.0340	-63.0788
87.1926	44.2526	-339.4992	-8.1353	14.2206	-114.7309
-69.9638	18.9536	0.1511	302.8968	-124.2955	8.7989
62.5147	-18.9634	57.0134	-105.1557	-79.2573	-91.7920
-26.4943	-24.5629	112.8793	95.0282	24.8475	-338.2183

TABLE 4-4. IDENTIFIED VALUES OF TIME-DOMAIN MODEL PARAMETER UNDER VARIOUS CONDITIONS

	B			D			Open-Loop Vibration	
No Noise (Correct Value)	104.1	-134.8	40.4	173.7	-81.1	52.7	.1634	.6845
	-97.5	-52.4	26.9	-56.9	-45.0	4.3	-.4094	.2145
	1.0	-98.4	-198.2	4.6	-25.6	-196.6	.0269	.0362
5% Noise	103.6	-124.9	31.1	174.5	-87.0	56.2	.163	.684
	-95.2	-59.0	23.1	-67.9	-40.5	10.6	-.410	.214
	1.0	-98.2	-198.5	4.3	-25.9	-196.4	.027	.036
25% Noise	141.7	-168.2	-8.3	135.7	-73.6	46.5	.160	.701
	-111.7	-54.4	6.2	-82.5	-49.7	6.2	-.403	.209
	-.1	-102.8	-194.9	8.5	-20.8	-199.5	.026	.036
Pilot-Induced Variations in Open-Loop Vibration	232.4	-235.0	-96.6	101.8	52.4	152.7	.153	.689
	-49.2	3.4	4.03	-133.8	-36.0	70.6	-.414	.208
	7.5	-107.2	-206.3	2.95	-17.3	-192.7	.026	.037

TABLE 4-5. CLOSED-LOOP PERFORMANCE OF VARIOUS FREQUENCY-DOMAIN VIBRATION CONTROL LAWS UNDER VARIOUS CONDITIONS (VALUES ARE GIVEN FOR EACH OF THE THREE ONES)

Vibration	No Noise	5% Measurement Noise		25% Measurement Noise		Pilot-Induced Variation in Open-Loop Vibrations
		Sensor Output	Vibration	Sensor Output	Vibration	Vibration
$G = T^{-1}$	-	.0373	.0123	.1867	.0615	.0631
	-	.0246	.0072	.1232	.0358	.0424
	-	.0023	.0009	.0116	.0046	.0042
$G = 0.5T^{-1}$	.0132	.0379	.0145	.1796	.0394	.0840
	.0090	.0247	.0086	.1183	.0184	.0559
	.0008	.0024	.0010	.0112	.0030	.0053
$G = (T^TT+A)^{-1}$ (T^T+B) $A = 10^5$ $B = 400$	Unstable					
$G = (T^TT+A)^{-1}$ (T^T+B)	.0107	.0406	.0202			
	.0322	.0704	.0668	Not Com-puted	Not Com-puted	Not Com-puted
$A = 105$ $B = 0$	.0012	.0047	.0042			

TABLE 4-6 EIGENVALUES OF THE CLOSED-LOOP SYSTEM WITH $b = 3*10^8$

Open-Loop	Closed-Loop	Absolute Value of Closed-Loop Eigenvalue
0.9135 + 0.4067i	0.9035 + 0.4025i	0.9890
0.9135 + 0.4067i	0.9035 - 0.4025i	0.9890
0.9135 + 0.4067i	0.8918 + 0.3980i	0.9766
0.4000 + 0.0000i	0.8918 - 0.3980i	0.9766
0.4000 - 0.0000i	0.8891 + 0.3970i	0.9737
0.4000 + 0.0000i	0.8891 - 0.3970i	0.9737
0.9135 - 0.4067i	0.4000 + 0.0000i	0.4000
0.9135 - 0.4067i	0.3999 + 0.0000i	0.3999
0.9135 - 0.4067i	0.3999 + 0.0000i	0.3999

TABLE 4-7. CLOSED-LOOP VIBRATION

	Open-Loop Vibration	5% Measurement Noise		25% Measurement Noise		With Pilot (or Gust) Induced Variation in Open-Loop Vibration
		Based on Sample	Statistically Calculated	Based on Sample	Statistically Calculated	Sample Based
First Output	.7037	.0049	.0053	.0245	.0265	.0575
Second Output	.4622	.0015	.0025	.0074	.0125	.0496
Third Output	.0451	.0004	.0004	.0019	.0018	.0042

TABLE 4-8. COMPARISON OF THE CONTROLLERS WITH THREE DIFFERENT PENALTIES ON CONTROL INPUT

	High Control Weighting $b = 3 \times 10^8$	Medium Control Weighting $b = 3 \times 10^7$	Low Control Weighting $b = 3 \times 10^6$
Eigenvalue Magnitude	.9890 .9766 .9737	.9659 .9292 .9210	.9003 .8162 .8015
Convergence Time to 5% of Open-Loop Vibration (sample points)	271 123 113	86 41 36	29 15 14

TABLE 4-9. STEADY-STATE RMS VIBRATION FOR CONTROLLERS IN THE PRESENCE OF MEASUREMENT NOISE AND PILOT-INDUCED VARIATIONS IN OPEN-LOOP VIBRATION

Disturbance	Outputs	Slow Controller $b = 3 \times 10^8$	Medium Speed $b = 3 \times 10^7$	Fast Controller $b = 3 \times 10^6$
25% White Gaussian Measurement Noise	First	.0265	.0455	.0771
	Second	.0125	.0214	.0374
	Third	.0018	.0029	.0051
Pilot Induced Variation in Open-Loop Vibration	First	.0575	.0252	
	Second	.0496	.0280	
	Third	.0042	.0019	

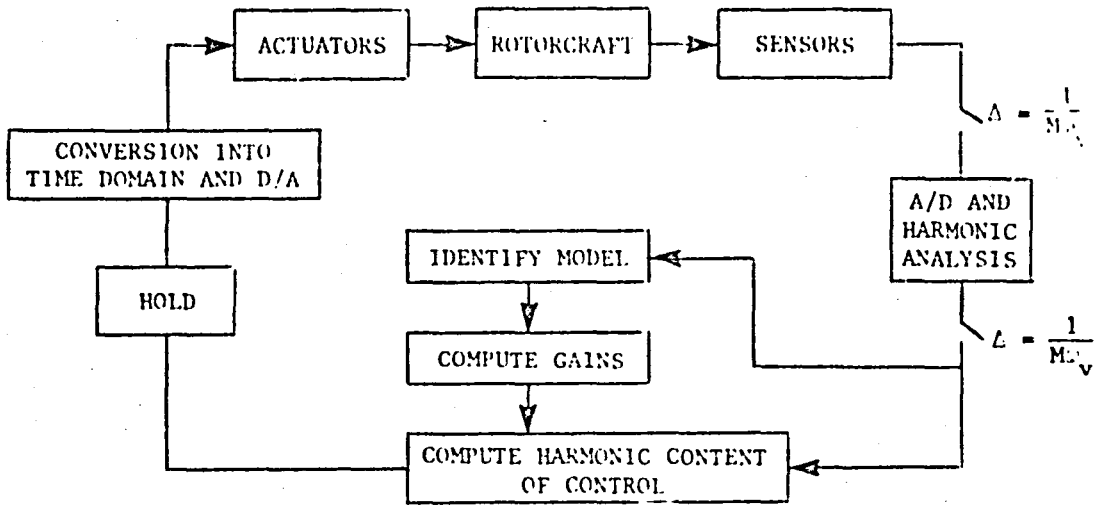

Figure 2-1. A Schematic Diagram of a Frequency-Domain Vibration Controller (M is sample points per vibration cycle and ω_v is the vibration frequency.)

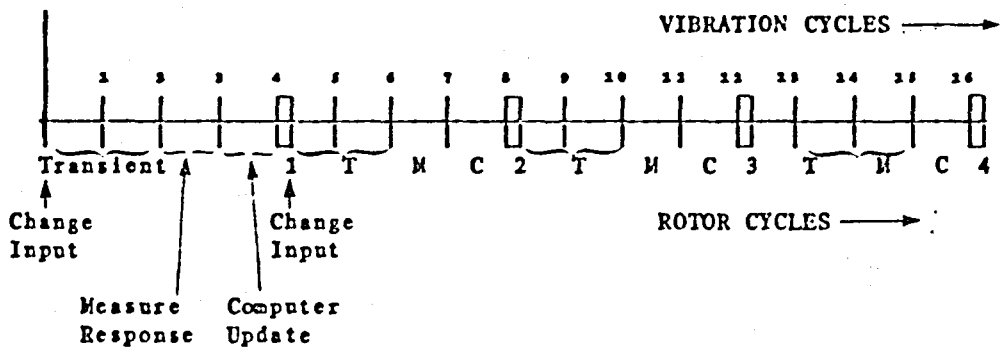

Figure 2-2. Feedback Control Implementation in the Frequency-Domain for a 4-Bladed Rotor (shows the transient setting, measurement, computation and input change cycles)

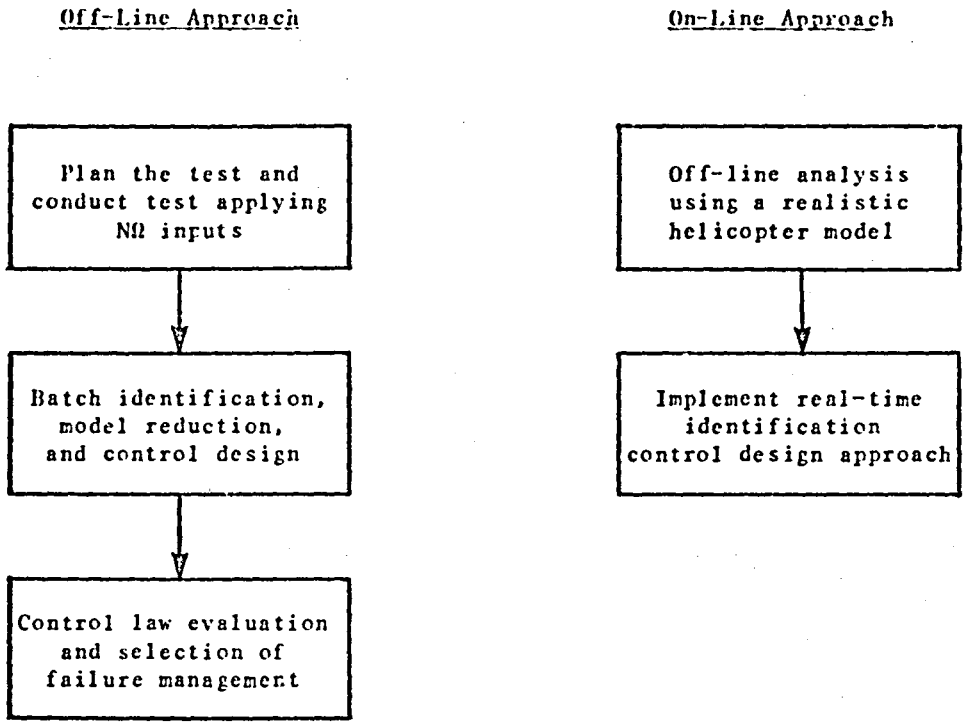

Figure 3-1. Off-Line vs. On-Line Identification for Helicopter Vibration Control

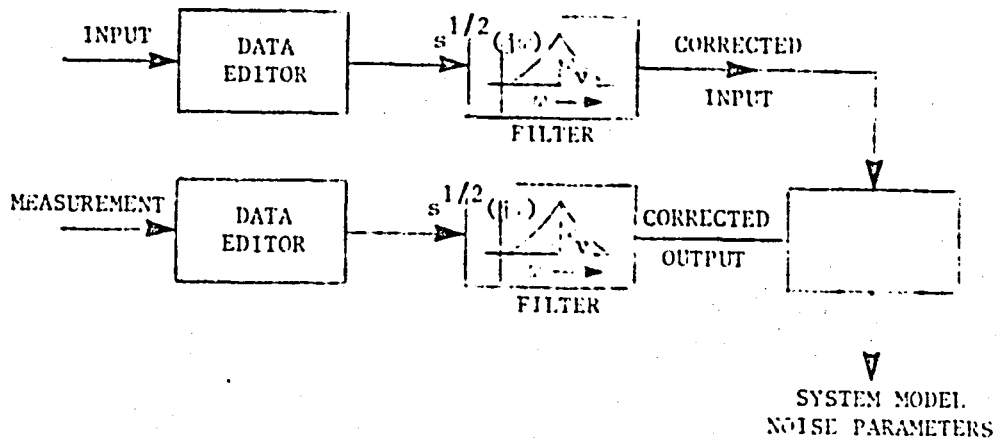

The filters cover a range around the vibration frequency.

Figure 3-2. Extension of Maximum Likelihood Method for Helicopter Vibration Control Model Identification

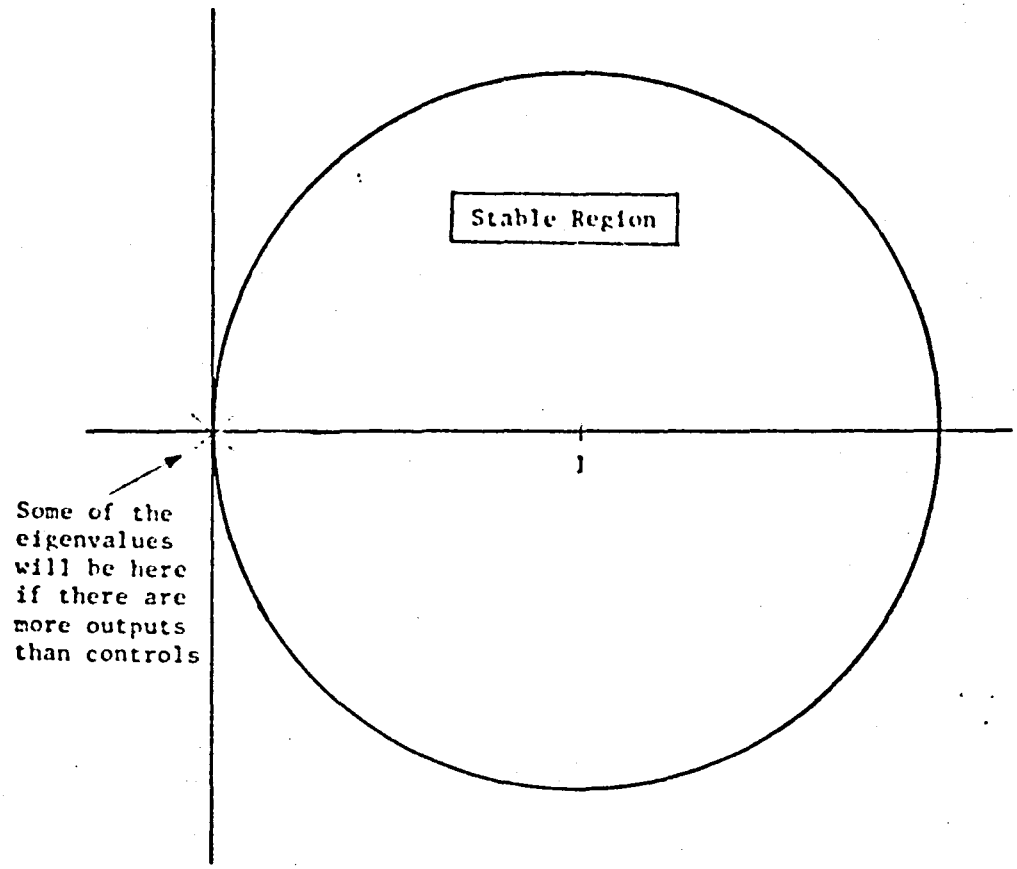

Figure 3-3. Location of the Eigenvalues of TG to Ensure Stability

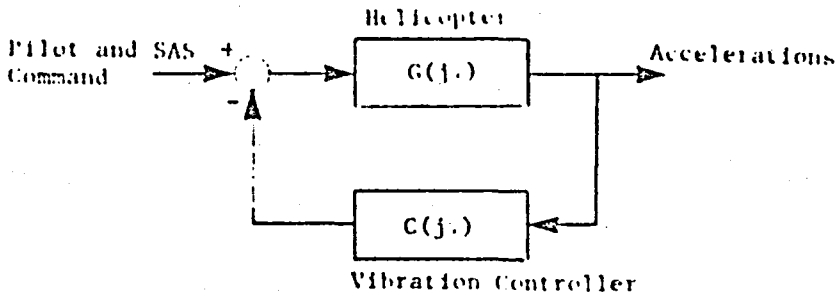

Figure 3-4. A Simple Flow Chart for a Vibration Control Law

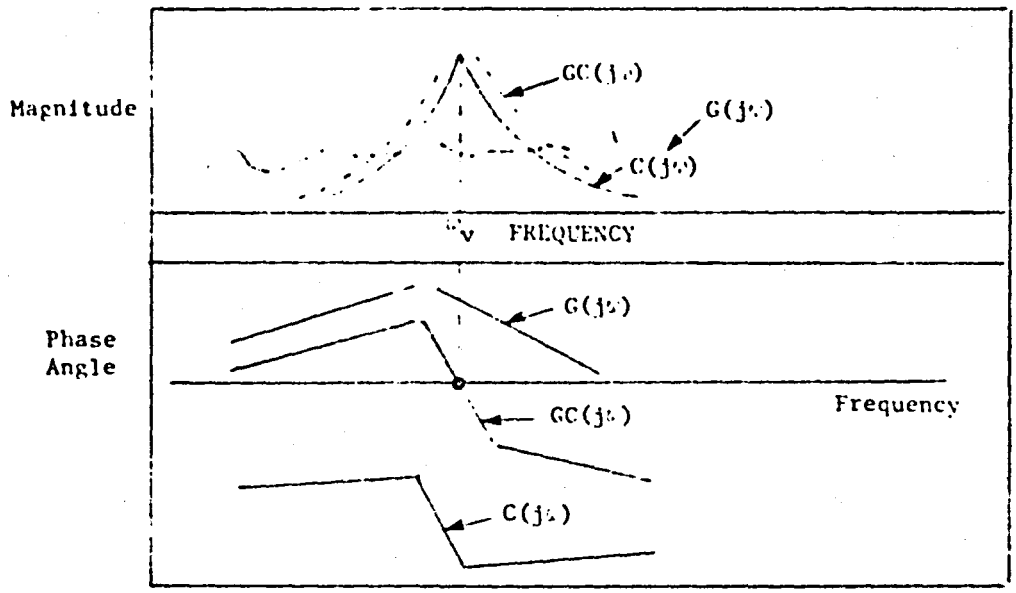

(a) Bode Plot

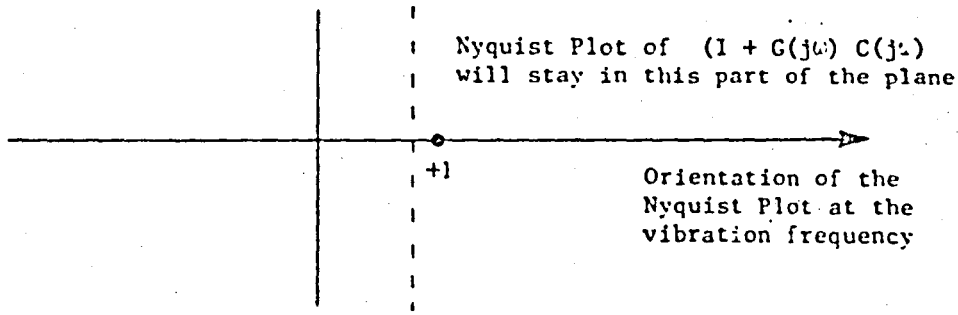

(b) Nyquist Plot

Figure 3-5. Bode and Nyquist Plots for the Vibration Controller

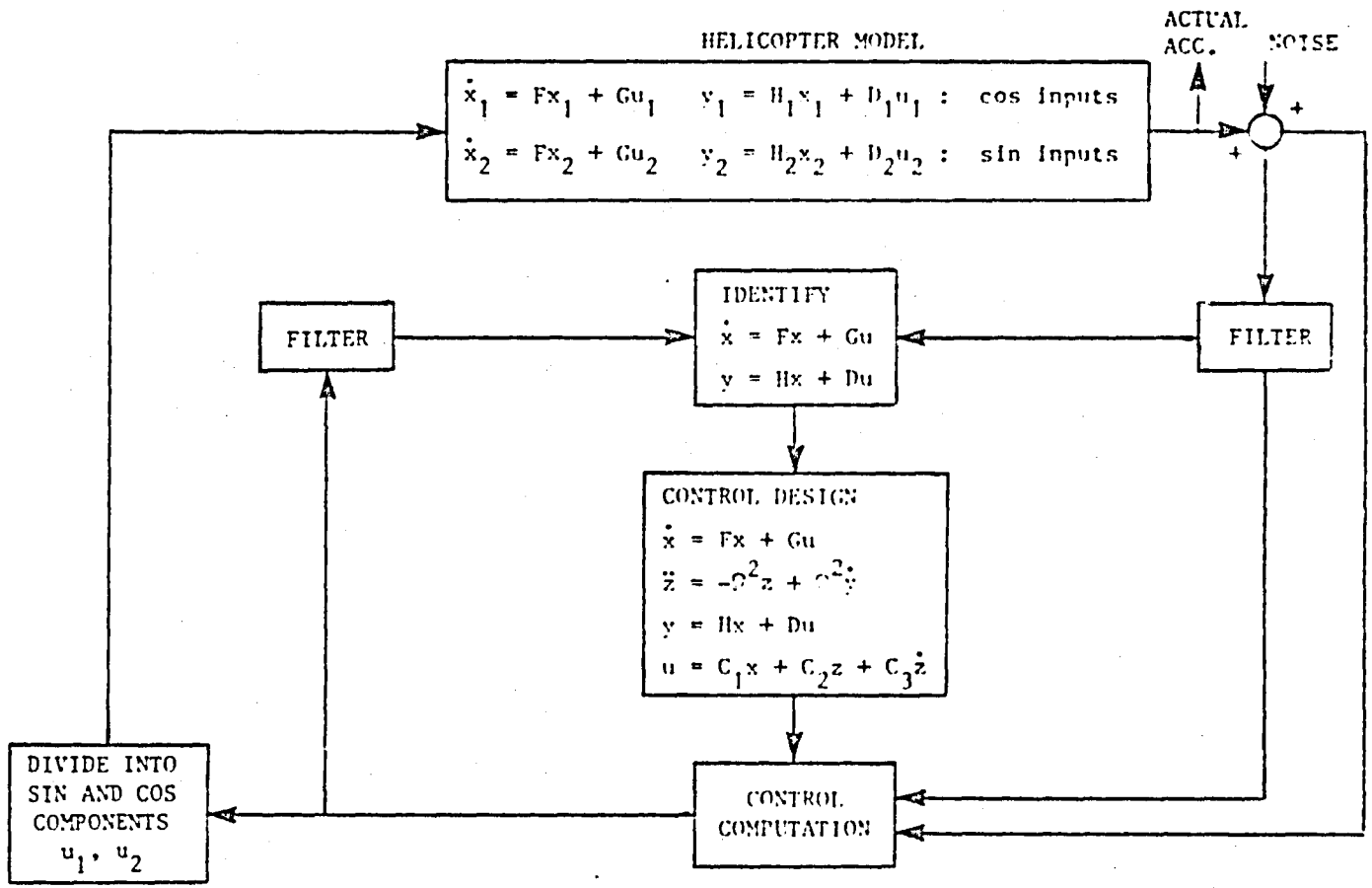

Figure 4-1. Evaluation Approach for the Time Domain Controller Based on the Frequency Domain Model

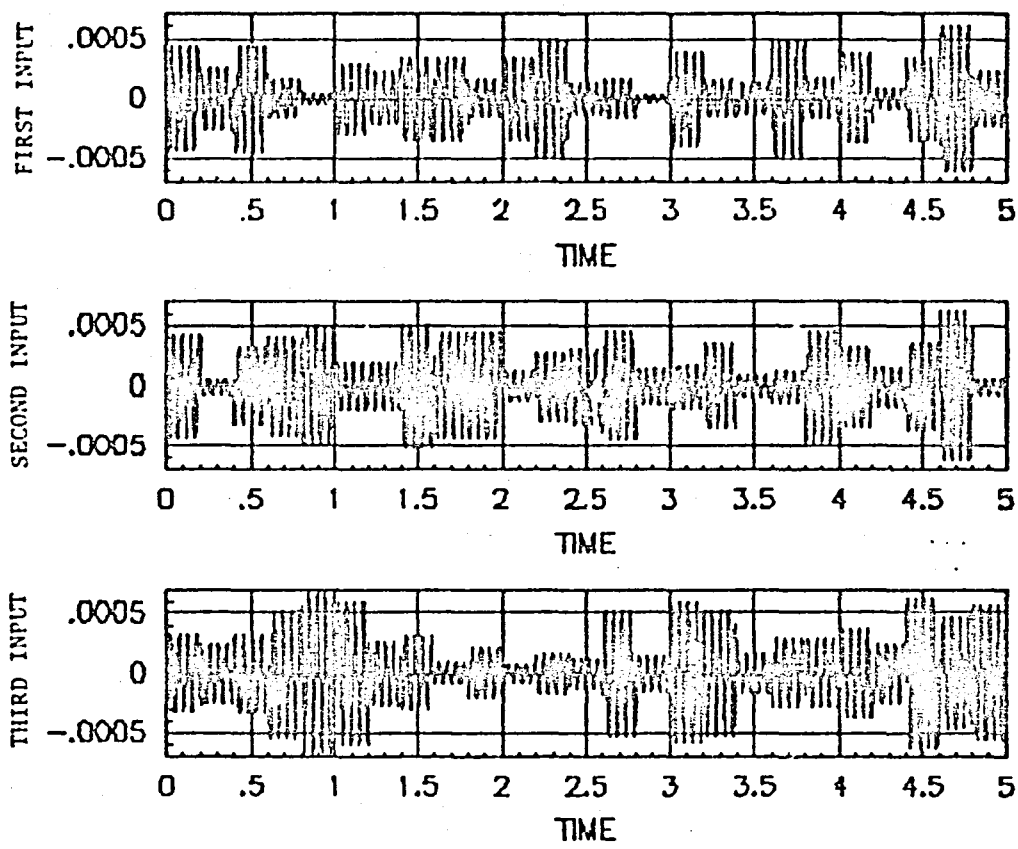

Figure 4-2. Inputs Used for System Identification (First Output - Vertical, Second Output - Lateral, Third Output - Longitudinal)

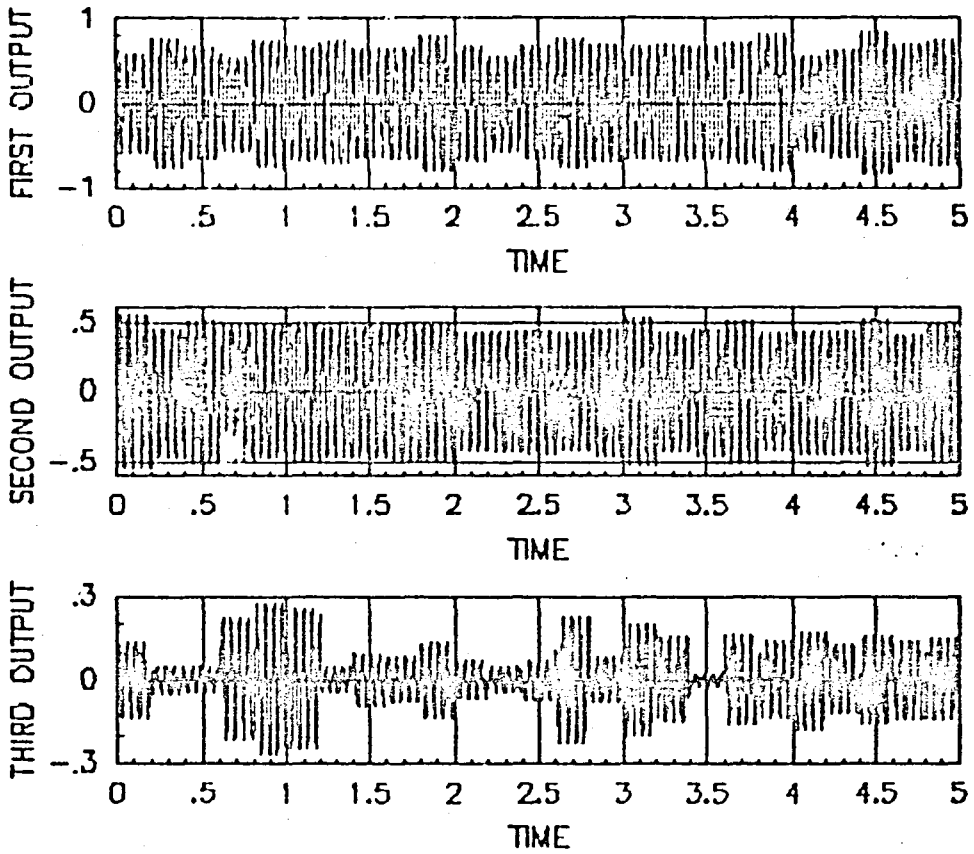

Figure 4-3. Noise Free Response of the Rotorcraft to Applied Inputs of Figure 4-2 (First Output - Vertical, Second Output - Lateral, Third Output - Longitudinal)

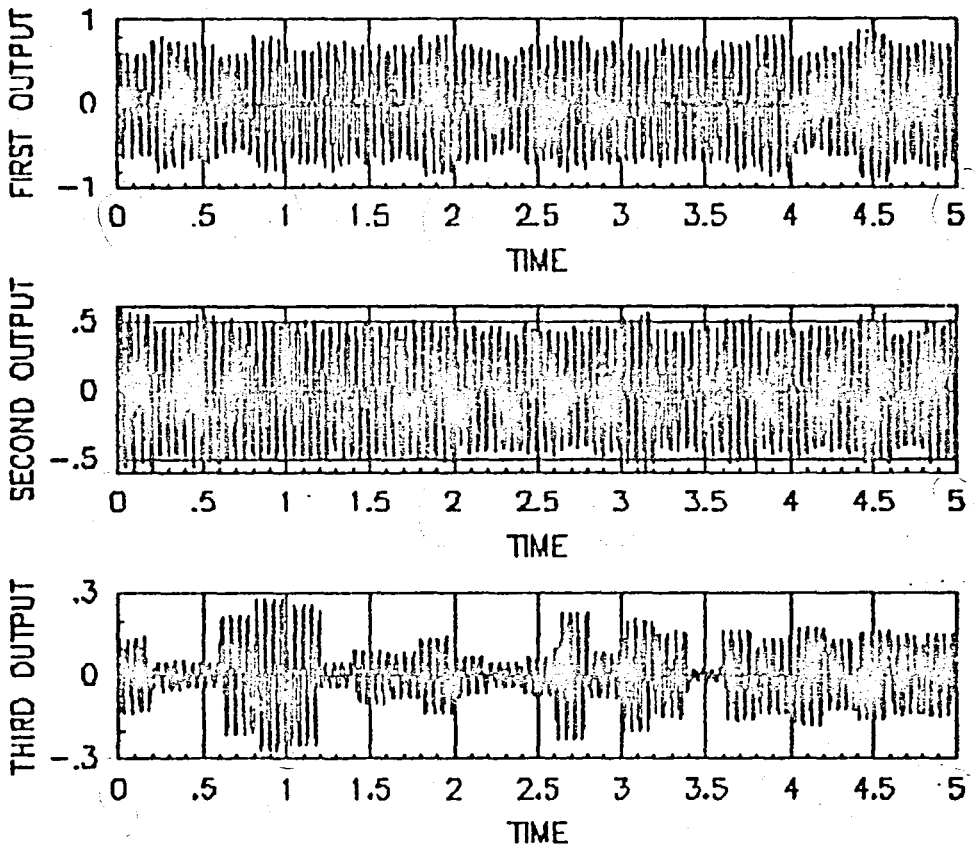

Figure 4-4. Rotorcraft Response to the Applied Inputs of Figure 4-2 with 5% Noise Level
(First Output - Vertical, Second Output - Lateral, Third Output - Longitudinal)

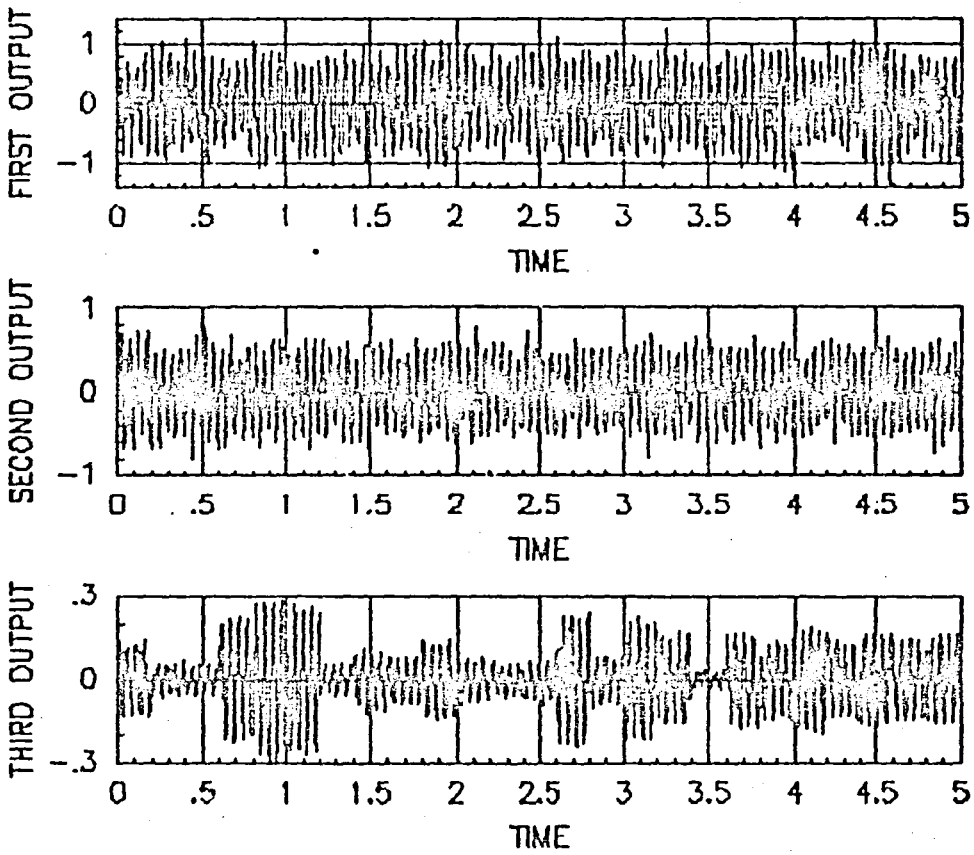

Figure 4-5. Rotorcraft Response with 25% Measurement Noise

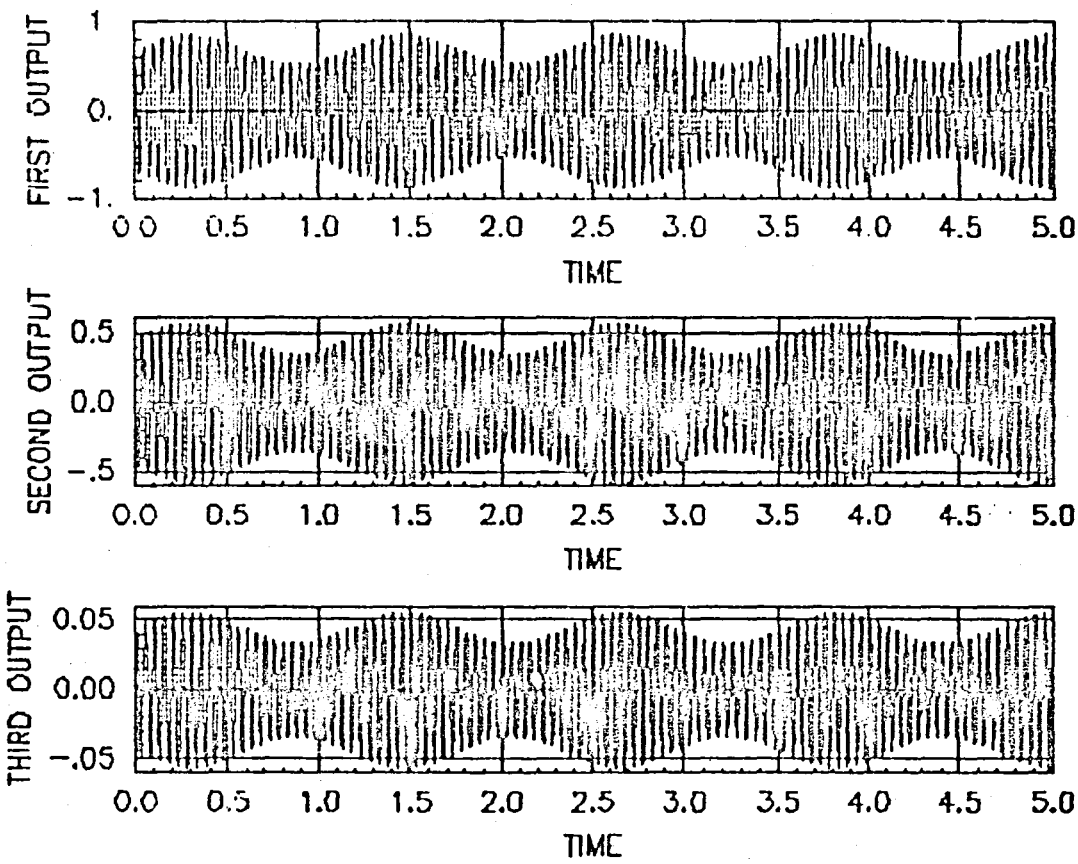

Figure 4-6a. Assumed Variation in Open-Loop Vibration Caused by a .85 Hz Pilot, SAS or Gust Induced Input

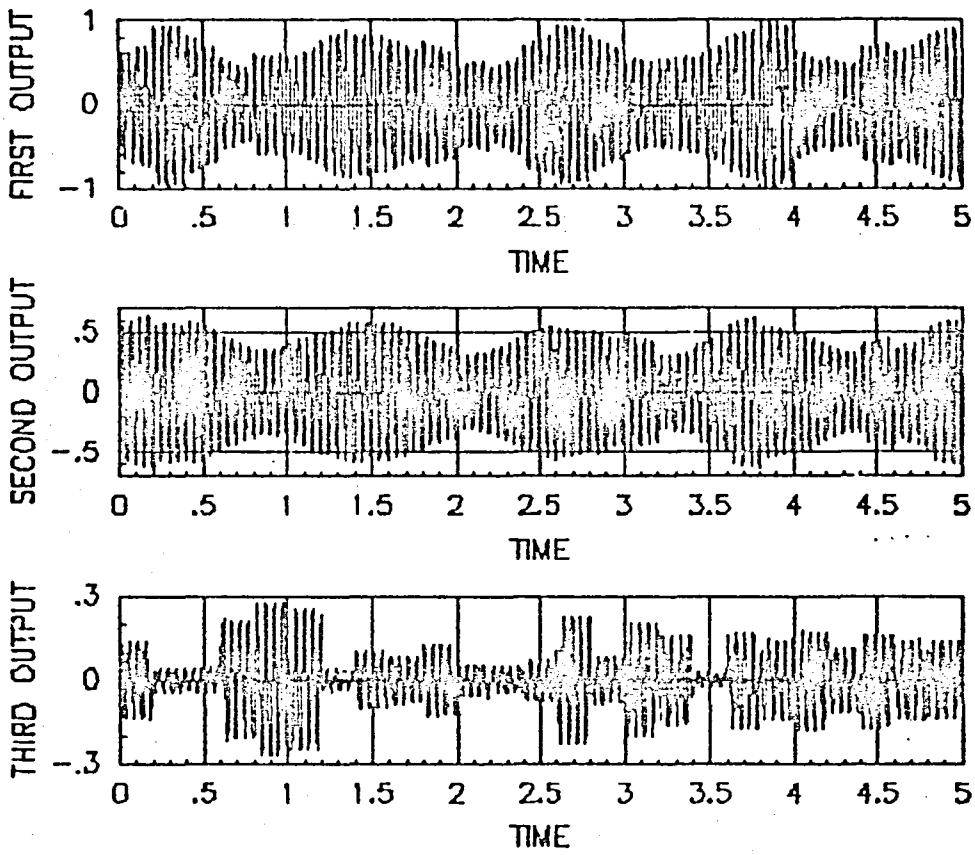

Figure 4-6b. Rotorcraft Response to Applied Input with Pilot-Induced Variation in Open-Loop Vibration

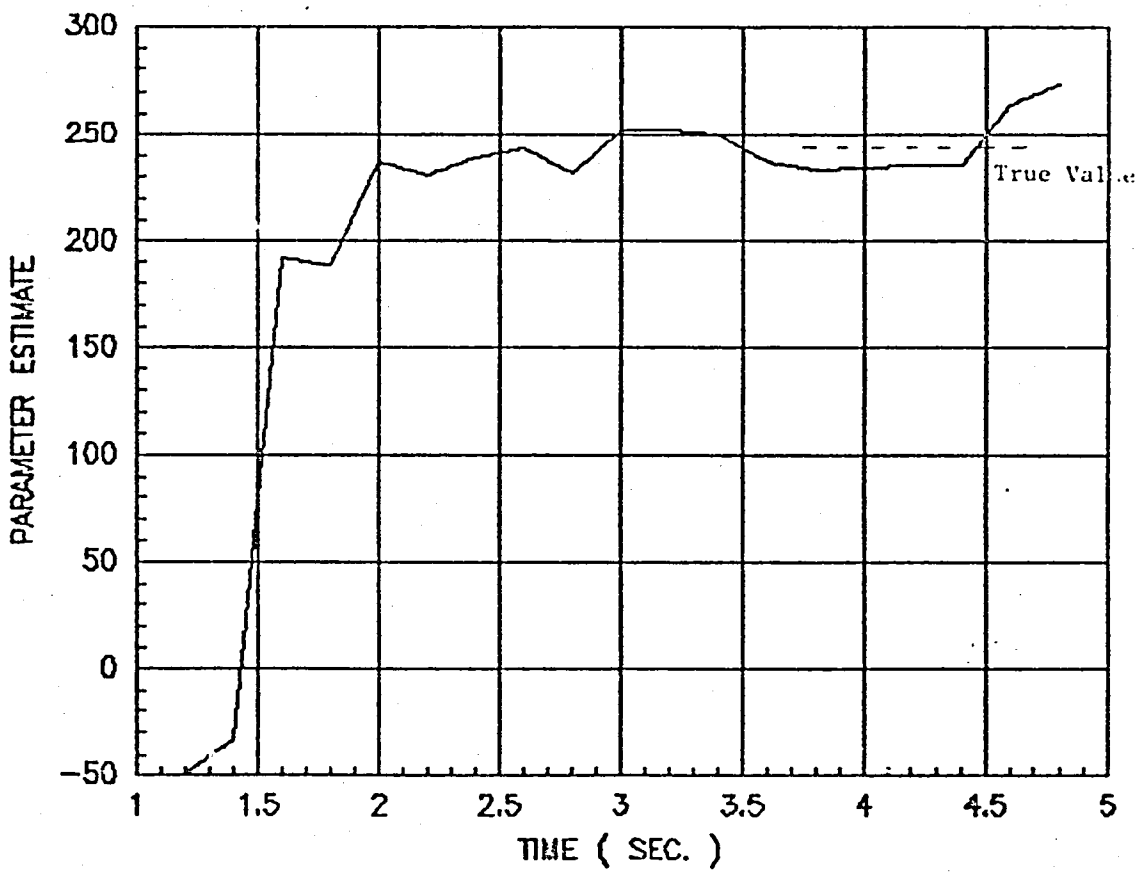

Figure 4-7a. Estimates of Parameter T_{11} as a Function of the Length of Data (5% Noise Level)

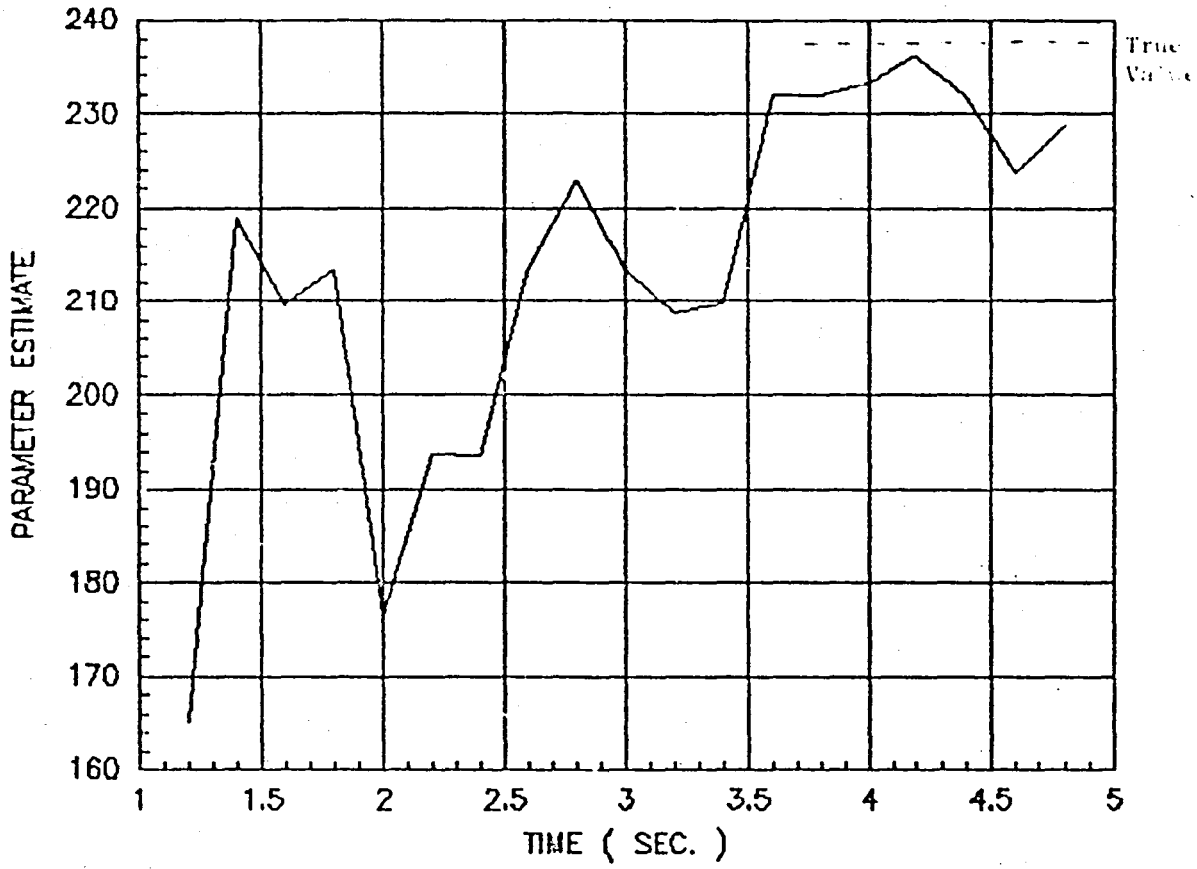

Figure 4-7b. Estimates of Parameter T_{11} as a Function of the Length of Data (5% Noise Level) (Another Sample Run)

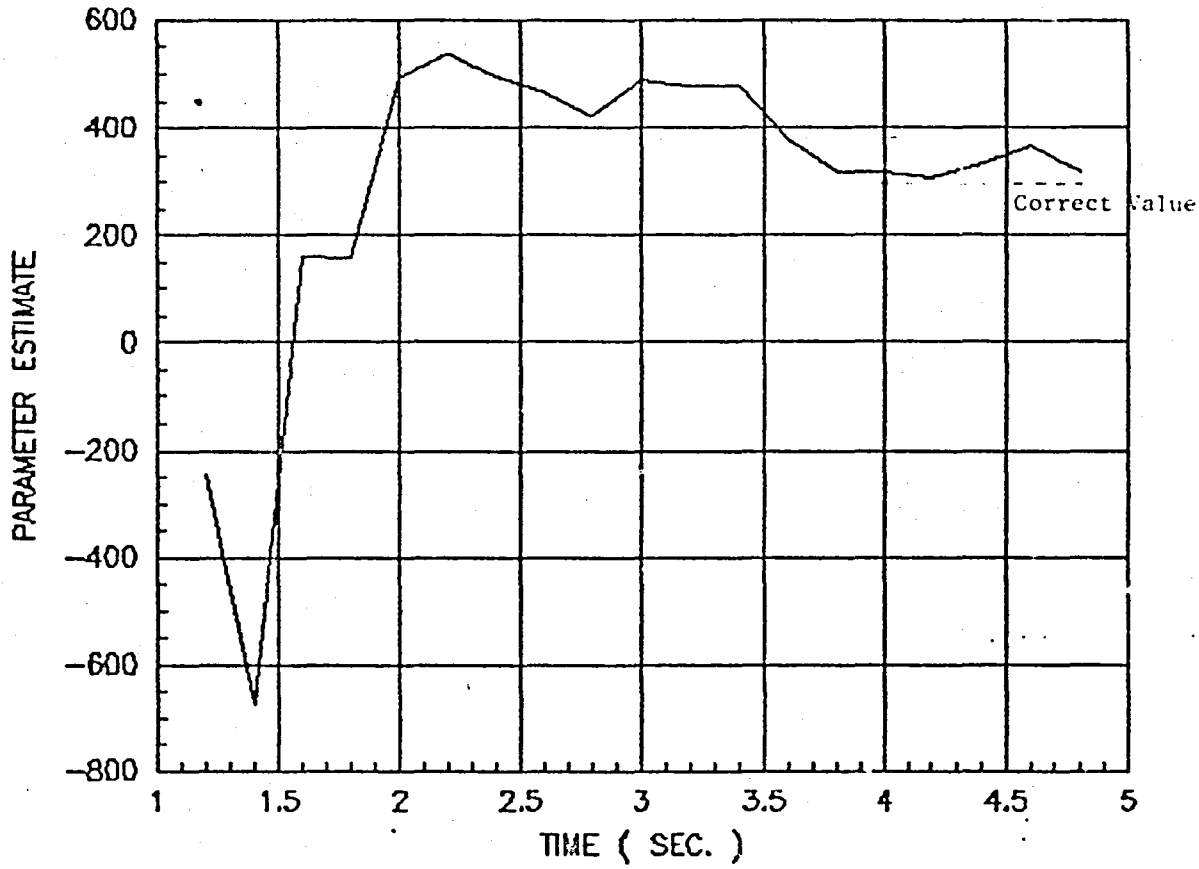

Figure 4-8a. T_{11} Parameter Convergence in the Time Domain
(for 25% Measurement Noise Level)

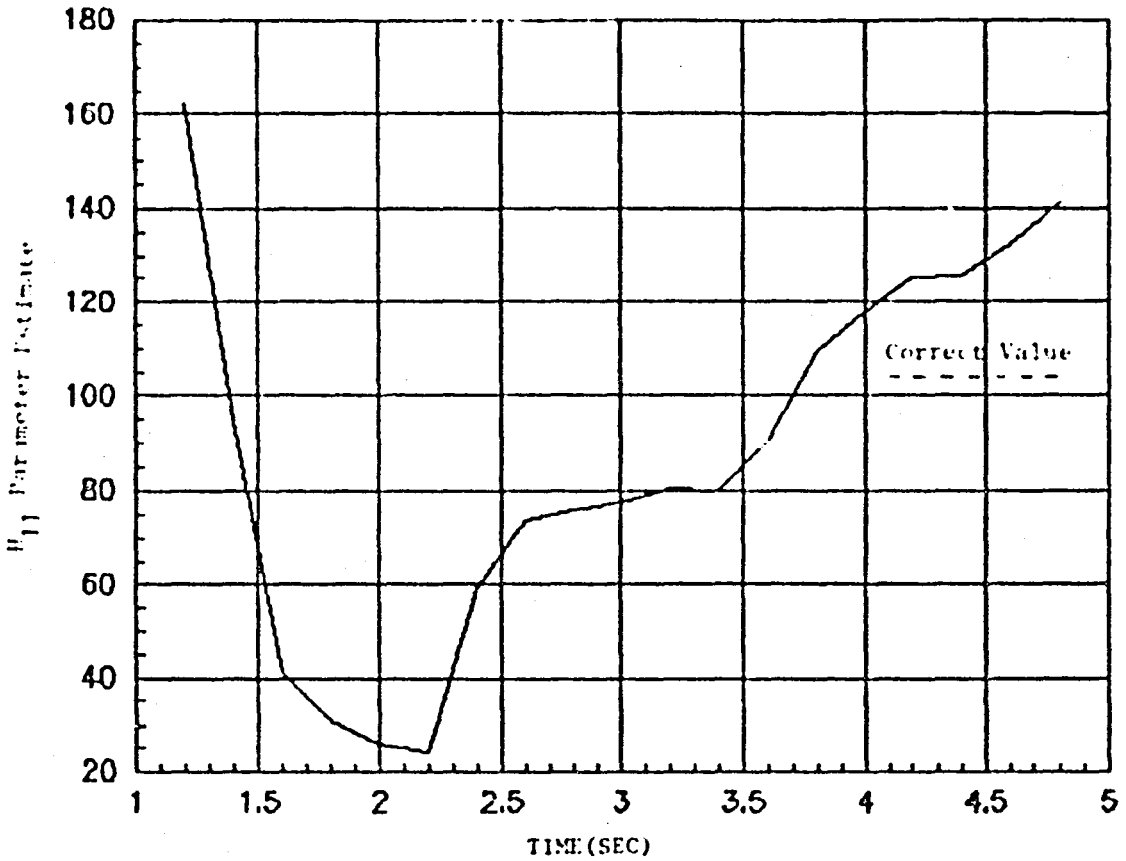

Figure 4-8b. Convergence Characteristics of Parameter B_{11} in the Time Domain (25% Measurement Noise Level)

C-2

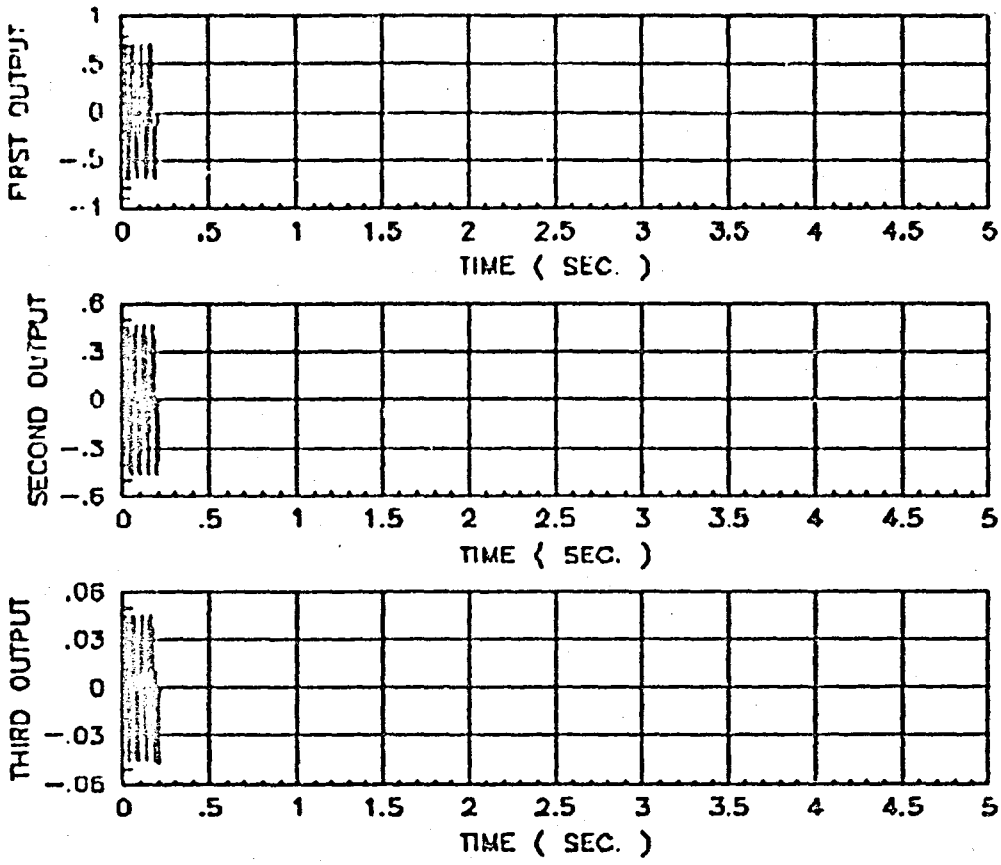

Figure 4-9. Frequency-Domain Control Law with No Noise and $G = T^{-1}$
(Sensor Output and Vibration)

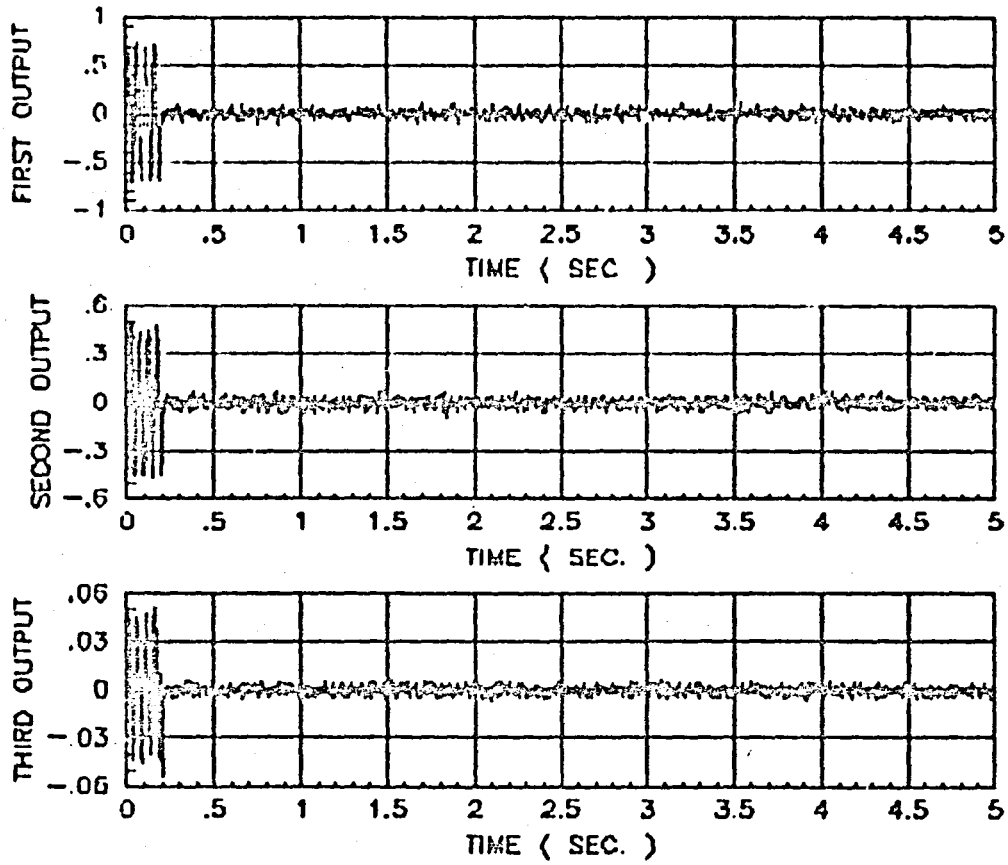

Figure 4-10a. Frequency-Domain Control Law with 5% Measurement Noise and $G = T^{-1}$ (Sensor Output)

(Note: Each second corresponds to 5 rotor cycles)

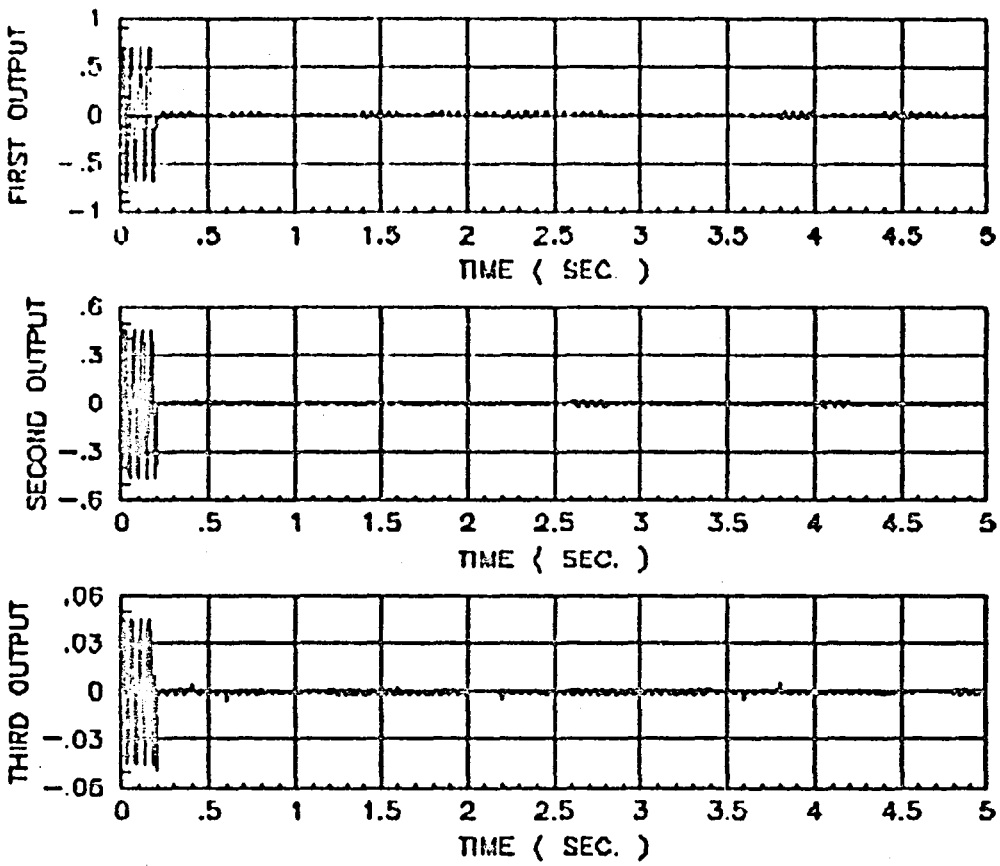

Figure 4-10b. Frequency-Domain Control Law with 5% Measurement Noise (Rotorcraft Vibration)

(Note: Each second corresponds to 5 rotor cycles)

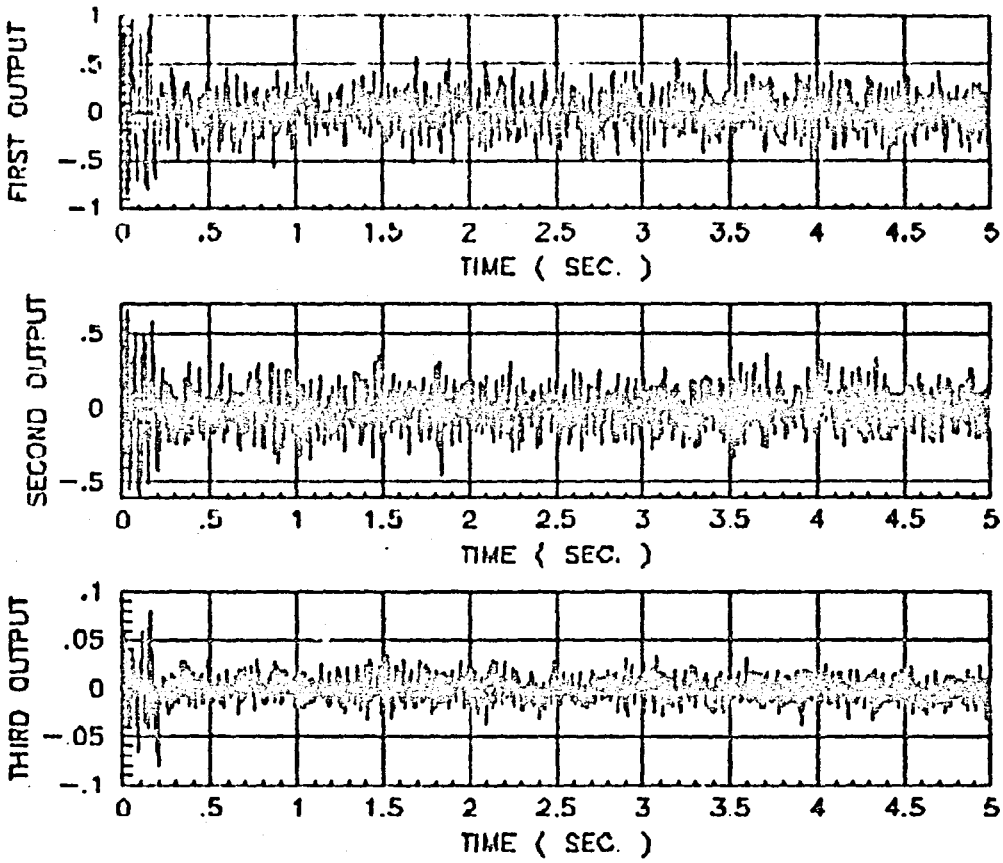

Figure 4-11a. Frequency-Domain Control Law with 25% Noise and $G = T^{-1}$ (Sensor Output)

(Note: Each second corresponds to 5 rotor cycles)

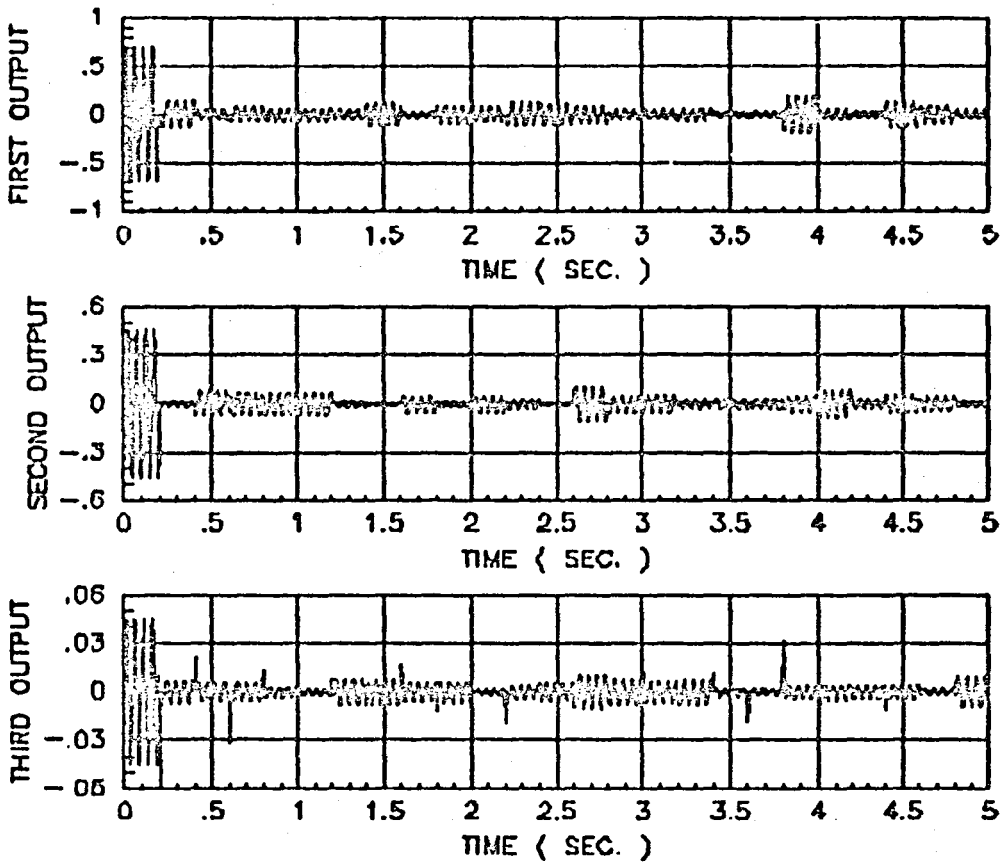

Figure 4-11b. Actual Rotorcraft Vibration Using Frequency-Domain Control with 25% Measurement Noise and $G = T^{-1}$
(Note: Each second corresponds to 5 rotor cycles)

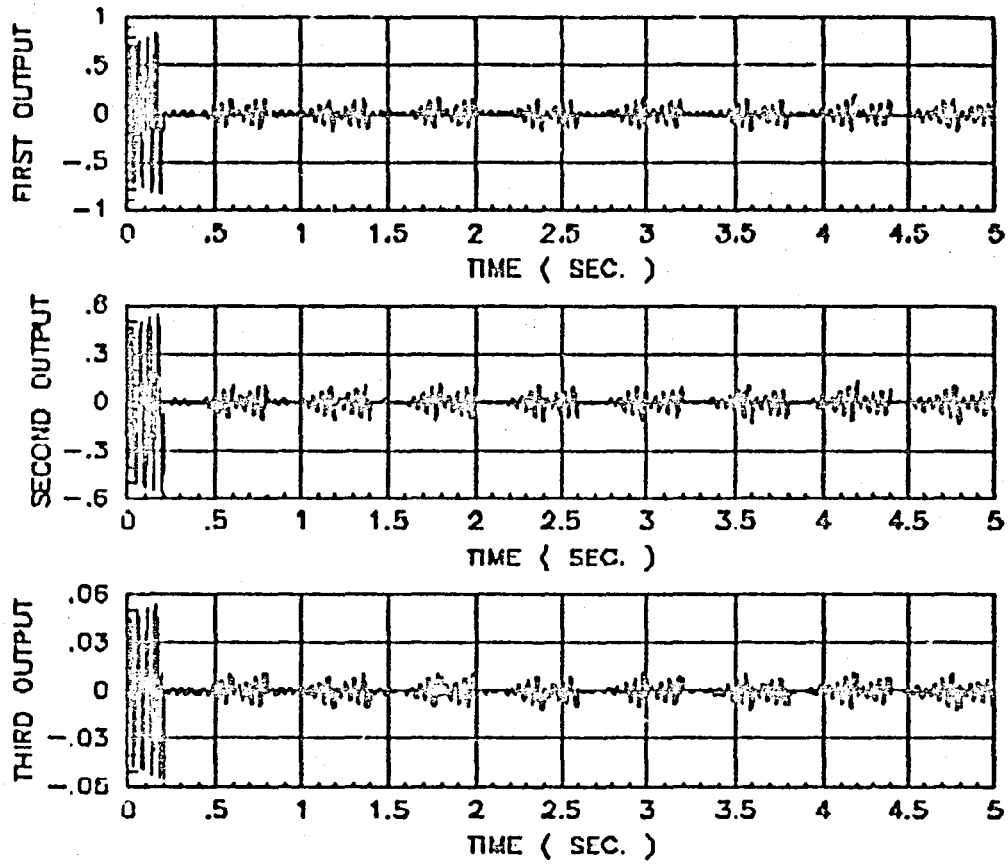

Figure 4-12. Rotorcraft Vibration with Frequency-Domain Control Law, Pilot-Induced Variation in Open-Loop Vibration and $G = T^{-1}$

(Note: Each second corresponds to 5 rotor cycles)

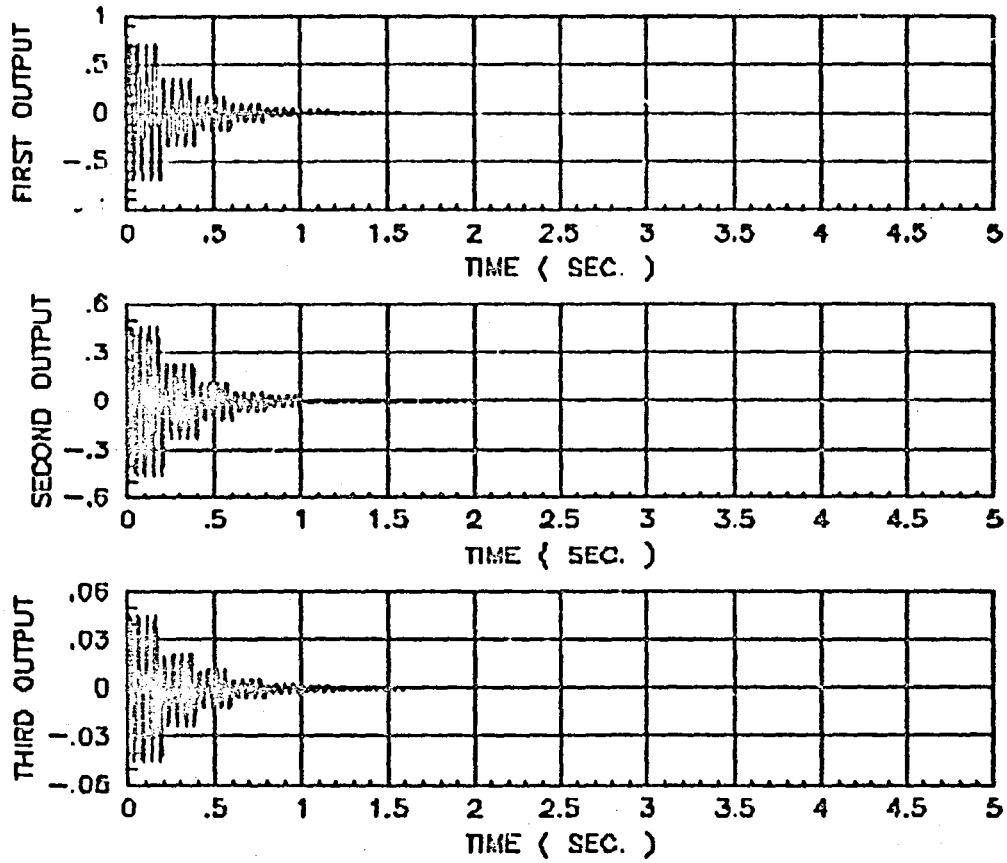

Figure 4-13. Closed-Loop Rotorcraft Vibration with No Measurement Noise and $G = 0.5\ T^{-1}$

(Note: Each second corresponds to 5 rotor cycles)

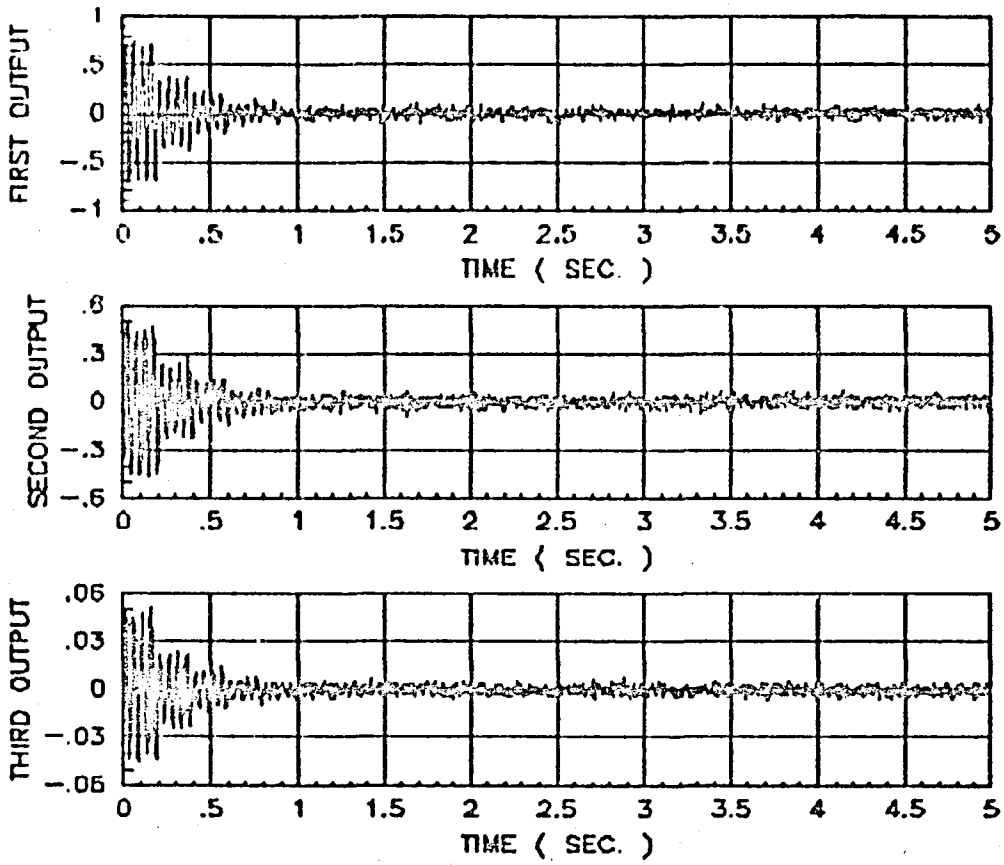

Figure 4-14a. Frequency-Domain Controller with 5% Measurement Noise and $G = 0.5\ T^{-1}$ (Sensor Outputs)

(Note: Each second corresponds to 5 rotor cycles)

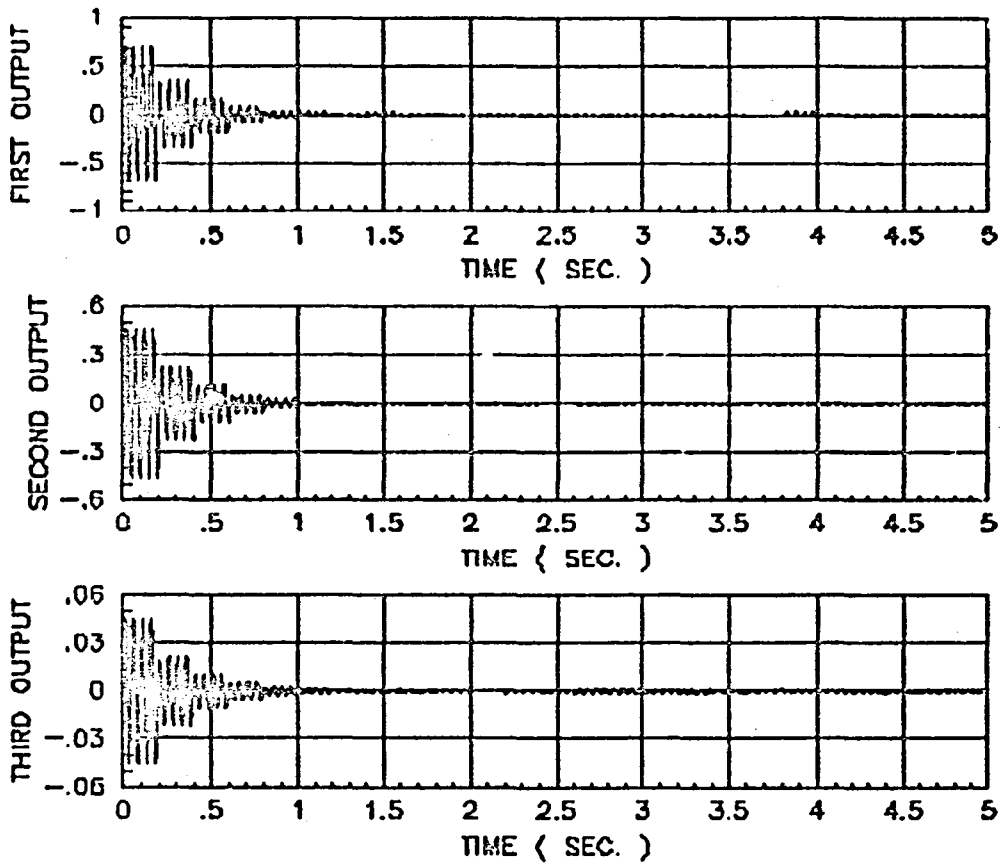

Figure 4-14b. Continued (Actual Vibrations)
(Note: Each second corresponds to 5 rotor cycles)

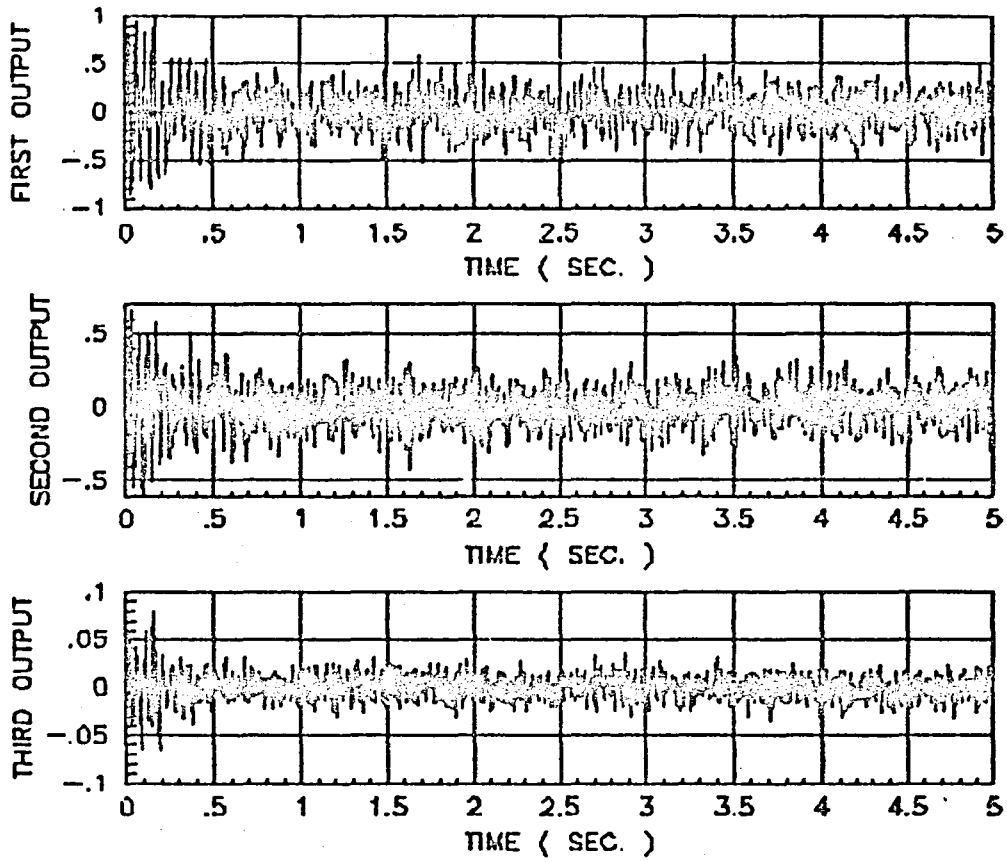

Figure 4-15a. Frequency-Domain Vibration Control Law with 25% Measurement Noise and $G = 0.5\ T^{-1}$ (Sensor Outputs)
(Note: Each second corresponds to 5 rotor cycles)

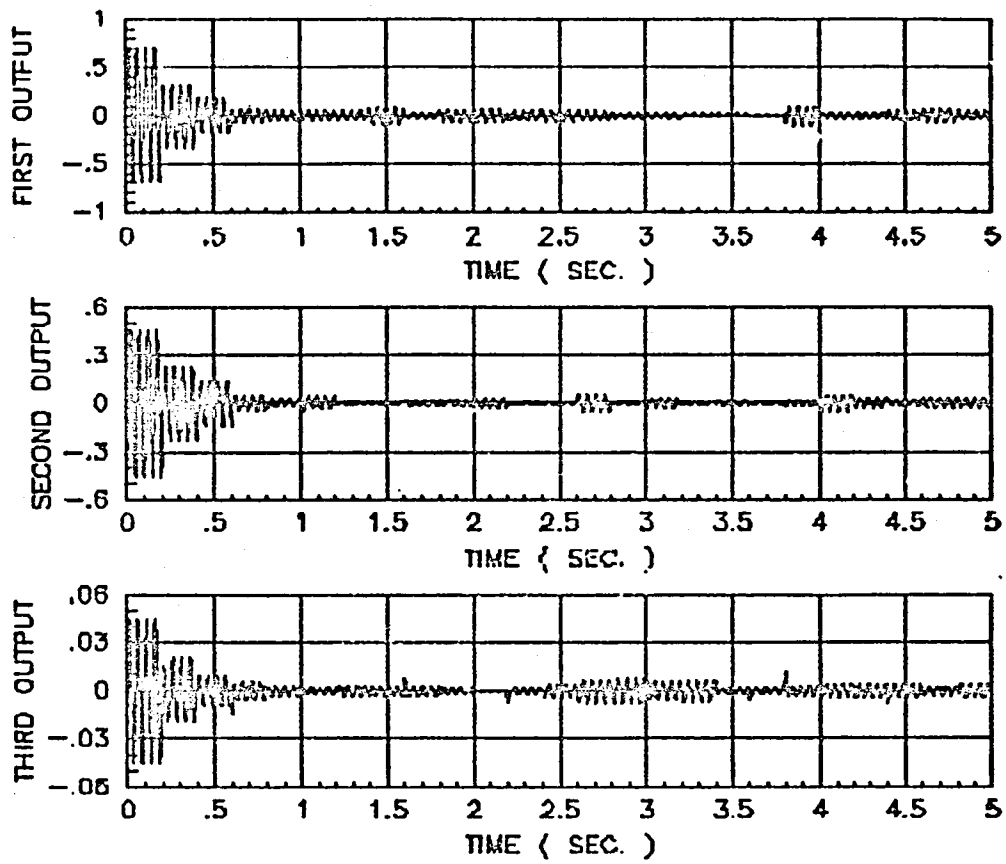

Figure 4-15b. Continued (Actual Vibrations)

(Note: Each second corresponds to 5 rotor cycles)

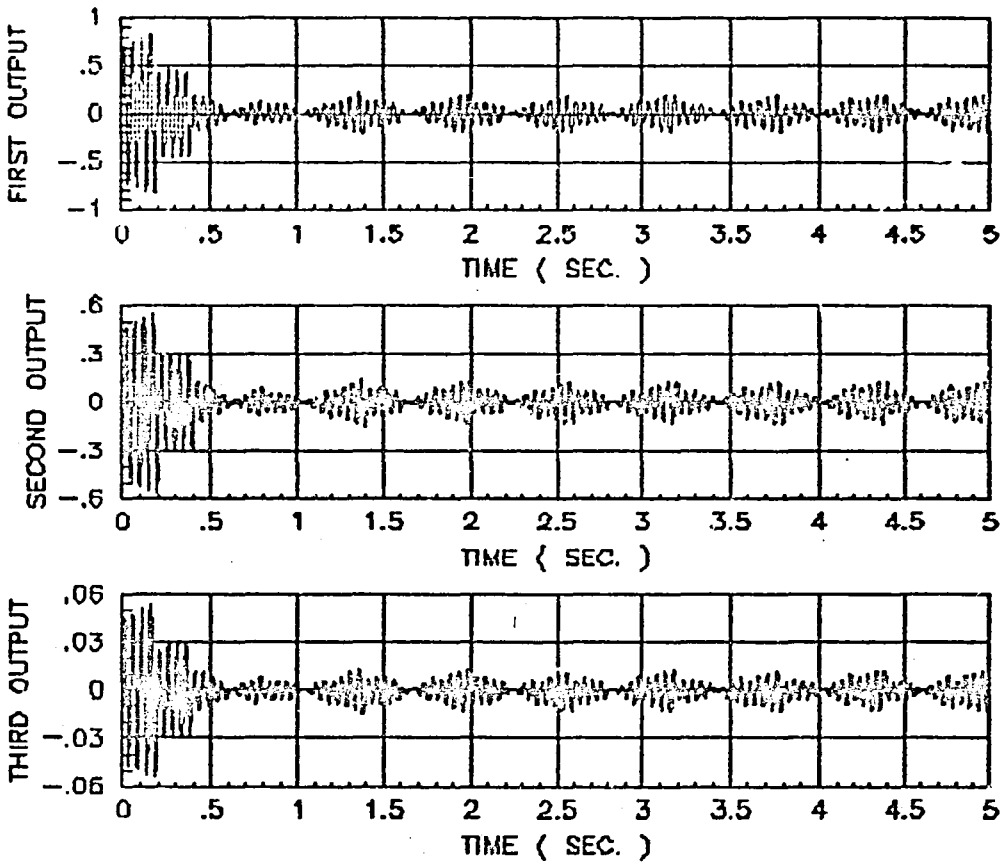

Figure 4-16. Actual Rotorcraft Vibration with Frequency-Domain Controller in the Presence of Pilot-Induced Variation in Open-Loop Vibration and $G = 0.5T^{-1}$
(Note: Each second corresponds to 5 rotor cycles)

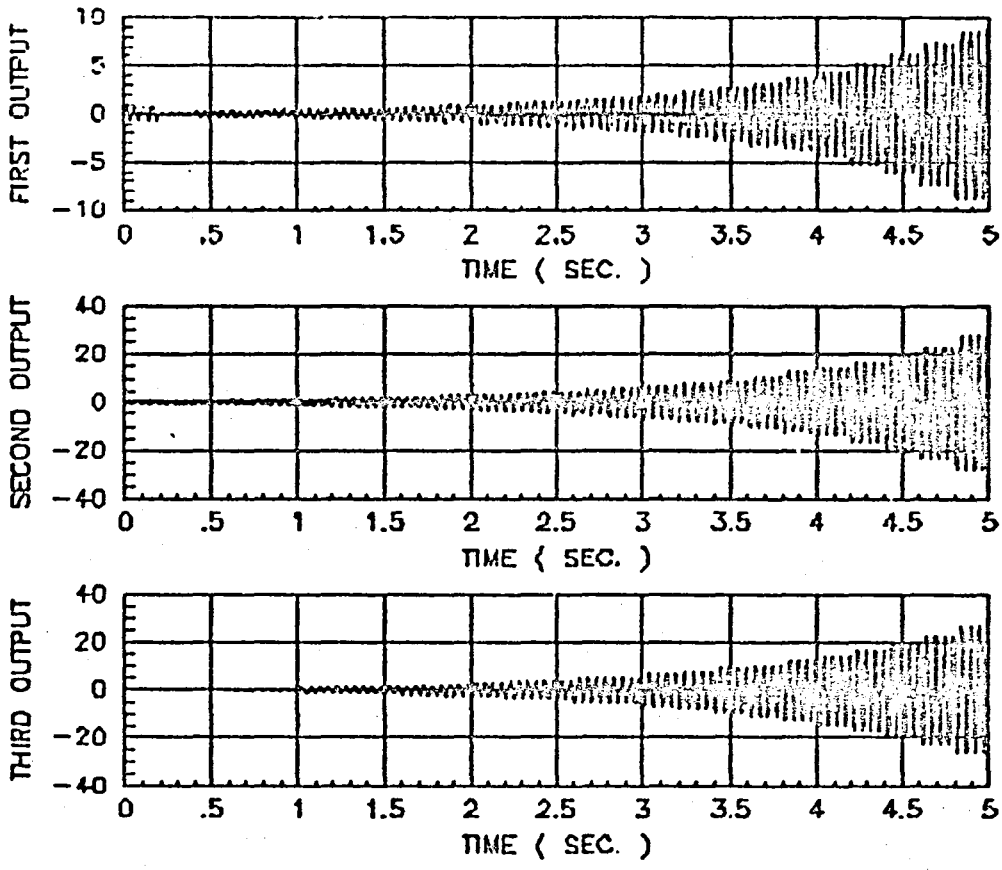

Figure 4-17. Frequency-Domain Vibration Control Law with 5% Measurement Noise and $G = (T^T T + A)^{-1}(T^T + B)$ ($A = 10^5$ and $B = 400$)

(Note: Each second corresponds to 5 rotor cycles)

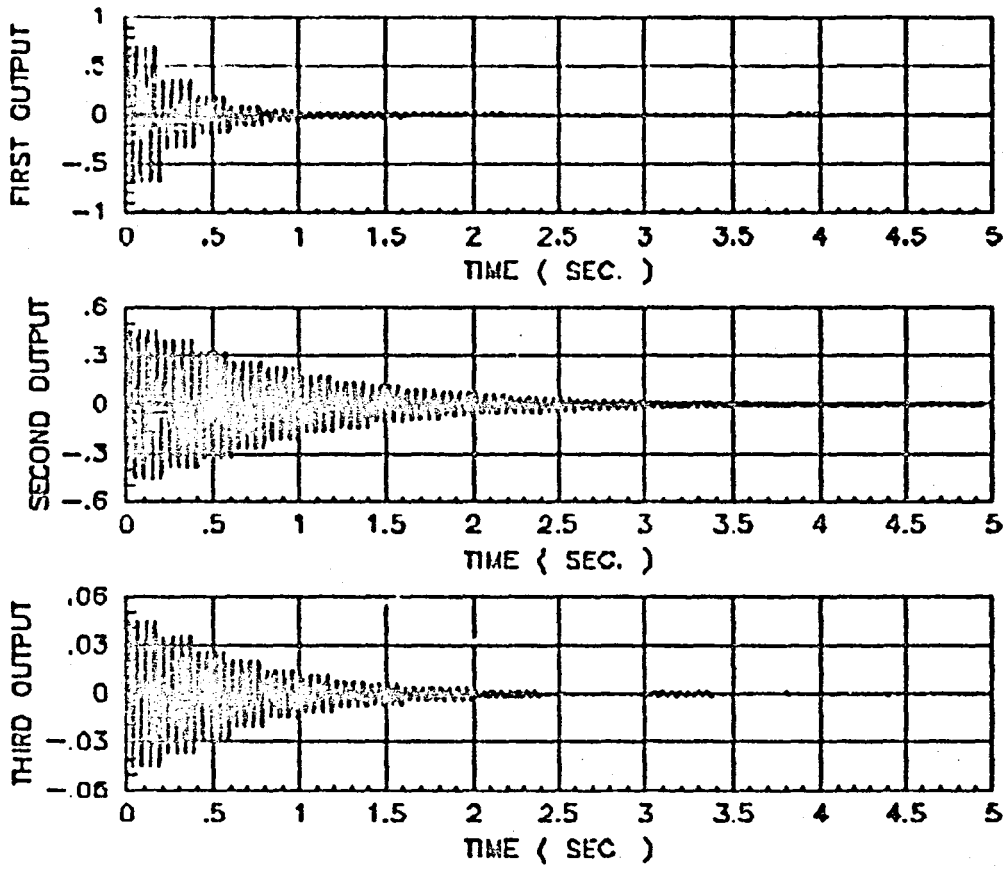

Figure 4-18b. Continued (Actual Vibration)

(Note: Each second corresponds to 5 rotor cycles)

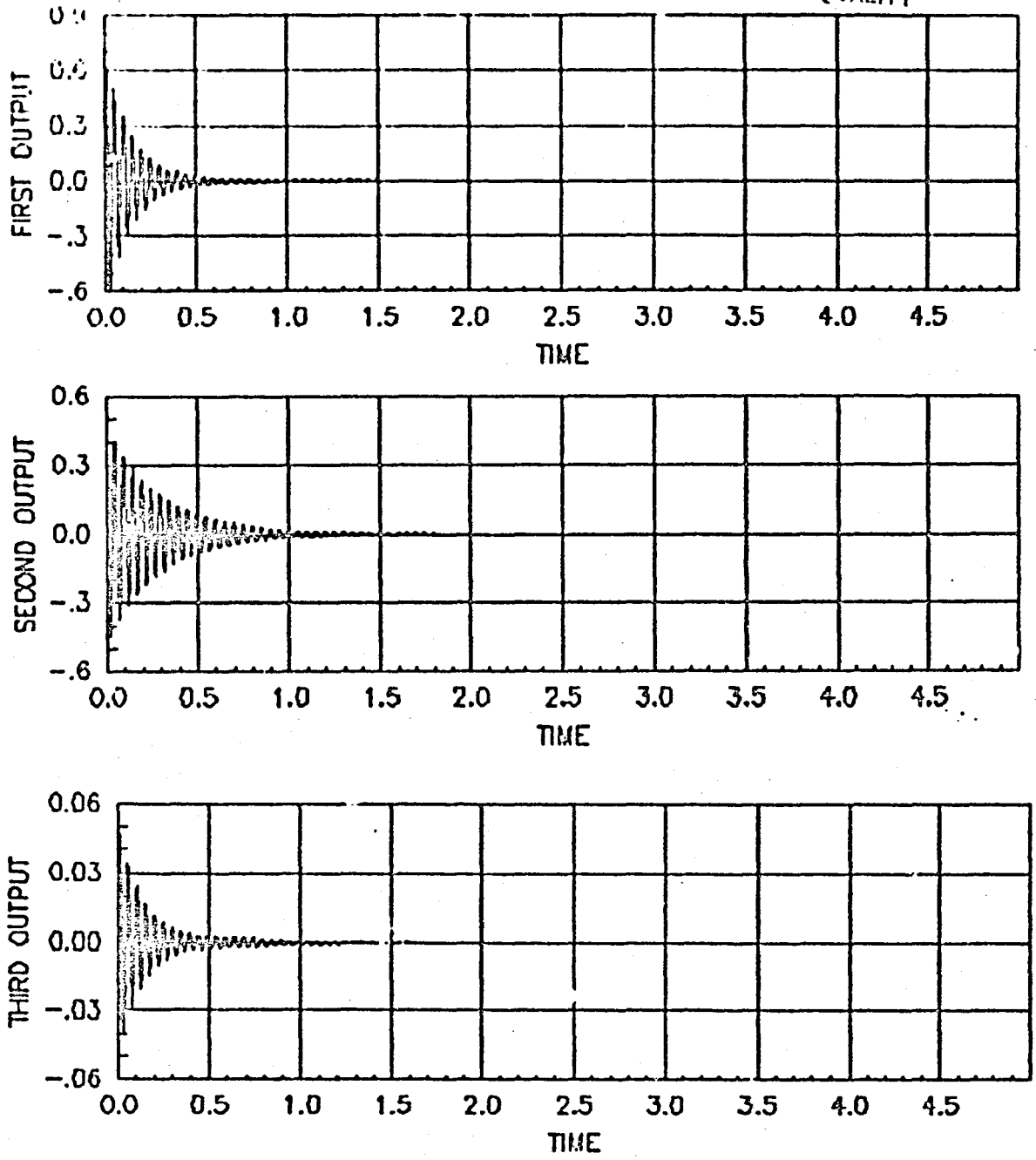

Figure 4-19. Response of the Closed-Loop System with $b = 3 \times 10^8$ and no Measurement Noise

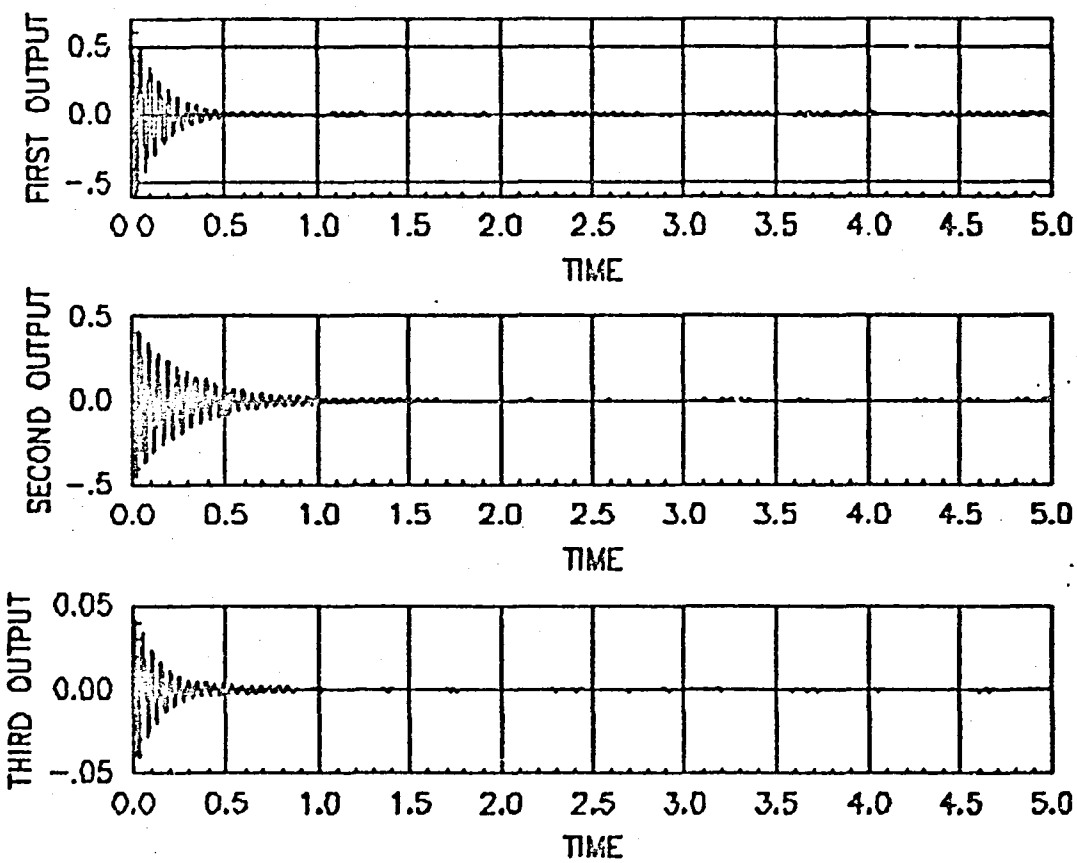

Figure 4-20. Closed-Loop Response with 5% Measurement Noise

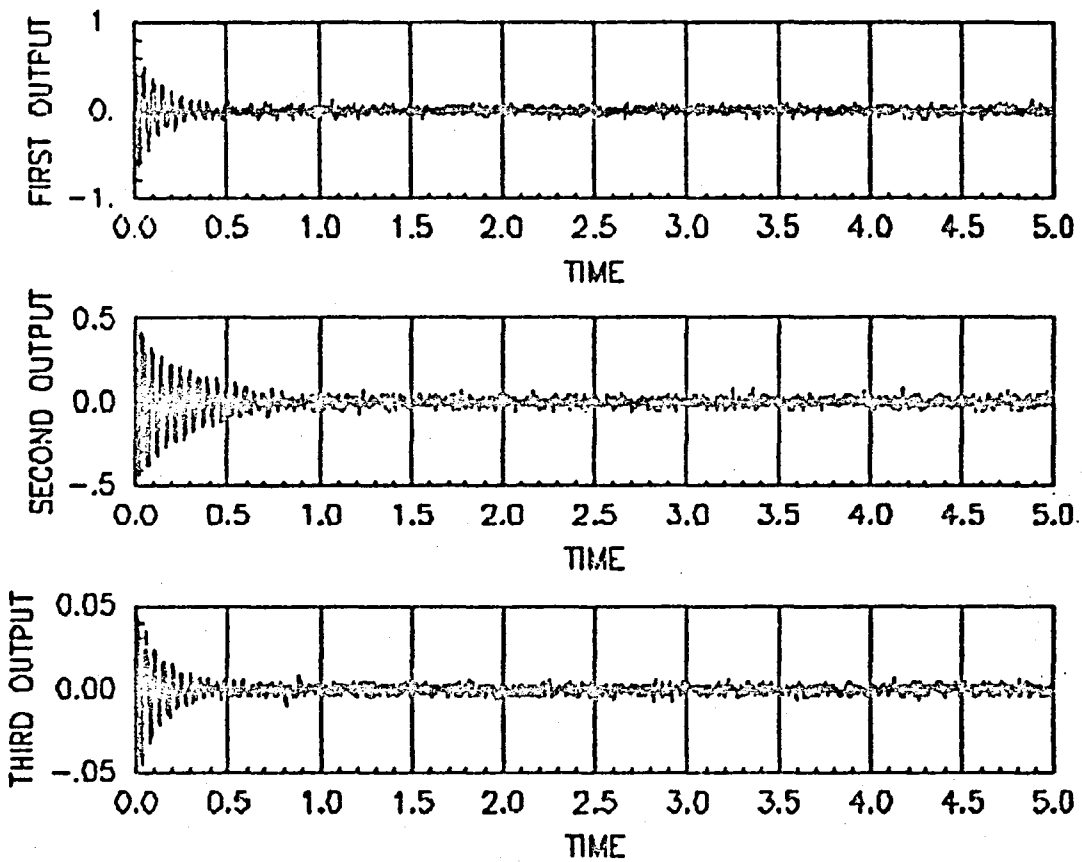

Figure 4-21. Measured Output with 5% Noise Level

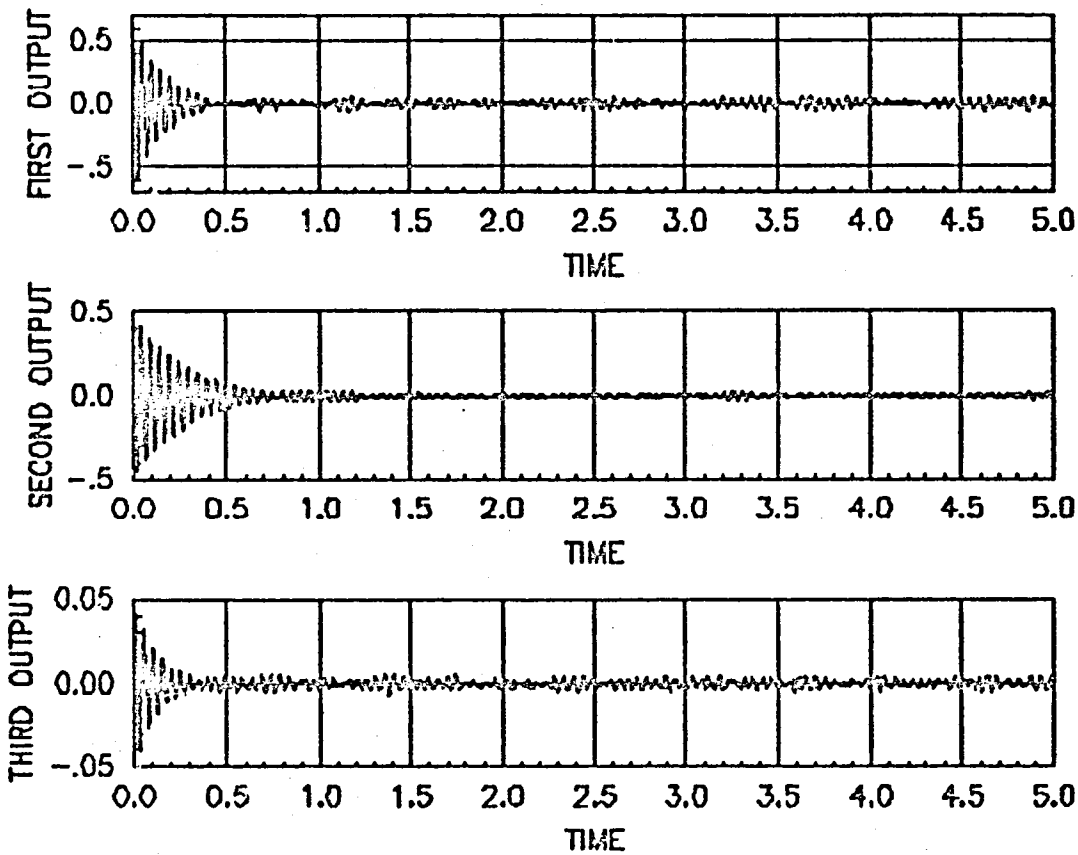

Figure 4-22. Closed-Loop Rotorcraft Vibration with 25% Measurement Noise

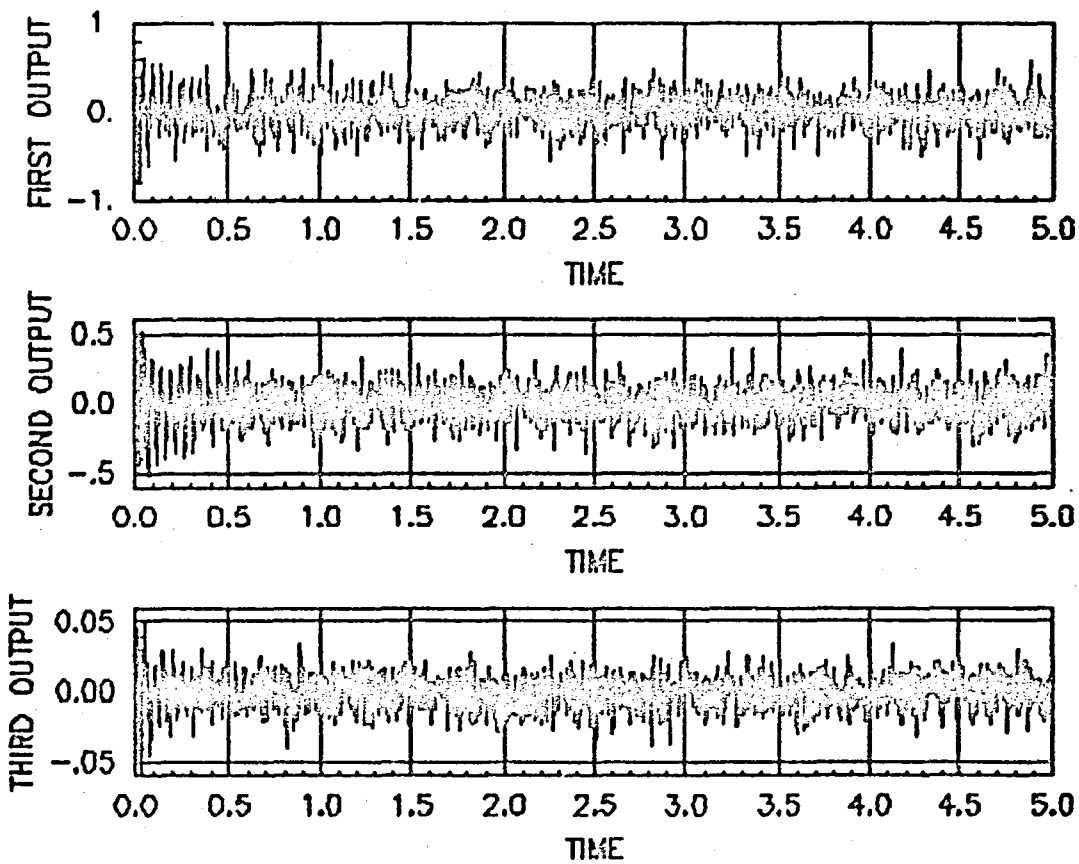

Figure 4-23. Measured Output with 25% Noise Level

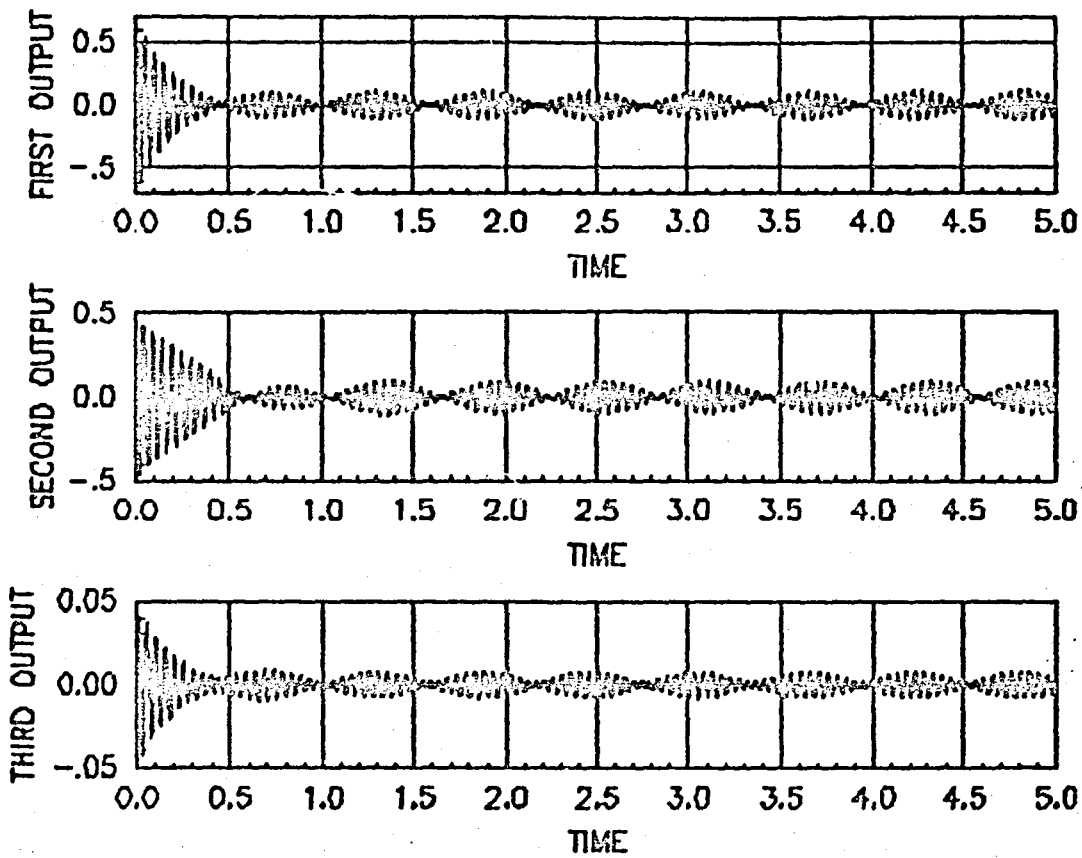

Figure 4-24. Closed-Loop Response of the System with Pilot Inputs

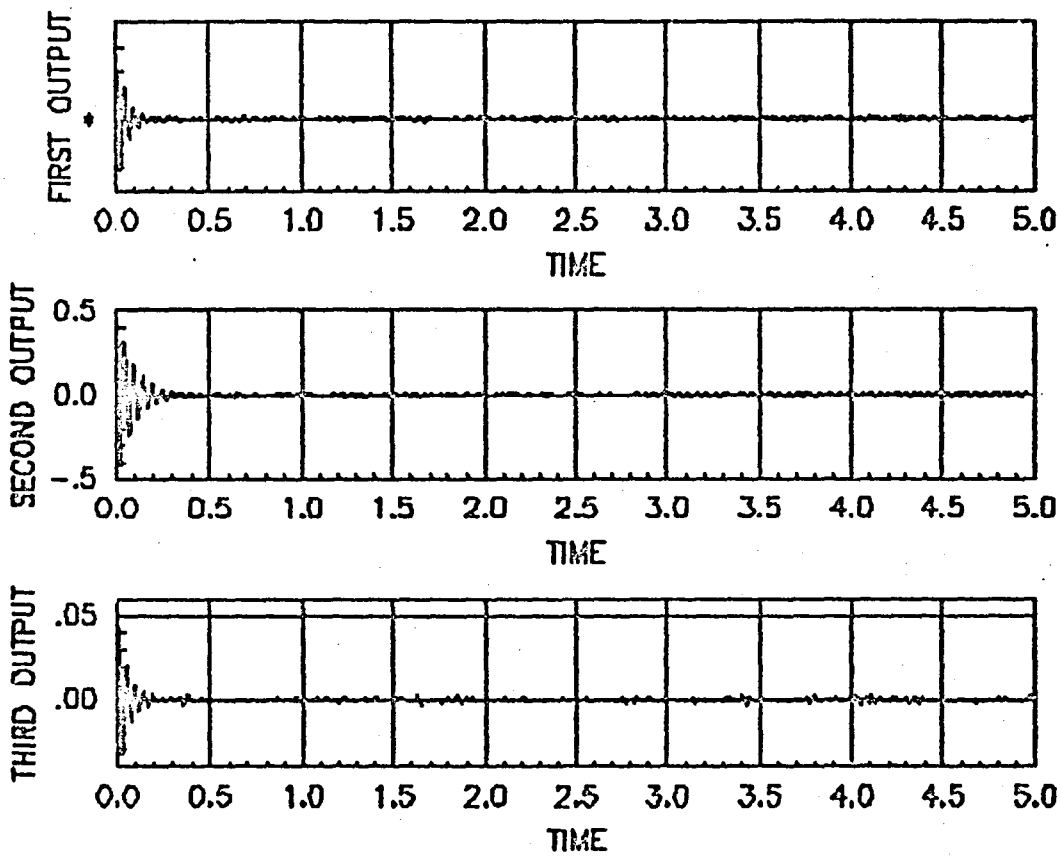

Figure 4-25. Closed-Loop Vibration with 5% Measurement Noise and $b = 3 \times 10^{7}$ (Controller with Medium Speed)

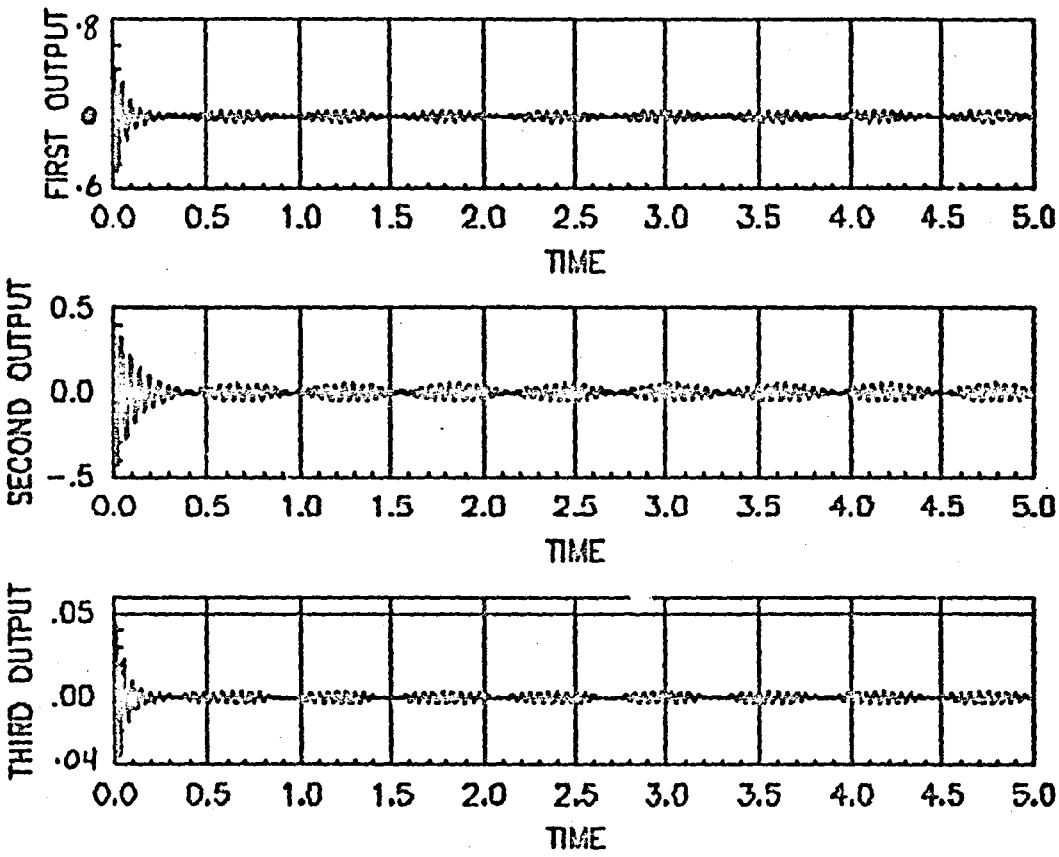

Figure 4-26. Closed-Loop Vibration with Pilot-Induced Variation in Open-Loop Vibration Time History (controller with medium speed)

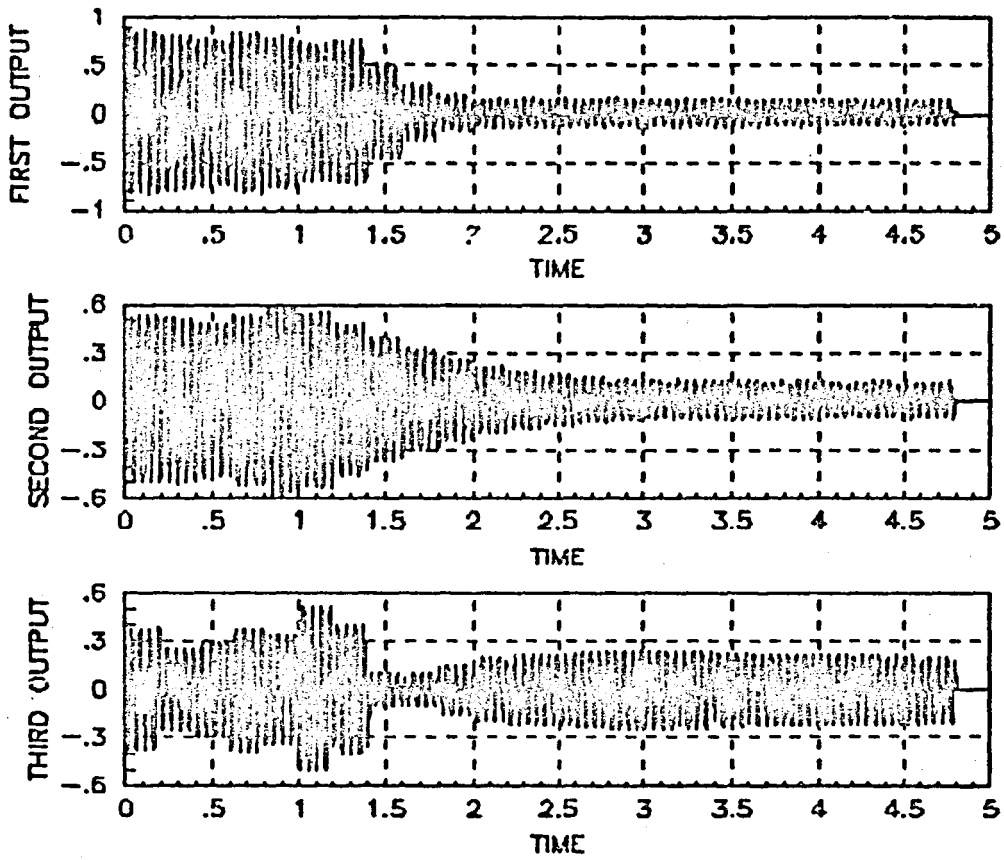

Figure 4-27. Measured Rotorcraft Vibration with Joint Estimation and Frequency-Domain Control (5% Measurement Noise)

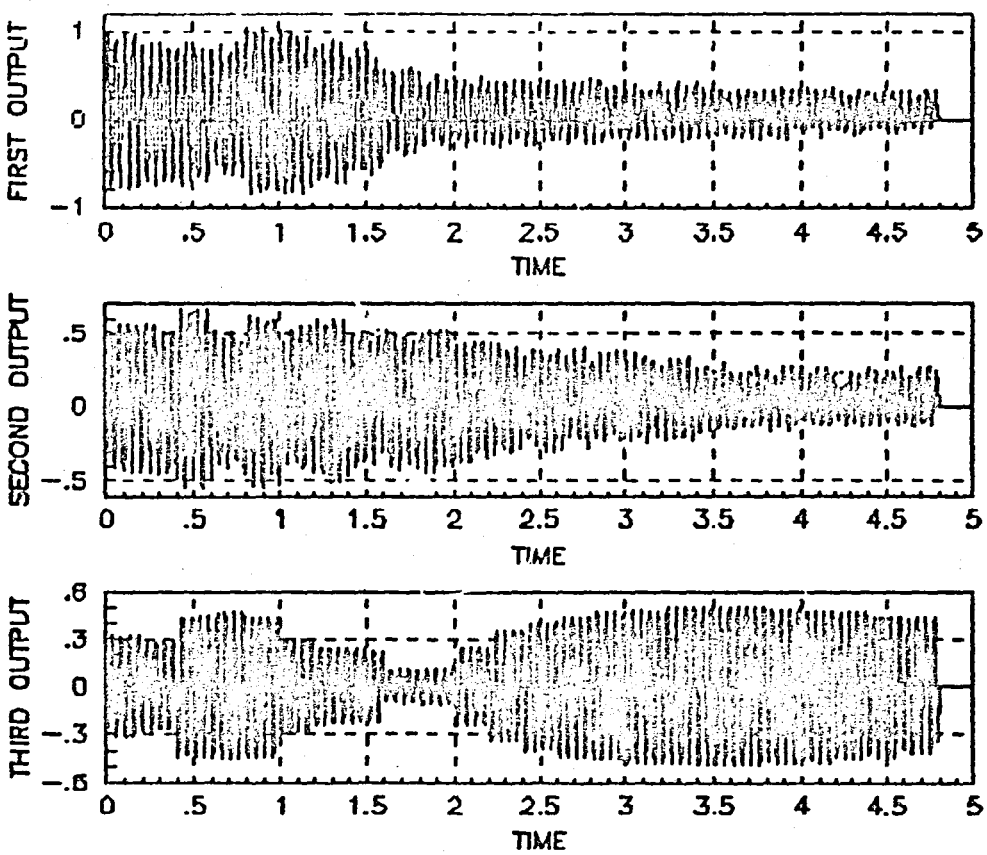

Figure 4-28. Measured Rotorcraft Vibration with Joint Estimation and Frequency-Domain Control (25% Measurement Noise)

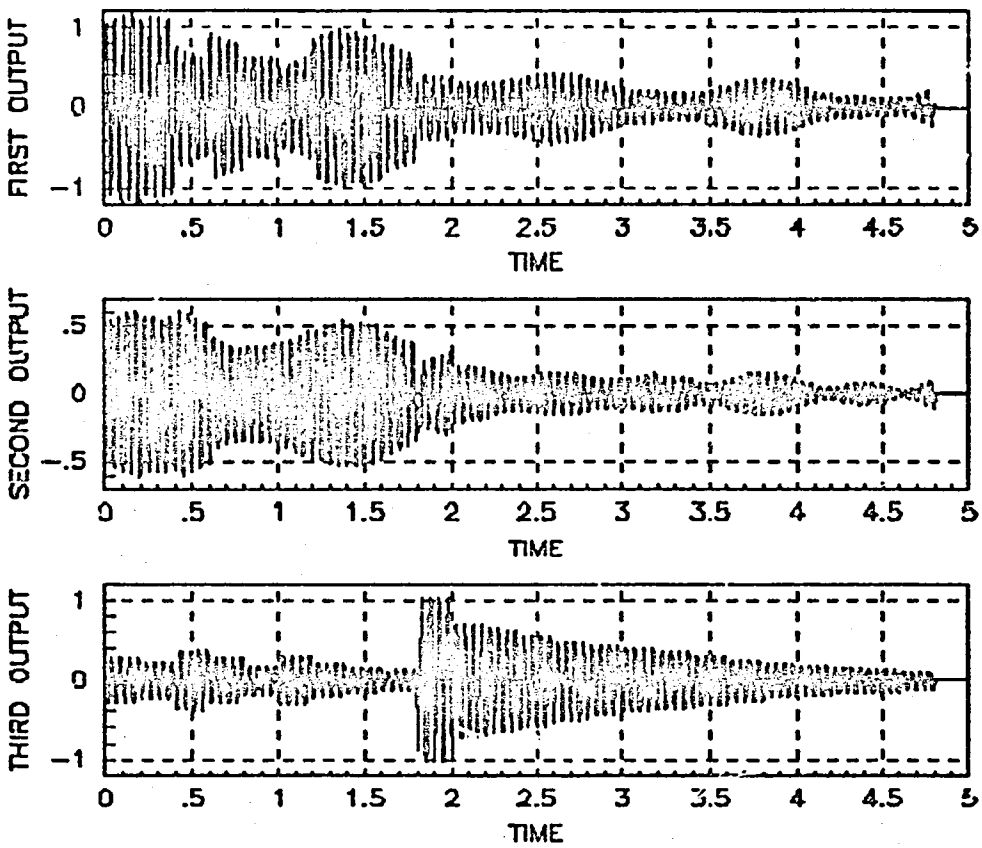

Figure 4-29. Measured Rotorcraft Vibration with Joint Estimation and Frequency-Domain Control (Variation in Open-Loop Vibration Due to Pilot Applied Inputs)

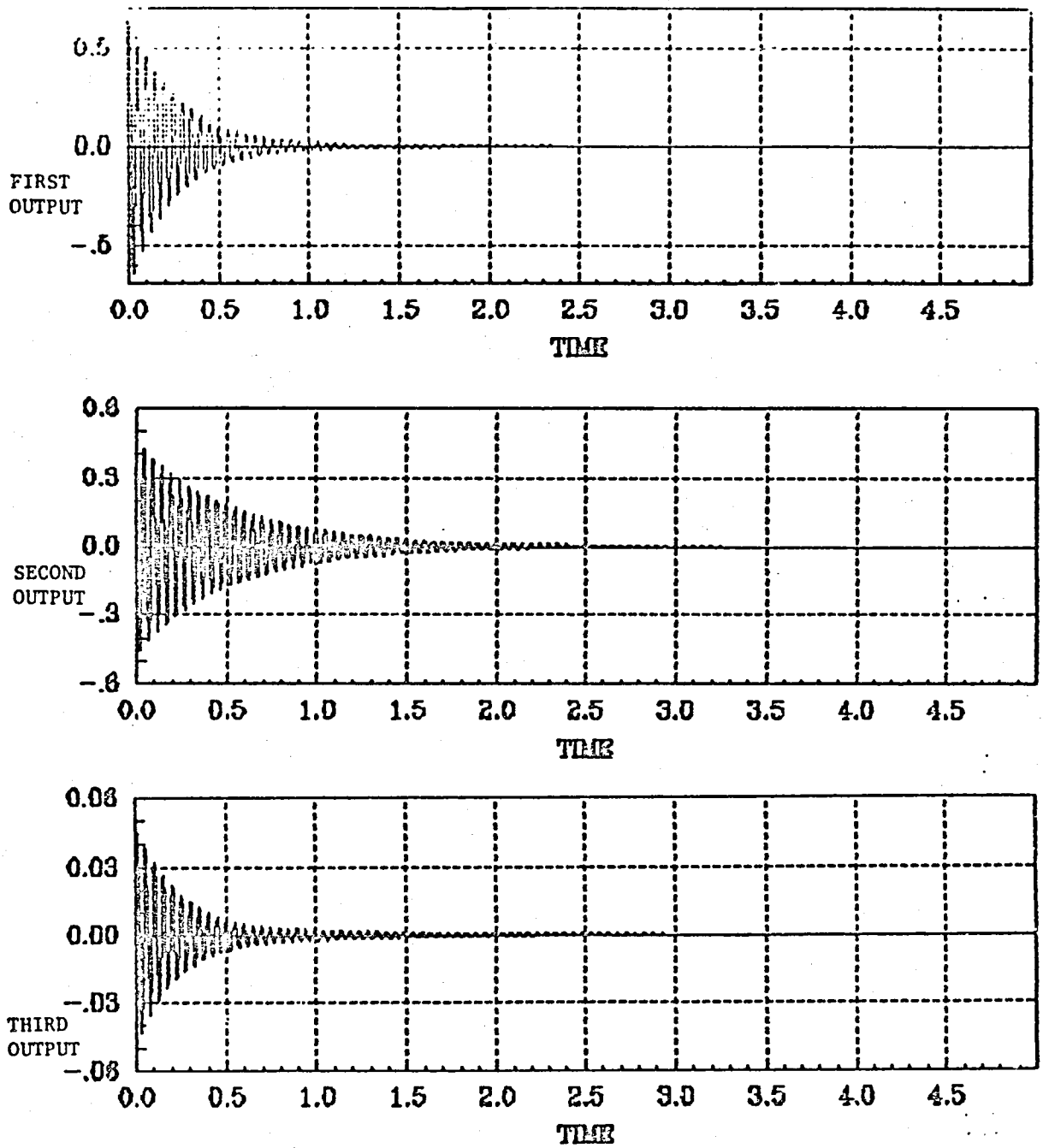

Figure 4-30. Response of the Time-Domain Controller with Real-Time Estimation and Control

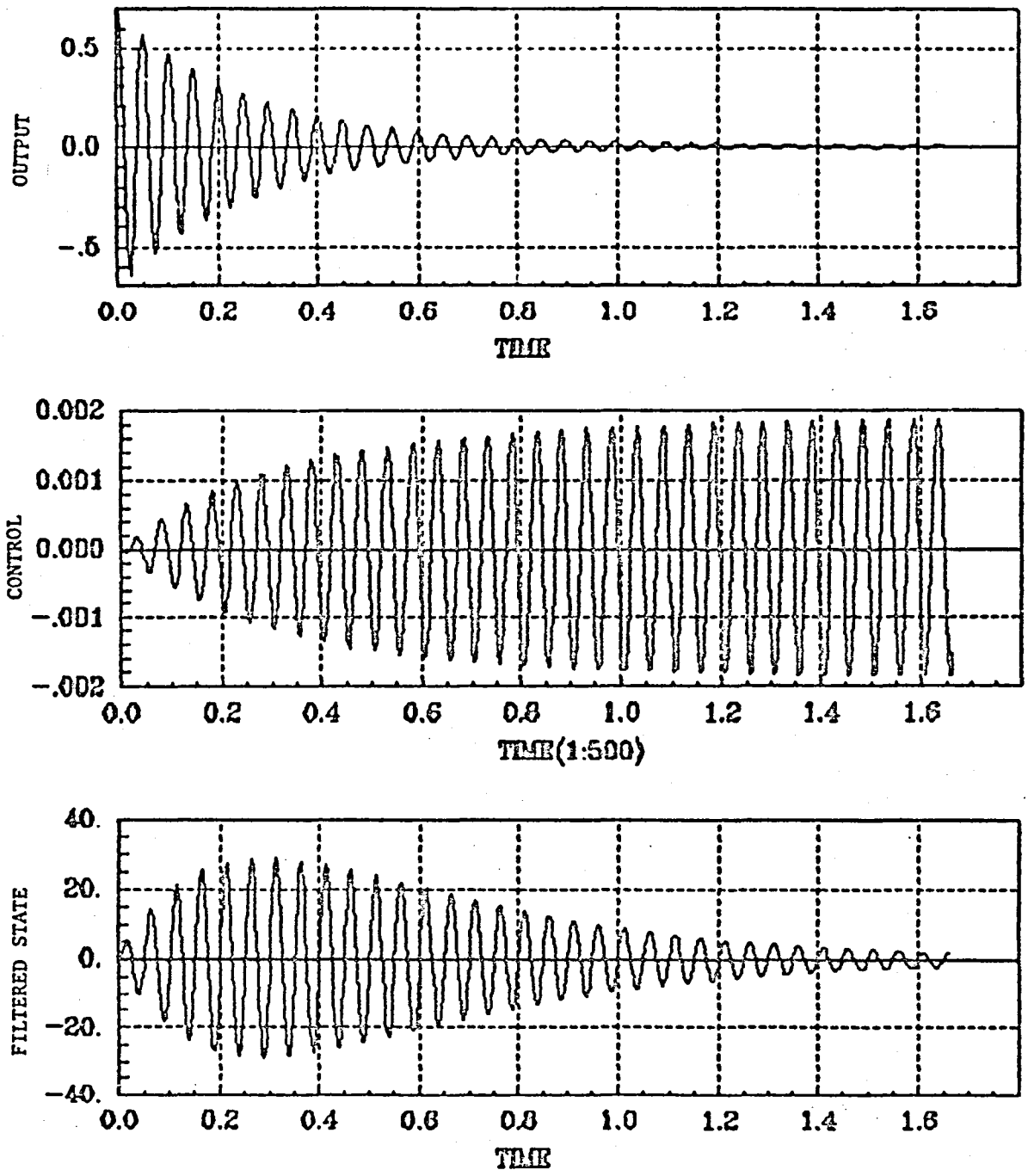

Figure 4-31. Time-Domain Controller with No Measurement Noise and On-Line Estimation

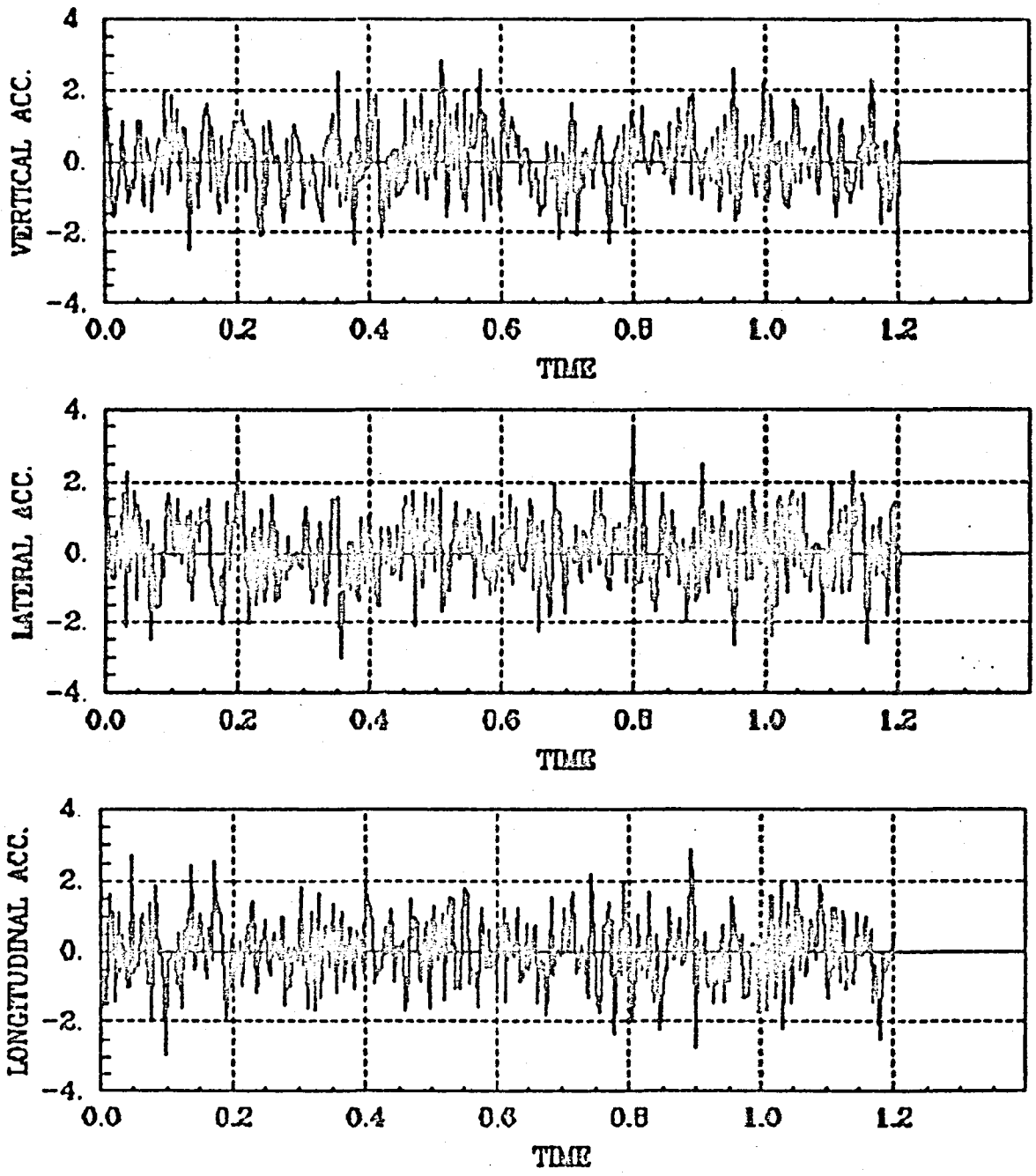

Figure 4-32. Measured Acceleration Time Histories with White-Gaussian Measurement Noise of RMS .6

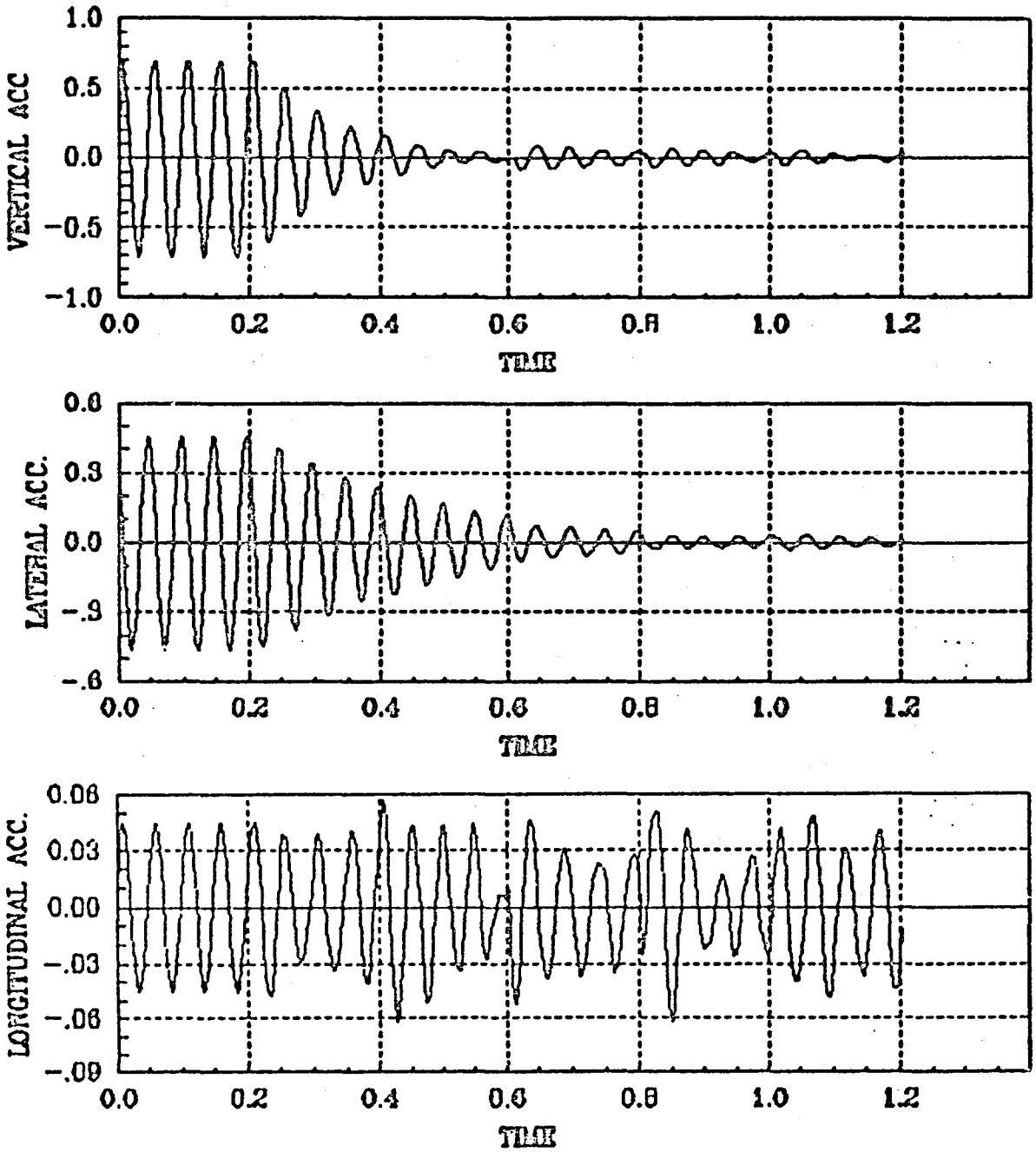

Figure 4-33. Actual Closed-Loop Accelerations in the Presence of Large white-Gaussian Noise

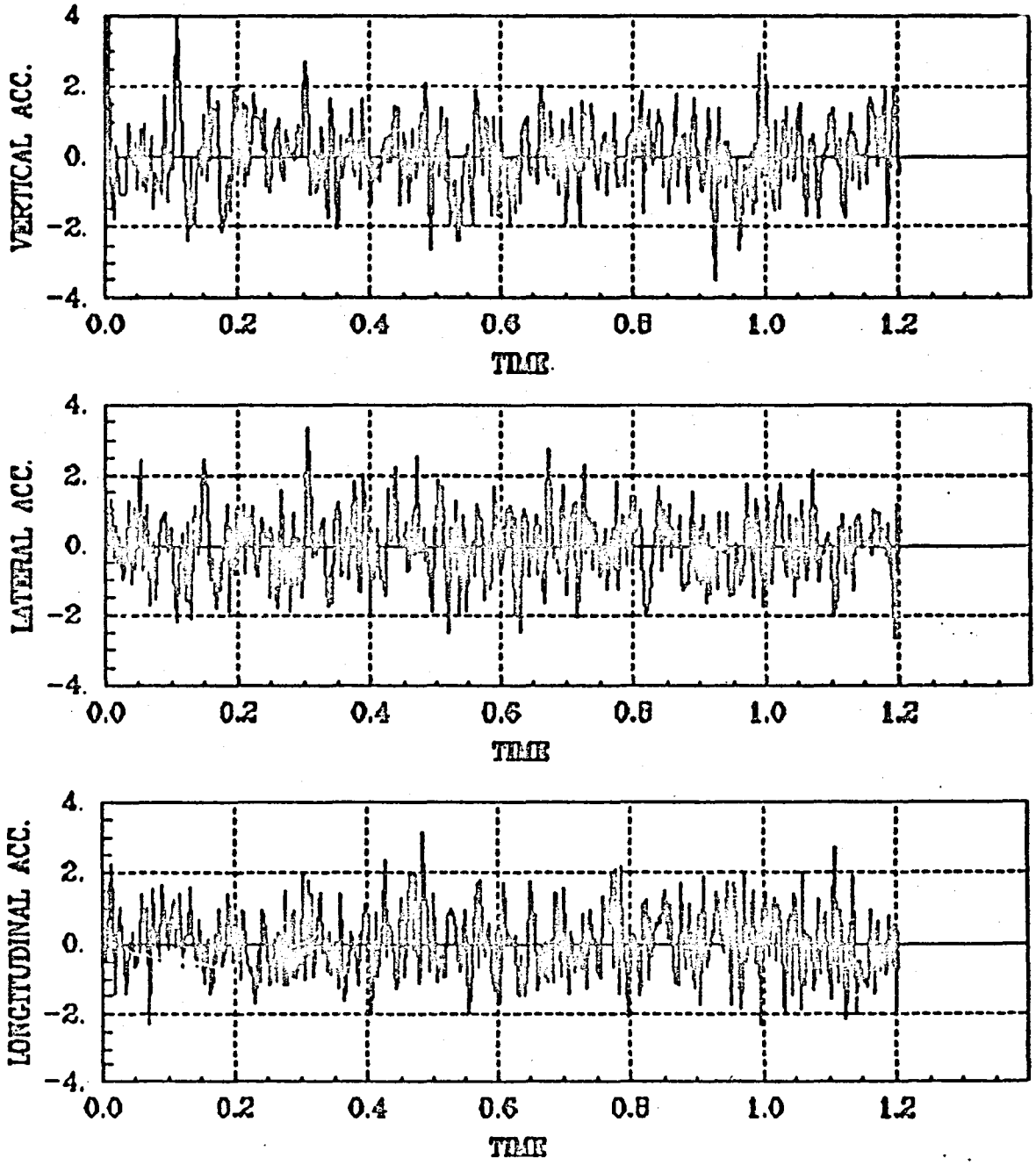

Figure 4-34. Measured Accelerations with Narrow-Band Noise
(Noise in ± 1/rev Around the Vibration Frequency)

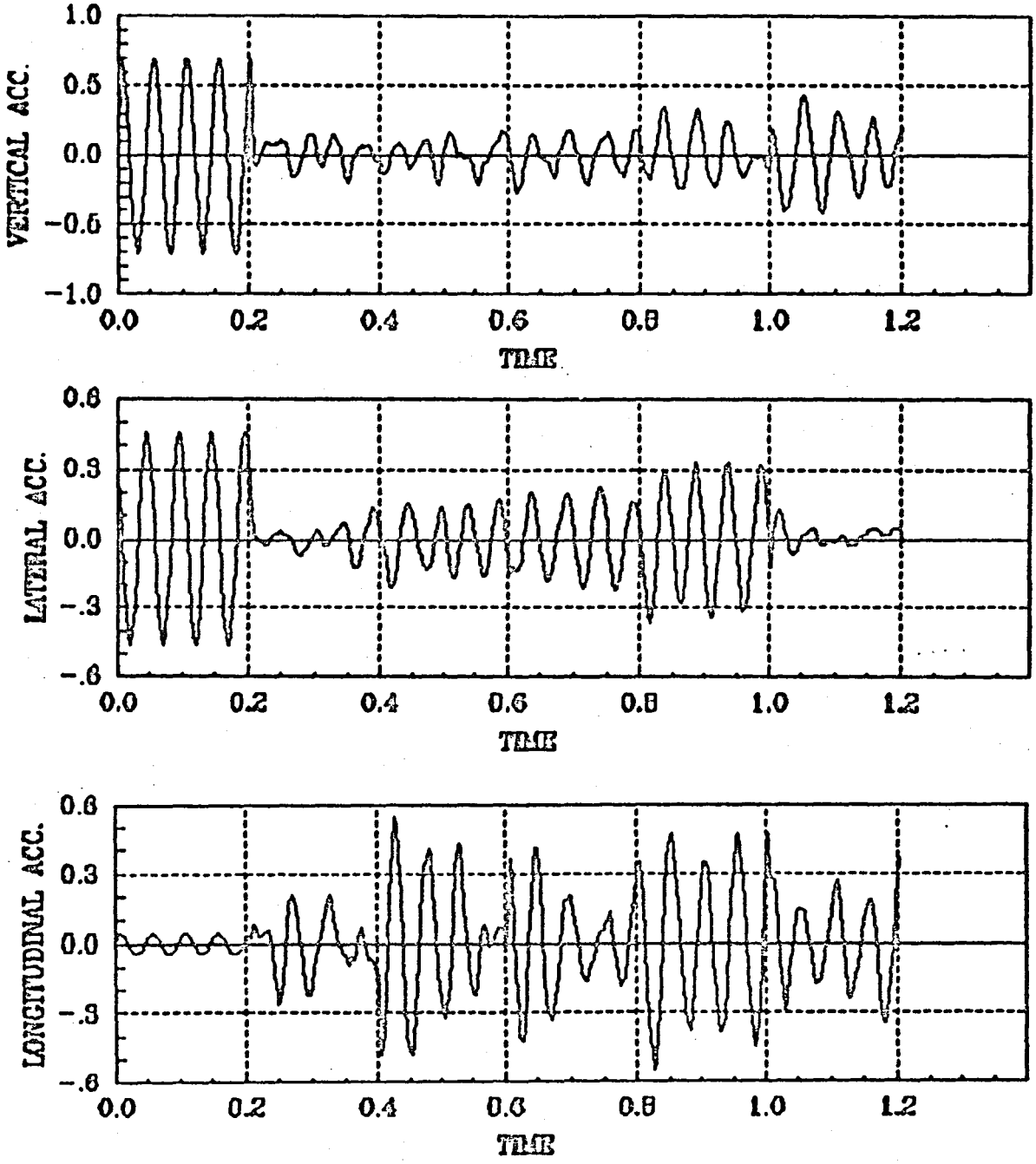

Figure 4-35. Closed-Loop Vibration with Narrow-Band Measurement Noise

APPENDIX A

MATRIX$_x$: A DATA ANALYSIS, SYSTEM IDENTIFICATION, CONTROL DESIGN, AND SIMULATION PACKAGE

MATRIX$_x$ is an interactive software system for the computer-aided-design and analysis of control systems for dynamic plants. In particular, data analysis, system identification, model reduction, control design, evaluation and simulation steps can be performed conveniently using MATRIX$_x$. A user-friendly interpreter incorporates powerful operations and easy-to-use graphics. The system can reduce control system design costs and provide capability for rapid analytical, laboratory and full scale testing of new control concepts.

DESIGN PHILOSOPHY

The design and development of MATRIX$_x$ is based on two simple ideas:

1. It should be possible to use most design and analysis techniques to solve any problem. The system must be responsive to the particular tastes of a control system designer. The outputs should be available in formats that are easy to comprehend.

2. A single computer program must be capable of performing most operations of interest to a control design engineer, because transferring files and data from one program to another can consume a major portion of an analyst's time.

MATRIX$_x$ implements commonly used design and analysis methods and facilitates using other current techniques and even algorithms which might be developed in the future. The software does not advocate any particular philosophy for control design or system identification. For example, both transfer-function and state variable control system design techniques are offered and can be applied to the same problem with equal ease. The overall flexibility of the package will become apparent as the software is described.

MATRIX$_x$ provides a comprehensive set of capabilities in a single integrated package with uniform data structures and file formats (see Figure A-1). Most 'bookkeeping' chores are performed by the software, leaving the control designer free to tackle control problems. It is even possible to implement linear control laws and estimators designed by MATRIX$_x$ directly into a multivariable control processor, MCP-100, designed and built by Integrated Systems, Inc. This implementation requires no knowledge of assembly language or other real-time programming techniques.

MATRIX$_x$ STRUCTURE

The structure of the software has been optimized for flexibility, ease of use, expansion capability and to reduce the need for the control systems experts to learn the details of operating systems and programming languages. Command inputs and graphics or alpha-numeric outputs are in clearly understandable formats.

Figure A-2 shows the overall structure of MATRIX$_x$. The program uses a stack architecture for storing variables in current use, allowing excellent interactive response. Command files and data files, not in current use, are stored on disc. Macros and current data are available on the stack. File management is completely user transparent.

Macro* and command file capabilities are used to build a hierarchical algorithm structure in MATRIX$_x$. The most basic (and often the most used) algorithms are programmed as language primitives. Primitives are the easiest to use and will execute rapidly. Examples of primitives are

---

* Macro capability allows a particular string to be replaced by another (usually much shorter) string. This capability must exist in all good interactive programs or operating systems.

arithmetic operations on matrices, singular value decompositions, Riccati equation solution, fast Fourier transform (FFT) and square root estimate update. Specialized and less commonly used operations are written as macros or command files. When research leads to new algorithms, these algorithms are conveniently written as macros and command files during the 'experimental' stage. Only a selected set of algorithms should then be added as language primitives, if desired. A command file or a macro consists of a series of language primitives and other macros and command files.

$MATRIX_x$ borrows certain aspects of its architecture from MATLAB, a matrix laboratory developed by Moler at Stanford University and now at the University of New Mexico, Albuquerque. MATLAB is in the public domain.

$MATRIX_x$ CAPABILITIES

The overall capabilities of $MATRIX_x$ may be divided into the following broad categories:

1. Matrix, vector and scalar operations,
2. Graphics,
3. Control design,
4. System identification and signal processing, and
5. Simulation and evaluation.

The details on how each of these capabilities is utilized are shown in subsequent sections. A brief summary is given here.

Matrix, Vector and Scalar Operations (Table A-1)

Basic arithmetic operations on compatible matrices are performed using standard symbols for addition, subtraction, multiplication, division and raising to a power. For example, the square root of a matrix A is computed by the command

SQRT(A).

Basic algorithms for linear system solutions, eigensystem decomposition (including reliable determination of the Jordan form), singular value decomposition (SVD), QZ decomposition, and matrix algebraic operations are implemented as language primitives. Many of the primitives are inherited from MATLAB. Most commonly used operations on matrices are available.

Graphics (Table A-2)

A powerful, flexible, user-driven graphics capability is available in MATRIX$_x$. The command, PLOT(x,y), causes y to be plotted against x with automatic selection of scales, axis labels and area of the screen where the plot is to be made. Only a part of the screen is used for plotting, leaving the remainder for alpha-numeric output and command inputs.

Using English language commands, it is possible to change the size of the plots, x-axis or y-axis scales, location of the plot on the screen, axis labels, title, grid lines, tic marks and other variables. The available command structure makes graphics capability extremely useful and user-friendly.

Control Design (Table A-3)

In MATRIX$_x$, control design can be based on any of the following:

(a) Classical methods including Bode and Nyquist (including methods for multivariable plants),

(b) Linear-Quadratic-Gaussian (LQG) approach,

(c) Methods based on A-B invariant subspaces,

(d) Eigenstructure assignment and zero placement, and

(e) Adaptive control using self-tuning regulators and other techniques.

For the LQG problem, the algebraic Riccati equation is solved from extended Hamilton equations avoiding inverses, which are troublesome in the singular case. The equations are row compressed with an orthogonal transformation followed by the QZ pencil decomposition and a backward stable ordering of the eigenvalues.

Meaningful extensions to LQG methods require inclusion of dynamics of reference, disturbances, sensors and actuators. Appending of dynamics in frequency-shaped control design or model-following techniques involves forming augmented equations, which are easily accomplished with MATRIX$_x$ primitives. Use of frequency-shaped costs with singular value plots for robustness evaluation allow incorporation of engineering judgment in the control design.

Evaluation tools for linear systems include frequency response, power spectral density plots, time responses, transmission zeros and individual transfer function zeros. The principle vector algorithm (PVA) primitive for numerically reliable extraction of the Jordan Form (with discriminatory rank deflation of root clusters) is very useful in modal analysis of open-loop systems of vehicles and structures. PVA permits computation of residues or partial fraction expansions of multivariable systems.

Data Analysis and System Identification (Table A-4)

Data analysis and identification can be performed very efficiently and easily in MATRIX$_x$. Tied with a flexible graphics package, MATRIX$_x$ provides a production environment for batch and recursive identification methods. A universal interface to external simulations is provided to facilitate data transfer. Data can be censored, detrended and analyzed in MATRIX$_x$. Batch procedures include the standard regression methods with analysis of variance and step-wise regression. State-space and nonlinear batch maximum likelihood procedures are also available. Recursive algorithms such as the recursive least squares, recursive maximum likelihood and extended Kalman filter with Ljung's modification are available. All covariance factorizations and updates are in U-D form for numerical reliability. Non-parametric batch and semi-batch methods using the FFT are provided for auto/cross covariances/spectras. Adaptive control algorithms for

multivariable systems using U-D updates can be designed using simple commands.

Filter design facilities include Finite Impulse Response design in Chebyshev Norm, Wiener Filters, window-based designs, and Infinite Impulse Response design.

Simulation and Evaluation (Table A-5)

$MATRIX_x$ provides capabilities for efficient linear and nonlinear simulation. The linear simulation is performed with a discrete representation and is structured to fully utilize any sparseness in system matrices.

A general nonlinear simulation model may be directly connected to $MATRIX_x$. The software is capable of solving explicit differential equations as well as implicit equations of the form $g(x,\dot{x},t) = 0$.

Use of 'chopped arithmetic,' i.e., using various effective machine word-lengths, can provide performance evaluation of on-board small word-length control system implementations. Simulations with finite word-length processing elements can thus be performed efficiently.

NUMERICAL ALGORITHMS

Numerical reliability and stability are important in all of the analysis environments described above. Primitive matrix operations are based on the best available numerical software drawn from EISPACK, LINPACK and recent research in numerical techniques.

Reporting and control of numerical errors are comprehensive. All potential loss of accuracy that may be significant is reported to the user. Backward stable unitary transformations are performed on data whenever possible.

AVAILABILITY

MATRIX$_x$ is currently operational on VAX with VMS and UNIX operating systems, IBM 3033 and 3081 with MVS/TSO operating system and CDC series machines with NOS operating system. Implementation on other machines is now in progress.

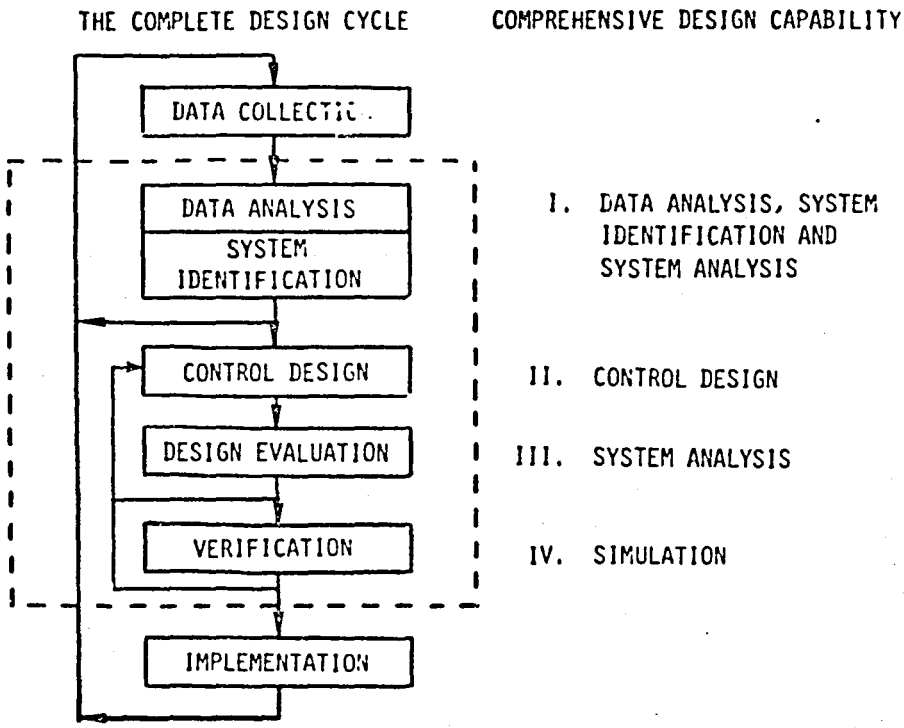

Figure A-1. MATRIX$_x$: A Data Analysis, System Identification, Control Design and Evaluation Package

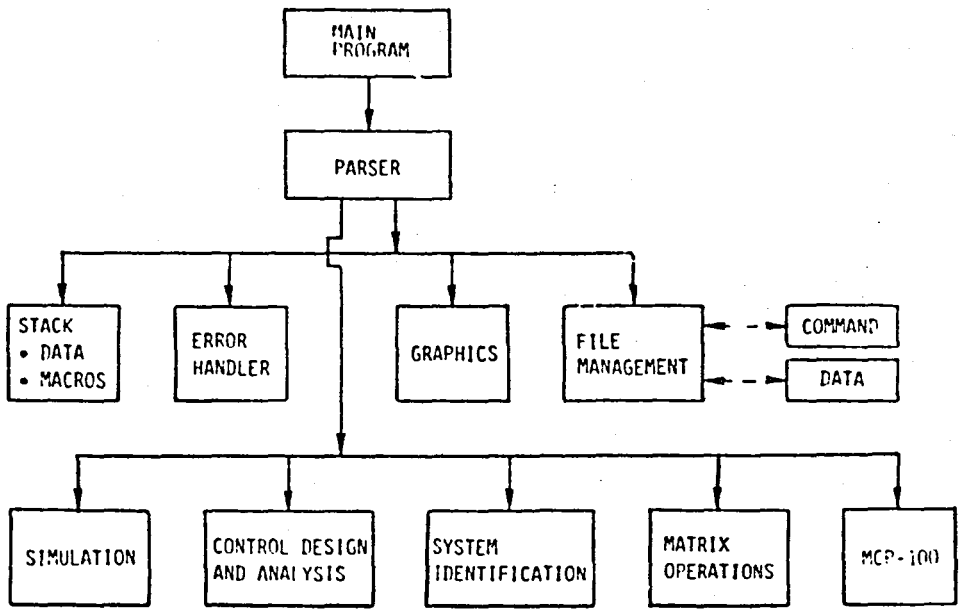

Figure A-2. MATRIX$_x$ Architecture

TABLE A-1. MATRIX$_x$ CAPABILITIES: MATRIX ARITHMETIC

Data Entering, Display and Editing
Addition, Subtraction, Multiplication and Division
Absolute Value, Real Part, Imaginary Part and the Complex Conjugate of a Matrix
Sum and Product of Matrix Elements
Element-by-Element Multiply and Divide
SIN, COS, ATAN, SQRT, LOG, EXP of Matrix Elements
Eigenvalue, Singular Value, Principal Values, Schur, LU, Cholesky and QR Decomposition of Matrices
Random Vector and Matrix Generation and Manipulation

TABLE A-2. MATRIX$_x$ CAPABILITIES: GRAPHICS

Flexible Commands
Multiple Plots
Axis Labels and Plot Title
Symbols and Lines
Tics and Grids
Log Scales
Bar Charts
Plot Location and Size
Personalizing the Plot Command
Report Quality Plots
3-D Graphics
Parallel and Perspective Projections
Surfaces
Curves
Viewing Transformations

TABLE A-3. MATRIX CAPABILITIES: CONTROL DESIGN AND SYSTEM ANALYSIS CAPABILITIES

Classical Tools (applicable to multivariable systems)

- Bode Plots
- Nyquist Plots
- Root Locus (with Zoom Capability)

Modern Tools

- Optimal Control Design, Discrete and Continuous
- Optimal Filter Design, Discrete and Continuous
- Frequency-Shaping LQG Design
- Singular-Value Decomposition of the Return-Difference
- Eigensystem Decompositions Including the Jordan Cannonical Form
- Model Following Control
- Model Reduction
- Linearization of Nonlinear Systems
- Minimal Realization and Kalman Decomposition
- Geometric Control Algorithms
- Multivariable Nyquist Plots

TABLE A-4. MATRIX$_x$ CAPABILITIES: SYSTEM IDENTIFICATION, SIGNAL PROCESSING AND DATA ANALYSIS CAPABILITIES

Data Display

- Time-History Plots
- Multichannel Cross-Plots
- Scatter Plots
- Frequency Plots
- Histograms

Data Transformations and Spectral Analysis

- Detrending
- Censoring
- Digital Filtering
- Discrete Fourier Transform
- Inverse Fourier Transform
- Autocorrelation
- Cross Correlation
- Autospectrum
- Cross Spectrum
- Decimation and Interpolation
- Maximum Entropy Spectrum Estimation

System Identification

- Step-Wise Regression and Model Building
- Maximum Likelihood Identification of State-Space Models and Nonlinear Models (generated by System-Build)
- Recursive Maximum Likelihood Identification
- Extended Kalman Filter Algorithm

Filter Design

- Window-Based Methods
- Wiener Filter
- REMEZ Exchange Algorithm for Finite Impulse Response Filters
- Elliptic, Chebyshev, Butterworth Infinite Impulse Response Design

TABLE A-5. MATRIX CAPABILITIES: SIMULATION AND *SYSTEM BUILDING CAPABILITIES

*Graphical Display of Block Diagrams and Interactive System-Building
Continuous and Discrete Systems
Linear and Nonlinear Components
Vector Signals and Multivariable Connections
Variety of Input Options for Linear Systems
State-Space
Transfer Functions
Pole-Zeros
Matrix Fractions
Multirate and Mixed System Analysis

* Interactive system-building will be released in June 1983.

APPENDIX B

OPTIMAL SELECTION OF FREQUENCY SHAPING FOR ESTIMATION

We want to minimize the determinant of the estimation error by a choice of the shaping function, F.

$$\sum = E(\Delta_p \Delta_p^T) = A^{-1} \int B(j\omega) N(j\omega) B^*(j\omega) d\omega \, A^{-1} \tag{B.1}$$

where

$$A = \int \left(\frac{\partial T_n u}{\partial}\right)^* (F^* R F) \left(\frac{\partial T_m u}{\partial}\right) d\omega \tag{B.2}$$

$$B = \left(\frac{\partial T_m u}{\partial}\right)^* (F^* R F) \tag{B.3}$$

Computation of the desired form for $F(j\omega)$ when $N(j\omega)$ is a general matrix leads to complex equations which cannot be used in practice. We drive the results for the case where $N(j\omega)$ is scaled by the same frequency function $g(j\omega)$, i.e., all measurement noises have the same spectrum. Then R will be selected such that

$$N(j\omega) = g(j\omega) R^{-1} \tag{B.4}$$

$$C = \int \left(\frac{\partial T_m u}{\partial p}\right)^* F^* R F \left(\frac{\partial T_n u}{\partial p}\right) (F^* g(j\omega) F) d\omega \tag{B.5}$$

Since A and B are both quadratic functions of F, a constant change in F at all frequencies will not affect the estimation error. Thus, we can impose the constraint

$$\int (F^* F) d\omega = 1 \tag{B.6}$$

Since the error covariance is a matrix, we must convert it into a scalar form for minimization. It is typically useful to minimize the determinant. Using Lagrange multipliers for the above constraint of Equation (B.6), we get

$$L = \det(\Sigma) + \lambda\left[\int F^{*}Fd\omega - 1\right]$$

$$= \frac{1}{(\det(A))^{2}}\left[\det\int\left(\frac{\partial T_{m}u}{\partial p}\right)^{*} F^{*}RF\left(\frac{\partial T_{m}u}{\partial p}\right) F^{*}g(j\omega)fd\omega\right] + x\int F^{*}Fd\omega - 1) \tag{B.7}$$

Taking derivatives with respect to $F^{*}F$, we get

$$\frac{\partial L}{\partial(F^{*}F)} = \frac{1}{(\det(A))^{2}}\ \mathrm{Tr}\left(C^{-1}\left(\frac{\partial T_{m}u}{\partial p}\right)^{*} R\left(\frac{\partial T_{m}u}{\partial p}\right) F^{*}g(j\omega)F\right.$$

$$\left. - A^{-1}\left(\frac{\partial T_{m}u}{\partial p}\right)^{*} R\left(\frac{\partial T_{m}u}{\partial p}\right)\right)$$

$$+ \lambda = 0 \tag{B.8}$$

The above equation is satisfied if

$$F^{*}g(j\omega)F = 1 \quad \text{at all frequencies} \tag{B.9}$$

or

$$F = [g(j\omega)]^{-1/2}$$

This equality is physically meaningful because it implies a filter which attentuates the measurements over that range of frequencies where measurement noise is large.

For a general $N(j\omega)$, the above equation is empirically extended to the following for $F^{*}g(j\omega)F = 1$, $A = C$. Thus, the quantity inside the bracket is zero for all ω.

$$R^{1/2}F(j\omega) = [N(j\omega)]^{-1/2}$$

END

DATE

FILMED

DEC 13 1984

End of Document